

EVALUATING THE EFFECTS OF COVALENCY ON IMMUNE FUNCTION

EVALUATING THE EFFECTS OF COVALENCY ON ANTI-TUMOUR IMMUNE  
FUNCTION USING A SYNGENEIC TUMOUR MODEL

BY: AKSHAYA RAAJKUMAR, B.Sc.

A Thesis Submitted to the School of Graduate Studies in Partial Fulfilment of the Requirements  
for the Degree Master of Science

McMaster University, MASTER OF SCIENCE (2022) Hamilton, Ontario

TITLE: Evaluating the Effects of Covalency on Anti-Tumour Immune Function Using  
Syngeneic Tumour Models

AUTHOR: Akshaya Raajkumar, B.Sc.

SUPERVISOR: Dr. Anthony Rullo

NUMBER OF PAGES: 107

## Abstract

Synthetic immunology aims to utilize synthetic chemistry and molecules to modulate natural immunological functions against cancer cells. Synthetic molecules developed for use in immunotherapy are antibody recruiting molecules (ARMs) that can utilize antibodies in human serum as a weapon against cancer cells. The development of ARMs has inspired the creation of a novel class of synthetic immunotherapeutics - covalent antibody recruiting molecules (cARMs). cARMs not only bind but covalently label specific antibodies to recruit them to the tumour cell surface. First generation cARM molecules consist of a human prostate specific membrane antigen (hPSMA) target binding domain, an antibody labeling acyl imidazole ester domain, and an anti-dinitrophenyl (DNP) antibody binding domain. The ALD domain instigates an irreversible covalent bond to label anti-DNP antibodies which enables the generation of a tumour therapeutic antibody directly *in vivo* which can enact immune cell function against tumour cells. cARMs have been proven to recruit anti-DNP antibodies to hPSMA expressing cells and mediate selective antibody-dependent cellular phagocytosis/cytotoxicity (ADCP/ADCC) against cancer cells in *in vitro* assays.

Following the development of a mouse model, initial *in vivo* studies demonstrated significantly improved survival in tumour bearing mice that were treated with ARM and cARM. *In vivo* labeling studies displayed successful labeling of anti-DNP antibodies in circulation by cARMs and the presence of labeled antibodies for at least 72hrs in circulation. Conversely, ARM mediated antibody binding was considerably less at all examined time points. Resolving autoinhibition limitations of cARMs allowed for enhanced and improved labeling of anti-DNP antibodies both *in vitro* and *in vivo*. This enhancement in labeling could allow for improved ternary and immune active quaternary complex formation to mediate tumour cell death. *In vivo* tumour studies demonstrated increased survival in tumour bearing mice treated with non-autoinhibited cARM when compared to ARM. Furthermore, innate immune cell populations were shown to increase in peripheral blood of tumour bearing mice treated with ARM and cARM. While cARM treatment dosing and concentration are yet to be optimized, this thesis demonstrates the potential of cARMs as an immunotherapeutic. cARMs can be synthesized to target a variety of cancer cell specific antigens, selectively label antibodies, and has the potential to recruit multi-specific therapeutic antibodies against heterogeneous tumours.

## Acknowledgements

Foremost, I would like to acknowledge and express my sincere gratitude to my supervisor Dr. Anthony Rullo for the continuous support of my research, sharing his enthusiasm of science and comradery when results don't pan out. His guidance and mentorship helped me immensely throughout my time in his lab. I could not imagine having a better advisor, one who allowed me to make mistakes and be self-sufficient.

I would like to thank Dr. Scott Walsh. He played a crucial part in this research and offered his extensive knowledge of immunology and animal work. He helped guide my project and my experimental plans while teaching me a wide array of skills.

I would like to thank my thesis advisory committee - Dr. Yonghong Wan and Dr. Sheila Singh for their support, feedback, questions, and insightful suggestions. I would also like to thank my external examiner, Dr. Amy Gillgrass, for her comments and recommendations.

Graduate school is a difficult and daunting journey - one that requires friends and support. As such, I'd like to thank the members past and present of the Rullo Lab. I thank Benjamin Lake and Nick Serniuck who developed the molecules used in my experiments. I'd also like to thank Eden Kapcan, Harrison McCann, and Pooja Mangalor. I thank my good friends and fellow lab members Rebecca Turner, Sissi Yang and Sarah Eisinga for their support throughout my project. They made going into the lab everyday more enjoyable.

Finally, I'd like to thank Mom, Dad, Kani, Lisa, Kairav & Lucas for all their love and encouragement through all my endeavours.

**Table of Contents**

<b>Descriptive Note</b>	<b>ii</b>
<b>Abstract</b>	<b>iii</b>
<b>Acknowledgments</b>	<b>iv</b>
<b>Table of Contents</b>	<b>v</b>
<b>List of Figures &amp; Tables</b>	<b>vii</b>
<b>List of Abbreviations</b>	<b>ix</b>
<b>Chapter 1: Introduction</b>	
1.1 Cancer	1
1.2 The Immune System & Cancer	1
1.2.1 Tumour Immunogenicity	1
1.2.2 Innate Immune Cells	2
1.2.3 Antibodies & Immune Function	4
1.3 Cancer Immunotherapy	8
1.3.1 Therapeutic Monoclonal Antibodies	8
1.4 Antibody Recruiting Molecules	11
1.4.1 Antibody Binding Domain	12
1.4.2 Target Binding Domains	12
1.5 Covalent Antibody Recruiting Molecules	15
1.5.1 Antibody Labeling Domain	16
1.6 Ternary & Quaternary Complexes	18
1.6.1 ARM Mediated Complexes & Immune Function	18
1.6.2 cARM Mediated Complexes & Immune Function	19
1.6.3 ARM/cARM Function <i>in vitro</i> & <i>in vivo</i>	20
<b>Chapter 2: Hypothesis &amp; Specific Aims</b>	<b>22</b>
<b>Chapter 3: Results &amp; Discussion</b>	
3.1 B16hPSMA Mouse Model Development	23
3.1.1 B16hPSMA Cells	23
3.1.2 B16hPSMA-cARM Binding	26
3.1.3 Anti-DNP Antibody Boosting in Mice	27
3.1.4 B16hPSMA Tumour Growth in Mice	30

3.1.5 Mouse Model Development- Discussion	36
3.2 Examine cARM/ARM Efficacy <i>in vivo</i>	42
3.2.1 ARM Efficacy Against B16hPSMA Tumours	42
3.2.2 cARM & ARM Efficacy Against B16hPSMA Tumours	46
3.2.3 cARM/ARM Efficacy – Discussion	48
3.3 ARM/cARM - Anti-DNP Antibody Binding	52
3.3.1 <i>Ex vivo</i> Binding/Labeling	52
3.3.2 <i>In vivo</i> Binding/Labeling	53
3.3.3 ARM & cARM Binding/Labeling – Discussion	56
3.4 Enhance & Optimize cARM Platform	60
3.4.1 Monoclonal Antibody Development	60
3.4.2 ARM vs. Ejection cARM vs. Non-Ejection cARM	62
3.4.3 ARM vs. cARMS <i>in vivo</i>	65
3.4.4 Immune Cell Presence in Tumour Bearing Mice	67
3.4.5 Treatment Platform Optimization – Discussion	69
3.5 Fc Dependent Target Cell Killing <i>in vitro</i>	73
3.5.1 Mouse Effector Cells for ADCC Assays	73
3.5.2 Antibody Dependent Cellular Phagocytosis	74
3.5.3 <i>In vitro</i> Approaches – Discussion	76
<b>Chapter 4: Conclusion</b>	<b>78</b>
<b>Chapter 5: Supplementary Figures</b>	<b>79</b>
5.1 Anti-DNP Antibodies	79
5.2 Non-Ejection cARM Structures	81
5.3 Rhamnose Mouse Model	82
5.4 Folate Mouse Model	83
<b>Chapter 6: Materials &amp; Methods</b>	<b>84</b>
<b>Chapter 7: Works Cited</b>	<b>92</b>

**List of Figures & Tables**

<b>Figure 1.1.</b> Antibody dependent immune function	7
<b>Figure 1.2.</b> ARM function to bridge antibody to tumour cell	14
<b>Figure 1.3.</b> ARM and cARM chemical structures	15
<b>Figure 1.4.</b> Proposed mechanism of cARM labeling of anti-DNP antibodies	16
<b>Figure 1.5.</b> Ternary complex destabilization by ARMs	19
<b>Figure 1.6.</b> Schematic of cARM function against hPSMA target cells	21
<b>Figure 3.1.</b> B16-hPSMA monoclonal cell line selection	24
<b>Figure 3.2.</b> hPSMA staining of chosen cell line	25
<b>Figure 3.3.</b> cARM – B16hPSMA binding	26
<b>Figure 3.4.</b> DNP vaccination to boost anti-DNP antibodies	28
<b>Figure 3.5.</b> Anti-DNP antibody ELISA standard curve	29
<b>Figure 3.6.</b> cARM effect on tumour volumes	31
<b>Figure 3.7.</b> Mitigating effects of B16hPSMA tumour regression	33
<b>Figure 3.8.</b> Immune cell presence in depleted vs. untreated mice	35
<b>Figure 3.9.</b> ARM anti-tumour effects on B16hPSMA tumours	43
<b>Figure 3.10.</b> B cell depletion effects on ARM efficacy	45
<b>Figure 3.11.</b> cARM vs. ARM effects on B16hPSMA tumours	47
<b>Figure 3.12.</b> ARM vs. cARM binding of anti-DNP antibodies	52
<b>Figure 3.13.</b> ARM/cARM <i>in vivo</i> binding/labeling of anti-DNP antibodies	55
<b>Figure 3.14.</b> Mouse monoclonal anti-DNP antibody expression	61
<b>Figure 3.15.</b> hPSMA recruitment to cARM labeled anti-DNP antibody	62
<b>Figure 3.16.</b> <i>Ex vivo</i> labeling of anti-DNP antibodies	63
<b>Figure 3.17.</b> Mouse <i>in vivo</i> labeling with ejection and non-ejection cARMs	64
<b>Figure 3.18.</b> ARM vs. cARMs effects on B16hPSMA tumours	66
<b>Figure 3.19.</b> Immune cell presence in tumour bearing mice	68
<b>Figure 3.20.</b> mCD16 expression in HEK293T cells	73
<b>Figure 3.21.</b> RAW264.7 induced ADCP against B16hPSMA cells	75
<b>Figure 5.1.</b> Anti-DNP antibody presence in boosted mouse sera	79
<b>Figure 5.2.</b> Anti-DNP antibody labeling by ejection cARM	80
<b>Figure 5.3.</b> Chemical structures of non-ejection cARMs	81



<b>Figure 5.4.</b> Mouse monoclonal anti-rhamnose antibody expression	82
<b>Figure 5.5.</b> <i>In vivo</i> boosting of anti-rhamnose antibodies	82
<b>Figure 5.6.</b> Endogenous folate receptor expression on cancer cell lines	83
<b>Table 6.1.</b> Transfection plasmids & amounts	84
<b>Table 6.2.</b> Antibodies for flow & ELISA	87
<b>Table 6.3.</b> Vaccination dosing profile	89

**List of Abbreviations**

ABD	Antibody binding domain
ADA	Anti-drug antibodies
ADCC	Antibody dependent cellular cytotoxicity
ADCP	Antibody dependent cellular phagocytosis
ALD	Antibody labeling domain
ARM	Antibody recruiting molecule
B16	Mouse melanoma cells
BiTE	Bispecific T-cell engager
BLI	Biolayer interferometry
BSA	Bovine serum albumin
cARM	Covalent antibody recruiting molecule
CD	Cluster of differentiation
CDR	Complementarity determining region
DM1	Drug maytansinoid
DMEM	Dulbecco's modified eagle medium
DMSO	Dimethyl sulfoxide
DNP	2,4-dinitrophenol
ELISA	Enzyme linked immunosorbent assay
ERK	Extracellular signal – regulated kinase
Fab	Fragment antigen binding
Fc	Fragment crystallizable
Fc $\gamma$ R	Fc gamma receptor
FcR	Fc receptor
FOLR	Folate receptor
GEFs	Guanine exchange factors
GM-CSF	Granulocyte macrophage colony stimulating factor
GUL	Glutamate urea lysine
HEK293T	Human embryonic kidney 293T cells
HER-2	Human epidermal growth factor 2
hPSMA/mPSMA	Human/mouse prostate specific membrane antigen
HSA	Human serum albumin
IFN $\gamma$	Interferon gamma
IgG	Immunoglobulin G
ITAM	Immune tyrosine activating motifs
KIR	Killer immunoglobulin-like
KLH	Keyhole limpet hemocyanin
mAb	Monoclonal antibody
MAC	Membrane attack complex
MEM- EARLES	Minimum essential medium with earle's salts
MFI	Mean fluorescence intensity
MPLA	Monophosphoryl lipid A
NF- $\kappa$ B	Nuclear factor $\kappa$ B
NK	Natural killer
PBS	Phosphate buffered saline
PI3K	Phosphatidylinositol-3-kinase

PSA	Prostate specific antigen
RAW264.7	Mouse macrophage cell line
RT	Room temperature
TAM	Tumour associated macrophages
TBD	Target/tumour binding domain
TLR	Toll-like receptor
TME	Tumour microenvironment
WT	Wild type

## **Chapter 1: Introduction**

### **1.1 Cancer**

Cancer remains as a leading cause of death around the world. In 2020, there were approximately 19.3 million new cancer cases worldwide and approximately 10 million cancer related deaths<sup>1</sup>. Cancer affects almost every tissue type in the body due to a variety of mutations that affect a significant number of genes<sup>2</sup>. Despite substantial research, the disease remains a challenge due to its complex nature. In fact, the mortality rate for cancer has remained the same for the last 50 years wherein death rates for infectious and cardiac diseases have decreased by approximately 60%<sup>2</sup>. Cancer burden is growing rapidly worldwide affecting populations and healthcare systems. Advances in cancer research will not only need a deep understanding of cancer biology but utilize innovative approaches to develop new standards of care.

### **1.2 The Immune System & Cancer**

#### **1.2.1 Tumour Immunogenicity**

Genomic instability in cancer often results in accumulation of mutations leading to the development of tumour antigens<sup>3</sup>. These antigens can then be recognized by the immune system and trigger an immune response<sup>3</sup>. As such, the immune system is vital in immunosurveillance within the tumour microenvironment (TME) and regulates disease development<sup>4</sup>. The innate immune cells, such as natural killer (NK) cells and macrophages, contribute to tumour suppression by killing tumour cells directly and by initiating adaptive immune responses<sup>5</sup>. In turn, adaptive immune cells, such as T cells and B cells, play a role in cell-mediated and antibody responses, respectively<sup>6</sup>. While immune responses are powerful against tumour cells, cancer cells have developed escape mechanisms to reduce immune cell function. As a result, the

immune system is not only involved in protective mechanisms against tumours but shapes tumour immunogenicity<sup>3</sup>.

Immune pressure results in tumour immunoediting, which is categorized into three phases. The elimination phase consists of coordinated innate and adaptive immune responses against tumour growth<sup>3</sup>. If cancer cell variants escape the eradication in the elimination phase, it enters the next phase of equilibrium<sup>3</sup>. This phase consists of dormant tumour cells and control of possible outgrowth by the adaptive immune system. The final phase of immunoediting is the escape phase wherein tumour cells can escape immune effector function and recognition. Tumour cell populations can escape immune function due to modifications resulting in loss of antigens or resistance to effector cells effects<sup>3</sup>. As such, tumour cells become inherently less immunogenic and acquire the ability to grow deprived of immune system control. Furthermore, tumour cells may escape due to the development of an immunosuppressive environment within the TME mediated by immunosuppressive cytokines and regulatory immune cells<sup>7</sup>. However, most tumours are antigenic and studies have shown that they can be eliminated by the immune system under certain conditions<sup>8,9</sup>. Consequently, the lack of immunogenicity is due to a lack of immune response induced by the tumour<sup>8</sup>.

### **1.2.2 Innate Immune Cells**

NK cells are innate cytolytic immune cells that are vital in controlling both viral infections and tumour cell growth<sup>10</sup>. NK cells are found in blood, spleen, bone marrow and lymph nodes and chemoattractants can cause migration to sites of inflammation<sup>11</sup>. NK cells express lytic machinery that can eradicate target cells without prior activation<sup>12</sup>. NK cell effector function is regulated by activating and inhibitory cell surface receptors<sup>12,13</sup>. NK cells use these receptors to recognize aberrant cells and mediate cytotoxicity, proliferation and cytokine production<sup>10</sup>. NK

cell function is suppressed by major histocompatibility complex (MHC) class I expression on cell surfaces as MHC class I molecules bind to killer immunoglobulin-like (KIR) family inhibitory NK cell receptors to prevent the killing of healthy “self” cells<sup>10,12</sup>. As such, NK cells can eliminate cancer cells which tend to downregulate MHC class I molecules<sup>14</sup>. Furthermore, cancer cells overexpress NK cell activating receptor ligands on cell membranes or secrete ligands to stimulate interferon- $\gamma$  (IFN $\gamma$ ) and tumour necrosis factor (TNF)<sup>15</sup>. Importantly, target cell recognition and effector function is also modulated by the cluster of differentiation-16 (CD16) receptor that is able to bind the constant region of immunoglobulins (IgG)<sup>14</sup>. Human NK cells are CD3<sup>-</sup>CD56<sup>+</sup> and encompass approximately 5-20% of peripheral blood lymphocytes<sup>16</sup>. These cells are divided into two major populations - CD56<sup>dim</sup>CD16<sup>+</sup> and CD56<sup>bright</sup>CD16<sup>-</sup>. The CD56<sup>dim</sup>CD16<sup>+</sup> population makes up 90-95% of NK cells and mediates high cytotoxic function<sup>16</sup>. Conversely, the CD56<sup>bright</sup> NK cells exhibit limited cytotoxicity and secrete cytokines when activated. On the other hand, mouse NK cells express CD27 instead of CD56. CD27<sup>bright</sup> mouse NK cells are able to produce copious amounts of cytokines as well as effect powerful cytolytic function<sup>17</sup>.

Macrophages are innate immune cells that are vital in tissue homeostasis. Macrophages are phagocytic cells that clear away apoptotic and aberrant cells, produce growth factors and modulate pro-inflammatory cytokine production<sup>18</sup>. Macrophage activation allows for phagocytosis of the target cell – resulting in phagolysosomal degradation, antigen presentation and cytokine secretion<sup>19,20</sup>. Macrophages, when activated, can either be proinflammatory & anti-tumour (M1 type) or anti-inflammatory & pro-tumour (M2 type)<sup>21</sup>. During initial tumour growth stages, tumour associated macrophages (TAMs) display an M1 phenotype and are activated by toll-like receptor (TLR) ligands and Th1 cytokines such as such as IFN $\gamma$ , TNF, and granulocyte-

macrophage colony stimulating factor (GM-CSF). M1-like TAMs mediate the eradication of immunogenic tumour cells via cytotoxicity and phagocytosis<sup>21</sup>. However, as tumour growth progresses, the TME induces the M2 phenotype of TAMs (via Th2 cytokines) that promote tumour growth. As a result, M2 TAMs stimulate cancer cell proliferation, limit anti-cancer therapies, and immunosuppress other immune cells<sup>21</sup>. Furthermore, TAMs secrete cytokines that impair effector T cell activity and inhibit immune cell maturation<sup>21</sup>. While TAMs play a protumourgenic role, they do display some anti-cancer effects wherein they inhibit some metastasis by NK cell recruitment and can display a phagocytic phenotype<sup>22,23</sup>.

### **1.2.3 Antibodies & Immune Function**

Antibodies are powerful proteins that bind antigens with substantial specificity and can be used to target tumour cells. Specifically, IgG antibodies play an important role as the principal isotype found in extracellular fluid and blood (10-20% of plasma protein) and bind to their target antigen with high affinity<sup>24</sup>. Antibody specificity is derived from the variable regions of the IgG heavy and light chains of the fragment antigen-binding (Fab) domain<sup>25</sup>. The genes that produce the heavy and light chains are created during B cell differentiation by junctional, diversity and variable (V) gene segment recombination<sup>19,25</sup>. The V<sub>H</sub> and V<sub>L</sub> of heavy and light chain regions allow for the complementarity determining regions (CDRs) which form the unique antigen binding site for the antibody. The Fab domain has neutralization and cell receptor recognition/blocking capabilities to limit tumour growth<sup>25</sup>. Conversely, the fragment crystallizable (Fc) region is formed by the constant regions (C<sub>H2</sub> and C<sub>H3</sub>) of IgG heavy chains and can induce immune responses through the engagement of Fc receptors and complement binding<sup>25</sup>. Specifically, the Fc region interacts with Fc receptors (FcR) on NK cells and macrophages to mediate antibody-dependent cellular cytotoxicity (ADCC) and antibody-

dependent cellular phagocytosis (ADCP)<sup>26</sup>. Of the IgG subclasses, human IgG1 interacts with FcR efficiently to mediate efficacious ADCC/ADCP<sup>27,28</sup>. Conversely, murine IgG2a is highly effective in FcR effector functions and complement activity<sup>29</sup>.

Antibodies can mediate anti-tumour effects through ADCC<sup>30</sup>. To stimulate ADCC functions, the Fab domain of IgG antibody binds to a specific molecule/antigen which is expressed on the cell surface (**Figure 1.1A**). Following binding, the antibody recruits effector cells such as NK cells. NK cells are powerful effector cells as they lack inhibitory FcγRIIb and express activating receptor CD16a (FcγRIIIa)<sup>31</sup>. ADCC mediated NK cell killing can occur through directed exocytosis of cytotoxic granules, TNF signaling and cytokine release. Upon CD16a binding to Fc domains of antibodies, a signaling pathway is stimulated within NK cells<sup>32</sup>. Specifically, CD16a associates with CD3-ζ or FcεRI-γ chains in the cell membrane which have immune tyrosine-based activating motifs (ITAMs) in their cytoplasmic tails<sup>33</sup>. ITAMs are phosphorylated upon FcγR binding and signal transduction through tyrosine kinases, and activation of phosphatidylinositol-3-kinase (PI3K), nuclear factor κB (NF-κB), extracellular signal-regulated kinase (ERK) pathways result in synapse formation and NK cell degranulation<sup>34</sup>. Lytic granules are transported on microtubules and are released at the synapse<sup>35</sup>. The exocytosis of cytolytic granules such as perforin and granzymes result in the perforation of target cells that causes osmotic lysis and granzyme inducing apoptotic death<sup>36</sup>. Interestingly, a single granule is adequate to lyse a target cell<sup>35</sup>. This degranulation process can be repeated and allows for the repeated killing of target cells<sup>35</sup>. Furthermore, TNF death receptor signaling results in target cell apoptosis<sup>34</sup>. Finally, cytokine production, such as IFNγ, stimulates proximal immune cell function in antigen presentation and induces augmented adaptive immune



responses<sup>34</sup>. CD16 is also expressed on activated macrophages as such, both NK cells and macrophages can contribute to ADCC effects<sup>37</sup>.

ADCP is a vital mechanism in antibody-directed, immune mediated tumour cell killing. Important effector cells in this process are macrophages which can clear antibody-opsonized cells and microbes by phagocytosis (**Figure 1.1B**)<sup>25</sup>. Human macrophages express all FcγR and upon FcγR binding (except inhibitory FcγRIIb) to Fc domains of antibodies that are bound to target cells, a signaling pathway is stimulated within macrophages<sup>38</sup>. This results in membrane receptor clustering and the phosphorylation of ITAMs found within the FcR cytoplasmic tail which results in signaling through Rac-guanine nucleotide exchange factors (GEFs) to stimulate phagocytosis<sup>39</sup>. A phagocytic synapse is formed followed by actin polymerization to mediate a phagocytic cup and pseudopod extension around the target cell<sup>38</sup>. Actin rearrangement then forms a phagosome within the macrophage which matures by fusing to lysosomes and endosomes to gain digestive enzymes and is concurrently acidified with proton pumps<sup>38,39</sup>. Finally, target cells are engulfed and digested.

IgG binding to antigens can initiate the classical pathway wherein immune complexes are formed to lyse target cells (**Figure 1.1C**). IgG Fc binding results in C1q recruitment and binding to exposed Fc region. A complement cascade is then initiated that involves sequential complement protein cleavage and activation of C4, C2, C3b, C5, C6, C7, C8 and C9 to form the membrane attack complex (MAC)<sup>40</sup>. The MAC complex creates a pore by inserting itself into the target cell membrane resulting in cell lysis<sup>40</sup>. Furthermore, complement activation also induces the activation of innate immune cells causing degranulation, phagocytosis and cytokine production<sup>40,41</sup>.

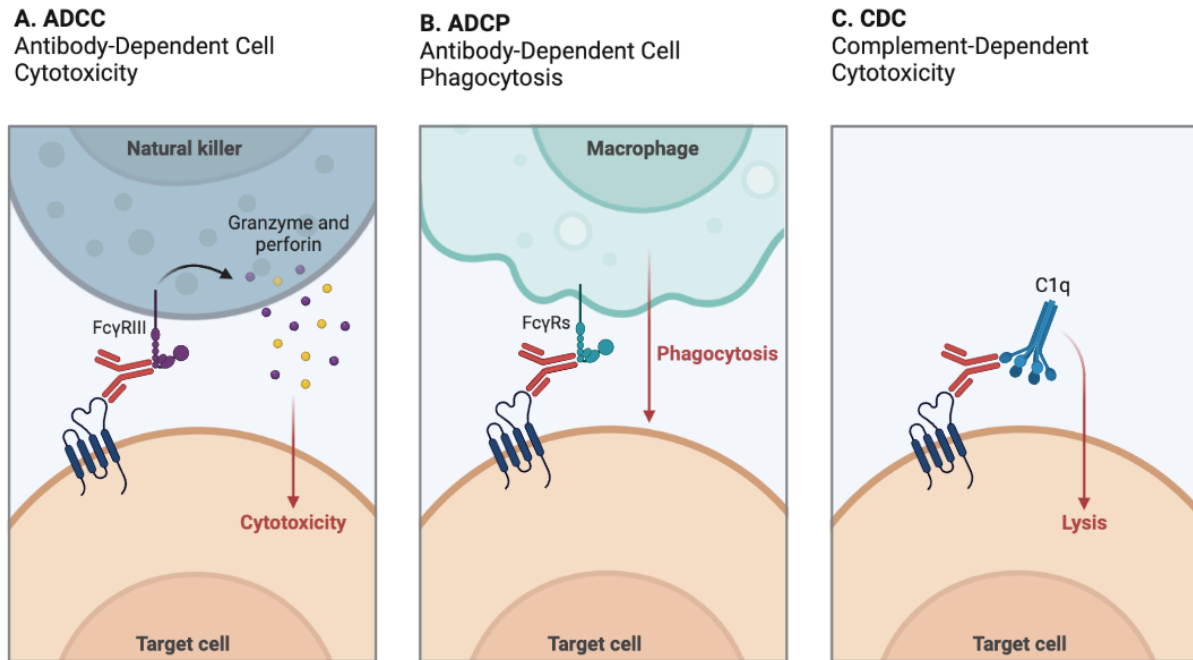


**Figure 1.1. Antibody dependent immune function.** (A) ADCC effects mediated by NK cells. Fab region of IgG antibody binding to antigen recruits NK cells binding through CD16 to Fc region. NK cell degranulation is activated to release perforin and granzymes to kill target cells. (B) ADCP effects mediated by macrophages. Fab region of IgG antibody binding to antigen recruits macrophage FcR binding to Fc region. Macrophage phagocytic functions are stimulated to phagocytose target cells. (C) CDC effects mediated by complement cascade. Fab region of IgG binding to antigen recruits C1q complement binding to IgG Fc. This stimulates a complement cascade and recruits C4, C2, C3b, C5, C6, C7, C8 and C9 to form the membrane attack complex.

### **1.3 Cancer Immunotherapy**

Currently, the recommended and conventional treatments for cancer include surgery to resect the tumour followed by radiation and/or chemotherapy<sup>42</sup>. Surgery is most effective at early stages however, there are limitations to this approach. Location of solid tumours, tumour growth rate and possible amputation or disfiguration are all considerations when deciding to resect tumours<sup>42</sup>. Radiation therapy, on the other hand, can harm healthy organs, tissues and cells<sup>42</sup>. Similarly, chemotherapeutic agents often harm healthy cells and pose many harmful side effects. Moreover, drug resistance to chemotherapy often develops in patients.

Cancer immunotherapy is a rapidly advancing field of research and novel standard of cancer therapy. It aims to exploit and harness the immune system to attack cancer cells by eliminating cancer immune evasion and augmenting tumour immunogenicity<sup>43</sup>.

#### **1.3.1 Therapeutic Monoclonal Antibodies**

Therapeutic monoclonal antibodies represent a major avenue of treatment in cancer immunotherapy as they are a powerful tool to target specific – disease associated cell surface proteins. Upon Fab binding to target antigens, they can affect a variety of functions. Tumour therapeutic antibodies are able to induce and recruit immune responses against tumour cells through ADCC, ADCP and CDC<sup>44-47</sup>. For instance, farletuzumab, a folate receptor  $\alpha$  targeting monoclonal antibody, has been demonstrated to induce lung cancer cell lysis through ADCC and CDC in preclinical trials<sup>48</sup>. Furthermore, therapeutic monoclonal antibodies can bind specific cell receptors or ligands to interrupt cancer cell signaling or carry toxins to target cells<sup>42</sup>. For example, a monoclonal antibody targeting human prostate specific membrane antigen (hPSMA) has been conjugated with drug maytansinoid (DM1) and examined in mouse models<sup>49</sup>. Following anti-hPSMA antibody binding, DMI (a microtubule depolymerizing drug) is released

during cellular internalization to induce mitotic arrest to limit cancer cell growth and delay tumour growth in tumour bearing mice<sup>49</sup>.

Antibodies travel through cell membranes poorly, thus anti-tumour antibodies are often limited to target membrane bound proteins, proteins that allow for internalization or extracellular antigens<sup>25</sup>. Preferably, the target antigen should be preferentially expressed on tumour cells to allow for specific targeting and minimal off target effects and toxicities<sup>25</sup>. Antibody therapy is also limited by antigen loss variant cells. Antigen loss variants can be selected during immunotherapy therefore limiting the potential efficacy of therapeutic antibodies. For instance, treatment of B-cell lymphoma with anti-CD20 antibodies resulted in a loss of CD20 expression in some cases<sup>50</sup>. Importantly, due to tumour cell genetic instability, antigenic variants are generated at a high rate<sup>25</sup>. Conversely, treatment of breast cancer with trastuzumab has not resulted in human epidermal growth factor receptor – 2 (HER-2) negative variants<sup>25</sup>. As HER-2 overexpression and signaling allows for cancer cell proliferation and increased oncogenicity, it is an important receptor to target<sup>51</sup>. Thus, targeting membrane bound proteins that are required for tumour cell growth and phenotype is vital in enhancing antibody anti-cancer effects.

While therapeutic monoclonal antibodies are efficacious, there are limitations to their anti-cancer effects. As antibody therapeutics contain “non-self” protein sequences and are large proteins (150kDa), this can induce an immune reaction against them. Anti-drug antibodies (ADA) can neutralize therapeutic antibodies which reduces the efficacy of these drugs<sup>52</sup>. Additionally, ADAs cause additional effects and can result in skin rashes and inflammatory response syndrome<sup>53</sup>. While humanized antibodies have reduced potential immune responses, they still retain murine CDR sequences. The CDRs could be viewed as foreign antigens and cause immunogenicity. For instance, in HER-2 positive breast cancer patients treated with

trastuzumab, a humanized antibody, ADA rates were 7.1%<sup>54</sup>. Intravenous administration of therapeutic antibodies could also result in IgE-mediated anaphylactic reaction, cytokine release syndrome, immunosuppression and serum sickness<sup>53,55</sup>. While the development of fully humanized antibodies have been approved for therapeutic use, they still induce ADA responses<sup>52,56</sup>. Lack of efficacy has been shown to correlate with ADA levels in patients with rheumatoid arthritis treated with adalimumab – a fully humanized antibody<sup>52</sup>. Similarly, 16% of rheumatoid arthritis patients treated with golimumab displayed ADA levels that correlated with reduced circulating levels of treatment antibody<sup>52</sup>. Thus, immunogenicity of humanized and fully humanized therapeutic antibodies remains a factor affecting efficacy. Furthermore, therapeutic antibodies lack oral bioavailability and have poor pharmacokinetics due to their large size and polar surface area<sup>57-59</sup>. Finally, the development and purification of therapeutic monoclonal antibodies is extremely expensive and time consuming. As antibodies are sizable multimeric proteins and large amounts of antibodies are required to reach clinical efficacy, high production costs are necessary. In 2012, the estimated cost for conventional chemotherapeutic drugs was \$17,500 per patient whereas therapeutic antibody treatment cost was \$30,400 per patient<sup>55</sup>. As such, there is a need to harness antibodies and their powerful biological properties affordably but without compromising efficacy and immunogenicity.

## 1.4 Antibody Recruiting Molecules

Synthetic immunology is a novel and exciting field of research that uses synthetic molecules to control and regulate immune responses. The development of bifunctional small organic molecules also known as “molecular glues” are promising in addressing many of the issues that therapeutic antibodies pose. Antibody-recruiting small molecules (ARMs) are bifunctional molecules that contain an antibody-binding domain (ABD) and a target binding domain (TBD), allowing them to redirect endogenous systemic antibodies to target cells<sup>60,61</sup>. This bridges antibodies to target cancer cells thereby enforcing proximity to induce potent immune function. Furthermore, ARMs are less immunogenic compared to therapeutic antibodies due to their small molecular size (1-2kDa)<sup>61,62</sup>. These small molecules can be produced at a large scale inexpensively and can be optimized for oral bioavailability<sup>63</sup>.

ARMs function by augmenting antibody opsonization of cancer specific targets. They can reprogram pre-existing antibodies in circulation that have no prior ability to localize to cancer cells (**Figure 1.2**). Following antibody recruitment, a ternary complex comprising the ARM, antibody and target cell antigen is formed. Subsequent immune FcR binding allows for the formation of an immune active quaternary complex to induce target cell killing. ARMs have been shown to induce strong antibody dependent immune responses such as ADCC, ADCP and CDC<sup>64,65</sup>. Specifically, ARMs mediate cancer cell killing in a target antigen and antibody dependent mechanism that minimizes off-target killing<sup>66,67</sup>. ARM treated mice that were immunized to express high antibody levels and engrafted with target antigen tumour cells displayed delayed tumour growth and enhanced survival<sup>68</sup>. Conversely, mice engrafted with antigen-negative cells or non-immunized were unaffected by ARM treatment<sup>67</sup>.

### 1.4.1 Antibody Binding Domain

The ABD of ARMs can bind and recruit anti-hapten antibodies, via small molecule ligands that bind endogenous antibodies. Specific endogenous antibodies such as anti- 2,4-dinitrophenyl (DNP) antibodies are found in abundance in human serum<sup>69</sup>. Approximately 1% of circulating endogenous antibodies in humans have been found to be anti-DNP antibodies<sup>64</sup>. Interestingly, their origin of antigenic exposure remains largely unknown although it is speculated to be derived from DNP-containing pesticides, preservatives and dyes and is present in a large portion of the population<sup>69,70</sup>. Importantly, the use of anti-DNP IgG antibodies have demonstrated powerful ADCC, ADCP and CDC functions to induce target cell killing<sup>41</sup>. Thus, anti-DNP antibodies represent a strategic choice to recruit to cancer cells. As such, the ARMs discussed in this thesis contain a DNP group at the ABD.

### 1.4.2 Target Binding Domains

Chemical biologists have developed ARMs targeting a variety of cancer proteins however, the focus of this thesis will be on prostate cancer targeting ARMs. hPSMA is a unique type II membrane bound glycoprotein that is greatly overexpressed (100-1000-fold expression) on the surface of prostate cancer cells and the neovasculature of many solid tumours<sup>71</sup>. Furthermore, hPSMA expression on normal, healthy tissues and benign prostate tissue is limited, thus making it an important marker and tumour target<sup>71</sup>. Moreover, hPSMA can be targeted by antibodies and has a characterized binding site to allow for targeting with small molecule ligands<sup>72</sup>. Additionally, hPSMA plays a vital role in prostate cancer progression wherein expression of hPSMA increases with cancer progression and aggressiveness<sup>67,73</sup>. hPSMA serves two enzymatic functions – folate hydrolase and NAALADase and contains a glutamate carboxypeptidase enzymatic pocket. Within the small intestine, it removes glutamates from  $\gamma$ -linked poly

glutamates and within the central nervous system, it metabolizes the neurotransmitter N-acetyl-aspartyl-glutamate<sup>71</sup>. The release of glutamate mediated by hPSMA can subsequently bind to receptors on cancer cells to activate PI3K signaling thus stimulating cell growth and proliferation<sup>74</sup>. As such, hPSMA serves as a powerful protein to not only target and identify cancer cells but also inhibit enzymatic function to reduce tumour growth.

Current studies exploiting hPSMA for immunotherapy are in preliminary stages and display varying results. The preclinical evaluation of an anti-hPSMA specific single-chain immunotoxin has demonstrated specificity and toxicity against hPSMA expressing cells *in vitro* and *in vivo*, however, high doses resulted in severe hepatotoxicity leading to animal death<sup>75</sup>. <sup>177</sup>Lutetium radiolabeled anti-hPSMA monoclonal antibodies induced antitumour activity in 4/35 patients. Prostate specific antigen (PSA) levels were used as a measure for antitumour activity and PSA levels decreased by ~50% for 3-8 months before levels returned back to normal<sup>76</sup>. Finally, hPSMA targeted bispecific T-cell engagers (BiTEs) have been examined in phase I clinical trials and demonstrated some dose dependent PSA response<sup>77</sup>. However, adverse reactions such as infections, fever and lymphopenia were observed in patients. Moreover, only 2 patients responded long-term to treatment<sup>77</sup>. As such, further immunotherapeutic approaches and mechanisms are required to target and eradicate hPSMA expressing cancer cells.

To utilize synthetic ARMs to target hPSMA expressing cells, small molecule ligands have been created to selectively bind hPSMA with high affinity. One such small molecule ligand is glutamate urea lysine (GUL) which has been shown to target hPSMA and inhibit enzymatic activity<sup>78</sup>. Prostate cancer targeting therapeutic ARMs contain GUL at the TBD to enable binding of hPSMA target cells (**Figure 1.3A**).



Alongside therapeutic ARMs, there are reporter versions developed and utilized to study the profile of these molecules. Importantly, versions containing small molecule biotin moieties at the TBD have been created (**Figure 1.3C**). The interaction between biotin and streptavidin is an extremely strong non-covalent bond and is extensively used to examine a variety of protein interactions due to their high affinity and specificity<sup>79</sup>.

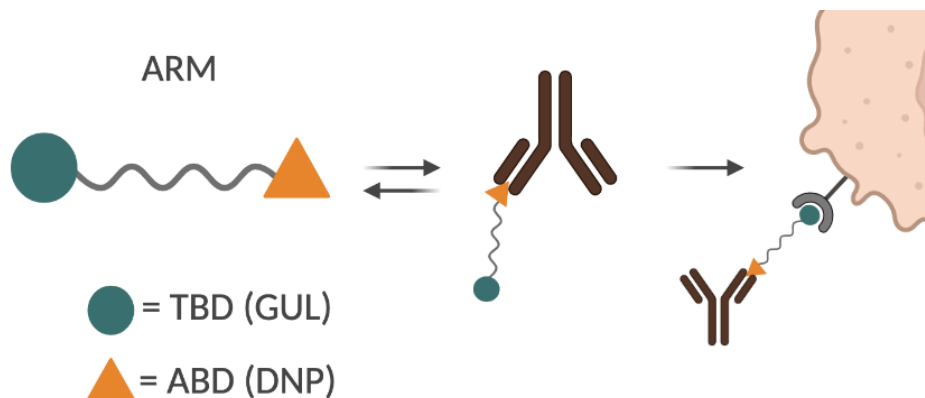


**Figure 1.2. ARM function to bridge antibody to tumour cell.** ARM ABD binds to anti-DNP antibodies in circulation. Following ABD binding, the bound antibody can be recruited to tumour cell surfaces and TBD binding allows for ternary complex formation and antibody mediated immune effects.

### 1.5 Covalent Antibody Recruiting Molecules

The Rullo lab has developed small molecule covalent immune recruiting technology which leverages proximity activated bio-conjugation chemistry with target immune protein binding. This technology has been applied to the recent development of covalent antibody recruiting molecules (cARMs) which contain small tumour antigen binding molecules and can selectively covalently link to natural serum antibodies<sup>80</sup>. First generation therapeutic cARM molecules (**Figure 1.3B**) consist of a hPSMA targeting TBD, an antibody labeling domain (ALD) and an anti-DNP antibody ABD<sup>80</sup>. Similarly, reporter molecules contain a biotin TBD, an ALD and a DNP ABD (**Figure 1.3D**). cARMs differ from ARMs as they form an irreversible covalent linkage to the antibody using proximal labeling chemistry.

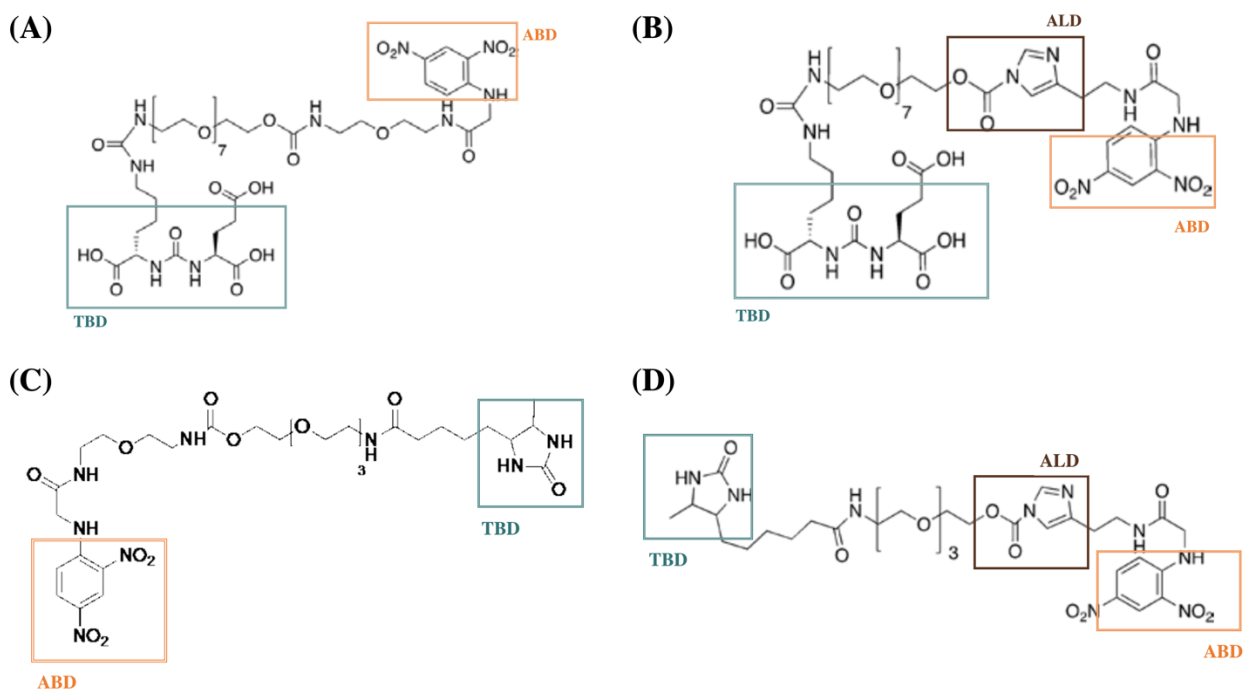


**Figure 1.3. ARM and cARM chemical structures.** (A) hPSMA targeting ARM. (B) hPSMA targeting cARM. (C) Streptavidin binding ARM. (D) Streptavidin binding cARM. (A-B) TBD contains GUL. (C-D) TBD contains a biotin moiety. (B-D) ALD contains an acyl imidazole group. (A-D) ABD contains a DNP group.

### 1.5.1 Antibody Labeling Domain

The addition of the ALD in cARMs allows for irreversible covalent binding to anti-DNP IgG at sub-saturating concentrations. The ALD functions post ABD (DNP) binding to the antibody (anti-DNP antibody). Once the ABD binds, a proximal lysine (lysine 59) residue found on anti-DNP IgG antibodies near the ABD-antibody binding site allows for covalent bond formation. The lysine residue attacks the electrophilic acyl imidazole group at the ALD, this results in the ABD acting as a leaving group (**Figure 1.4**). Anti-DNP IgG is then covalently linked to the TBD, thus allowing it to target hPSMA expressing tumour cells wherein it previously lacked an inherent ability to mark tumour cells for immune recognition/eradication.

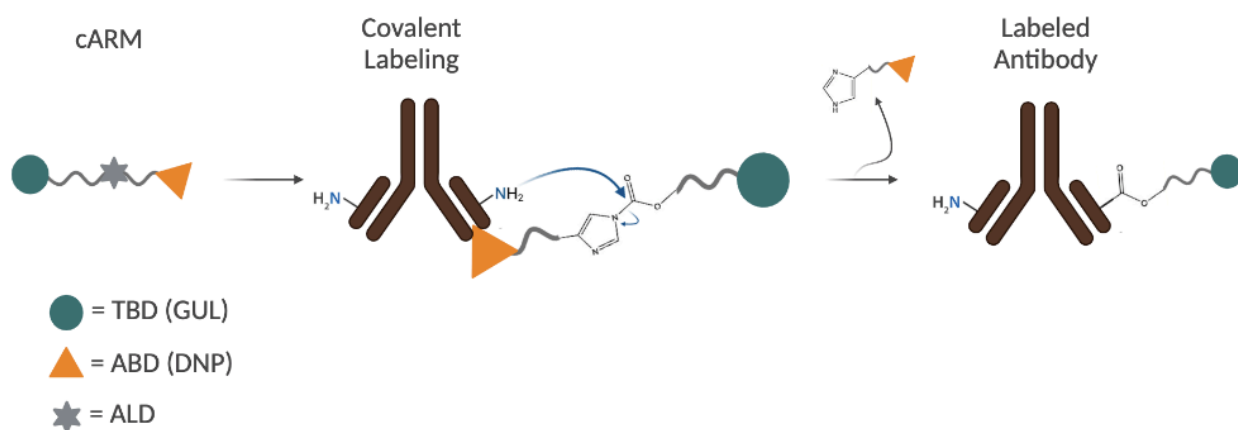


**Figure 1.4. Proposed mechanism of cARM labeling of anti-DNP antibodies.** cARM ABD binds to anti-DNP antibodies. Following ABD binding, a proximal lysine residue attacks the electrophilic acyl imidazole ALD to form an irreversible covalent bond. The ABD is ejected and this results in a labeled antibody covalently attached to the TBD.

Labeling specificity of cARM was confirmed to target anti-DNP IgG in the presence of other IgG antibodies and serum proteins. Specifically, control experiments using cARM and human non-DNP IgG antibodies demonstrated no covalent recruitment<sup>81</sup>. While control IgG contained several lysine residues, the covalent reaction could not be completed without previous DNP binding interactions<sup>81</sup>. Additionally, site selective maximal labeling of polyclonal anti-DNP IgG (0.2 $\mu$ M) was observed using a small excess of cARM (0.4 $\mu$ M) in 10% human serum<sup>80</sup>. There are several lysine residues found on anti-DNP IgG and a nonselective reaction would utilize more than 2 equivalence of cARM. Furthermore, cARM mediated labeling was observed when completed in 100% pooled human serum with low nM anti-DNP IgG and high concentrations of human serum albumin (HSA) which is known to sequester DNP<sup>80</sup>. In the presence of excess DNP-glycine competitor which competes with cARM for anti-DNP IgG binding, there was an observed reduction in anti-DNP IgG specific labeling when compared to samples with no competitor<sup>80</sup>. Similarly, cARM labeling decreased substantially when using pooled human IgG depleted of anti-DNP IgG, confirming cARM labeling specificity. cARM labeling was also conducted in anti-DNP IgG boosted mouse serum wherein successful labeling was observed when compared to a lack of labeling in non-DNP boosted mouse serum<sup>80</sup>. As such, cARM labeling is specific, reliable and functions according to the hypothesized binding mechanism.

## 1.6 Ternary & Quaternary Complexes

### 1.6.1 ARM Mediated Complexes & Immune Function

ARMs function by reversibly binding to anti-DNP antibodies, recruiting them to cancer cells and forming the ternary complex at the tumour cell surface. Following binding of an effector cell to the recruited antibody, the ternary complex then forms a quaternary “immune” complex with the FcR receptors on immune cells to trigger target cell death through ADCC and ADCP<sup>82,83</sup>. As such, the efficacy of ARMs is not only controlled by the number but also the stability of immune active quaternary complexes (**Figure 1.5**). The formation of the quaternary complexes *in vivo* is thereby dependent on ternary complex and ARM-antibody binary complex formation and stability. Ternary complex formation is fundamentally limited by ARM affinity to antibodies and sub-saturating antibody concentrations<sup>80</sup>. Antibody recruitment with ARM utilizing low serum antibody concentrations were not able to sufficiently mediate immune cell function against hPSMA target cells<sup>81</sup>. Furthermore, ternary complex dissociation is promoted by rapid ARM clearance<sup>66,80</sup>. However, attempting to mitigate this issue by administering excess ARMs results in autoinhibition of ternary complex formation<sup>80,84</sup>. This occurs as excess ARMs in circulation bind antibodies and tumour antigens separately, preventing ternary complex formation and instead, forming binary complexes<sup>68</sup>. As ARMs reversibly bind both to antibodies and targets, there are certain constraints on ARM efficacy and function that minimize antibody recruitment and immune function against cancer cells.

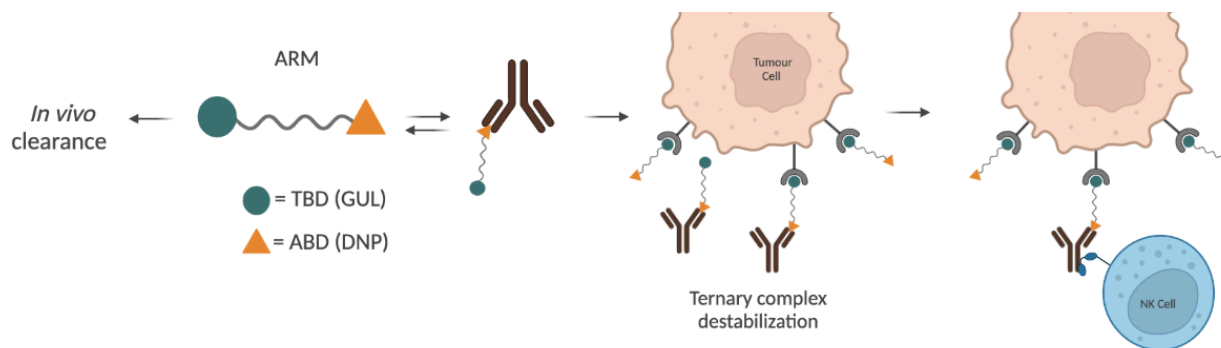


**Figure 1.5. Ternary complex destabilization by ARMs.** The reversible binding nature of ARMs results in destabilized ternary and subsequent quaternary complexes. Excess ARMs results in autoinhibition and drives high clearance when ARMs are unbound.

### 1.6.2 cARM Mediated Complexes & Immune Function

cARMs allow for an irreversible covalent linkage to antibodies thereby resulting in a stable cARM-antibody complex (**Figure 1.6**). This then allows for ternary and immune active quaternary complex simplification and stabilization. As such, cARMs can circumnavigate some of the limitations posed by ARMs. The resultant effect is enhanced immune cell recognition and tumour cell elimination. The Rullo Lab aims to probe this hypothesis and examine the effects of covalency on ternary and quaternary complex formation and stability.

Covalent antibody recruitment was able to induce increased immune cell recognition and function compared to ARMs *in vitro*. cARM labeled antibodies enhanced CD16 activation against hPSMA target cells at serum antibody concentrations wherein noncovalent ARM recruitment could not<sup>81</sup>. These results were consistent with cARM covalent recruitment of monoclonal anti-DNP IgG as well as serum anti-DNP IgG. Conversely, a lack of immune recognition was observed when anti-DNP depleted IgG was used – confirming selective antibody recruitment. However, autoinhibitory effects do come into play when there are excess cARM labeled antibodies resulting in immune complex dissociation due to competitive binding with FcRs<sup>81</sup>. Moreover, covalent antibody recruitment enhanced ADCP of target cells at low antibody concentrations compared to non-covalent antibody recruitment. Similarly, with lower hPSMA

expressing target cells, cARM mediated ADCP outperformed ARM recruitment<sup>81</sup>. As such, covalent formation of immune complexes induced by cARM antibody recruitment did enhance immune effector function. Additionally, the specificity of cARM function was described wherein cARM labeled antibodies only induced immune recognition and function with cell lines that expressed high hPSMA levels<sup>81</sup>.

cARMs heighten stability of immune active complexes. Data suggests that immune recognition and function is not only modulated by the amount of antibody recruitment but the kinetic stability of immune complexes as well. While cARM mediated antibody recruitment is higher at lower antibody concentrations, both noncovalent and covalent antibody recruitment reached similar maximal recruitment at higher antibody concentrations<sup>81</sup>. However, there was a lack of ARM function at these high antibody concentrations whereas strong cARM function was observed<sup>81</sup>. This difference in functionality could be attributed to ARM-antibody dissociation. Dissociation of ARM and antibody could disrupt active immune complexes wherein complex formation needs to remain intact to allow for immune signaling and activation. Thus, cARM induced covalent stabilization could increase immune complex stability to allow for receptor clustering and activation<sup>81</sup>.

### **1.6.3 ARM/cARM Function *in vitro* & *in vivo***

Thus far, hPSMA targeting cARMs and analogous ARMs have only been examined *in vitro* within the Rullo Lab. Through *in vitro* analysis, ARM and cARMs have successfully demonstrated anti-DNP IgG binding and recruitment. Furthermore, cARMs have displayed selective anti-DNP IgG labeling. Both constructs were utilized in *in vitro* ADCP and CD16a activation assays to study not only anti-DNP IgG recruitment to form ternary complexes, but molecule mediated immune function and activation. While this is extremely important analyses,

further examination into ARM and cARM mediated effects is required. Specifically, it is important to investigate the effects of covalency on tumour growth within *in vivo* tumour studies and the feasibility of *in vivo* labeling by cARMs. As such, much remained unknown about cARM behaviour within an *in vivo* model.

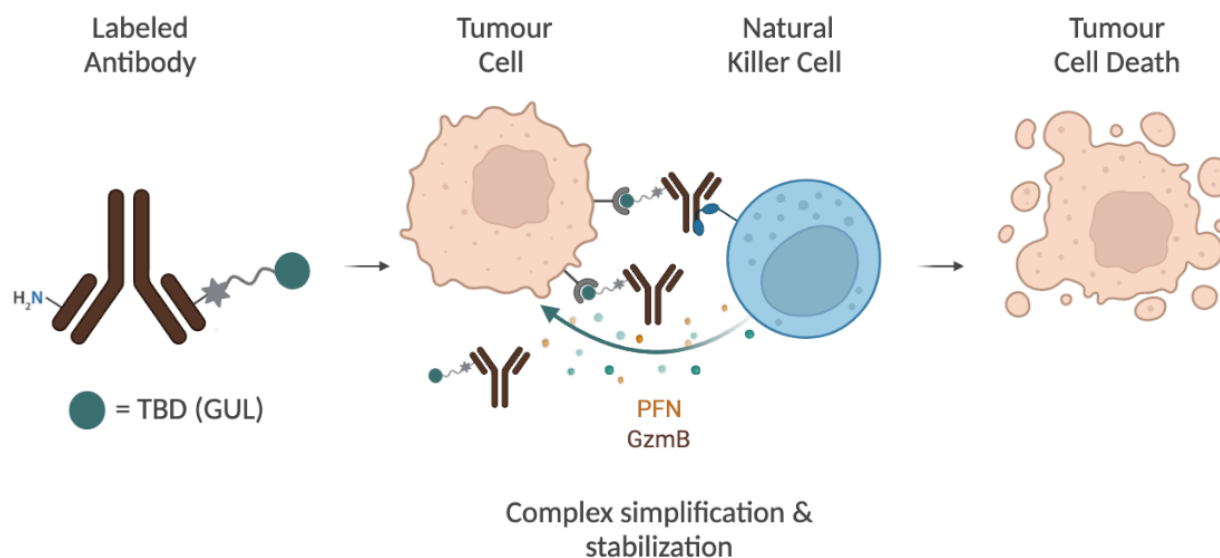


**Figure 1.6. Schematic of cARM function against hPSMA target cells.** The labeled and covalently bound antibody binds to hPSMA expressed on cancer cells. This simplifies and stabilizes ternary complex formation and subsequent quaternary immune active complexes. This machinery is able to recruit immune effector cells to induce antibody-dependent cellular cytotoxicity or antibody-dependent cellular phagocytosis to lyse target cancer cells.



## Chapter 2: Hypothesis & Specific Aims

cARMs display increased therapeutic efficacy *in vivo* when compared to analogous ARMs due to advantageous covalent interactions and effects. Specifically, covalent interactions between cARM and antibody allow for the simplification and stability of the ternary and quaternary complexes thereby resulting in higher cancer cell death, decreased tumour volume and increased survival.

While hPSMA targeting cARMs have been validated in *in vitro* functional assays, they have yet to demonstrate anti-cancer efficacy *in vivo*. As such, this is the next vital step in cARM validation and analysis. The overall goal of this thesis is the development and application of mouse *in vivo* and *in vitro* approaches to evaluate cARM vs. ARM immunotherapeutic efficacy/function and cARM pharmacokinetic properties vs. ARMs.

In this thesis, the above hypotheses were tested through the following specific aims:

1. Develop a mouse model to test anti-tumour efficacy and antibody recruitment of anti-DNP antibodies via ARMs and cARMs
2. Examine ARM vs. cARM efficacy in reducing/delaying tumour growth in a syngeneic hPSMA mouse model
3. Study ARM/cARM - anti-DNP antibody binding kinetics and selectivity *in vivo/in vitro*
4. Enhance and optimize cARM treatment platform utilizing results from previous aims
5. Evaluate Fc dependent target cell killing in mouse *in vitro* assays

## Chapter 3: Results & Discussion

### 3.1 B16hPSMA mouse model development

#### 3.1.1 B16hPSMA Cells

ARMs and cARMs have been designed in the lab to target tumour antigen hPSMA. To develop a mouse model to test these small molecules, mouse cells required sufficient hPSMA expression on the cell surface. As murine cancer cells do not endogenously express this human antigen, cells were transduced to express hPSMA.

To express hPSMA in a mouse cell line for tumour growth in mice, mouse melanoma B16F10 cells were chosen as the tumour model. Following transduction with a plasmid containing the hPSMA gene (Addgene), selection using Blasticidin and polyclonal cell population growth, monoclonal cell lines were cultured. Alongside wildtype (WT) hPSMA, there was also transduction of mutant (L5A) hPSMA to prolong hPSMA expression levels on the cell surface.

Following flow cytometry analysis of all WT and L5A clones, B16hPSMA L5A clone A (**Figure 3.1**) demonstrated the highest hPSMA expression (~400 MFI). Higher hPSMA expression would then allow for increased antibody recruitment and enhanced efficacy. This clone is the only one used in further experiments and in the *in vivo* model.

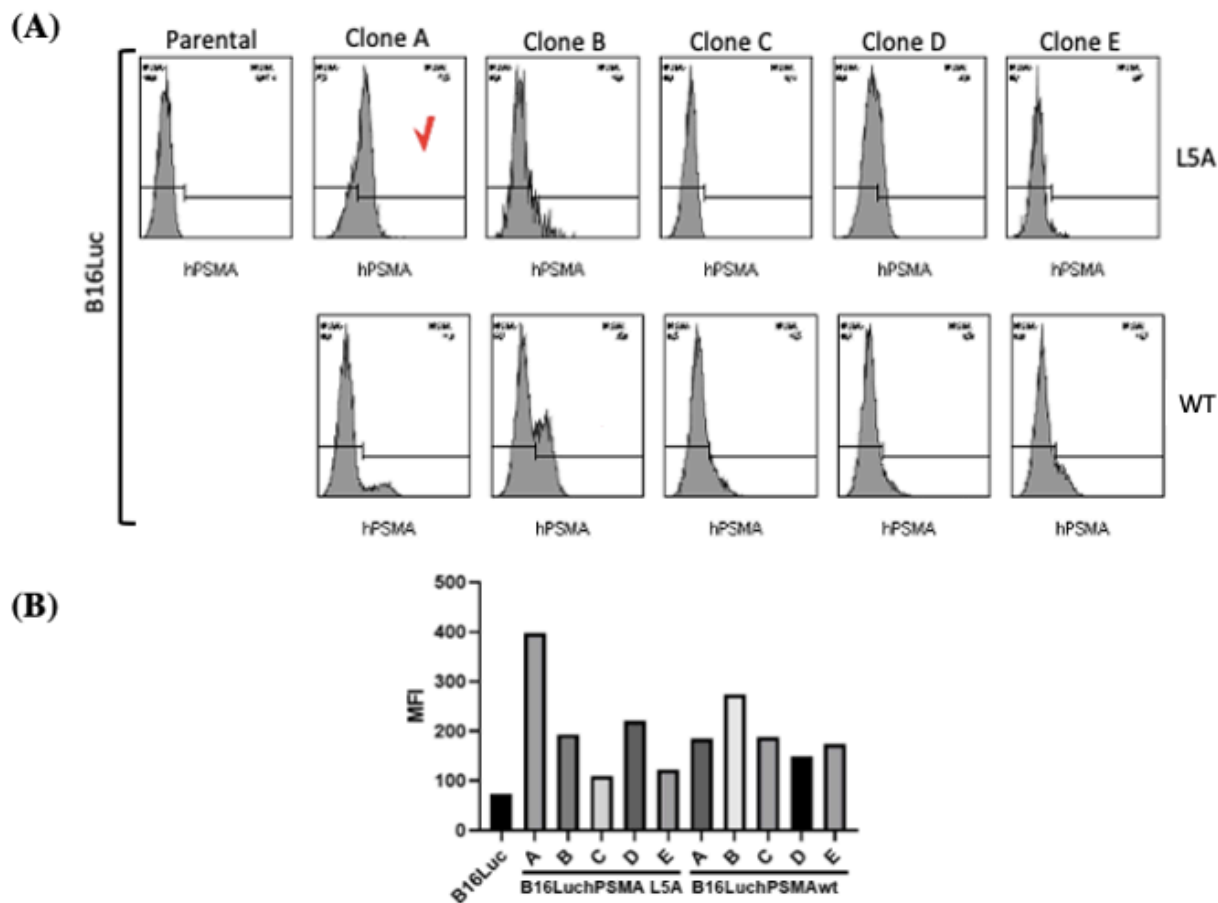


**Figure 3.1. B16hPSMA monoclonal cell line selection.** B16hPSMA monoclonal cell lines were analyzed through flow cytometry to characterize PSMA expression levels. Cells were stained with monoclonal anti-hPSMA antibody (Alexa Fluor 647). **(A)** Flow cytometry results of hPSMA-L5A mutants and hPSMA-WT monoclonal cell lines were compared to negative gated B16 parental cells. The shift in the histograms corresponds to cell populations expressing hPSMA compared to the negative parental populations. **(B)** Mean fluorescence intensity (MFI) of all the monoclonal cell lines cultured when compared with parental B16 cells.

The selected B16hPSMA L5A-A clone was stained with anti-PSMA antibody to confirm hPSMA expression following culturing, prior to tumour cell transplantation (**Figure 3.2**).

Alongside B16hPSMA cells, HEK293hPSMA cells were used as a positive control as they are readily used in the lab due to their high hPSMA expression. Flow cytometry results showed that when compared to parental B16 cells, the transduced B16hPSMA cells displayed higher expression of hPSMA on the cell surface.

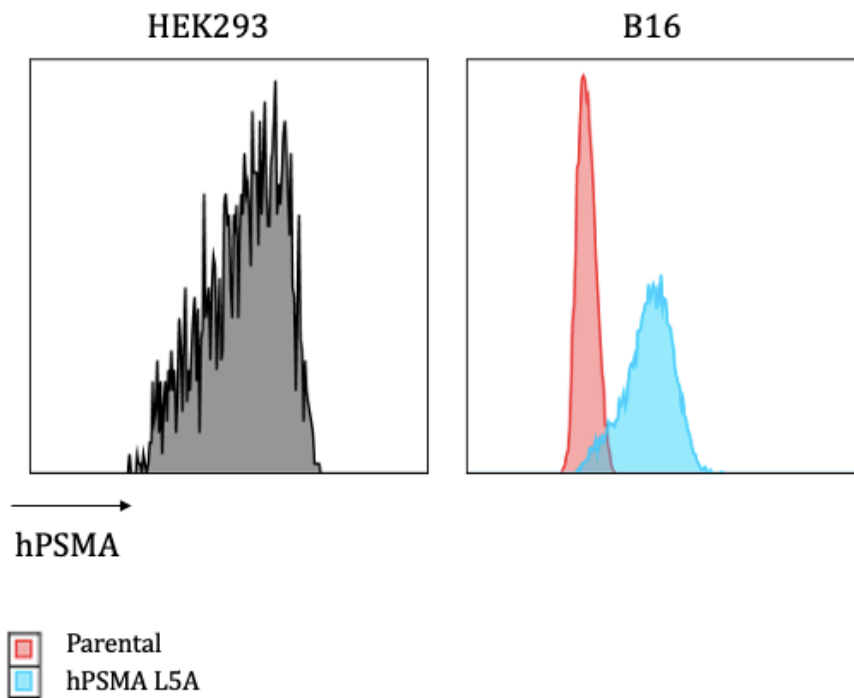


**Figure 3.2. hPSMA staining of chosen cell line.** Flow cytometry results of anti-hPSMA antibody staining to confirm hPSMA expression in transduced cell lines. B16 parental and B16hPSMA cells were stained with anti-hPSMA antibody (AlexaFluor 647) to visualize and confirm hPSMA expression. The parental cell lines were used as a comparative control. HEK293 cells were used as a positive control.

### 3.1.2 B16hPSMA – cARM Binding

As cARM/ARM require binding to tumour cell surfaces via the TBD domain, these molecules need to be able to bind to B16hPSMA cells. Flow cytometry analysis was completed to confirm cARM binding to B16hPSMA expressing cells, (**Figure 3.3**). Anti-DNP antibody (AlexaFluor 647) was incubated with cARM overnight to allow for saturated labeling. B16hPSMA, B16 parental and HEK293hPSMA (positive control) cells were stained with anti-DNP antibody alone to view background staining. Cells were also incubated with labeled anti-DNP antibodies to view cARM binding. Compared to cells that were stained with anti-DNP antibody alone, labeled antibody binding showed increased fluorescence. HEK293hPSMA showed a substantial increase in fluorescence from antibody alone to labeled antibody binding. On the other hand, B16 parental cells showed a very small shift in fluorescence with labeled antibody binding when compared to antibody alone. Comparatively, B16hPSMA cells showed an increased shift in fluorescence which corresponds to cARM binding to hPSMA.

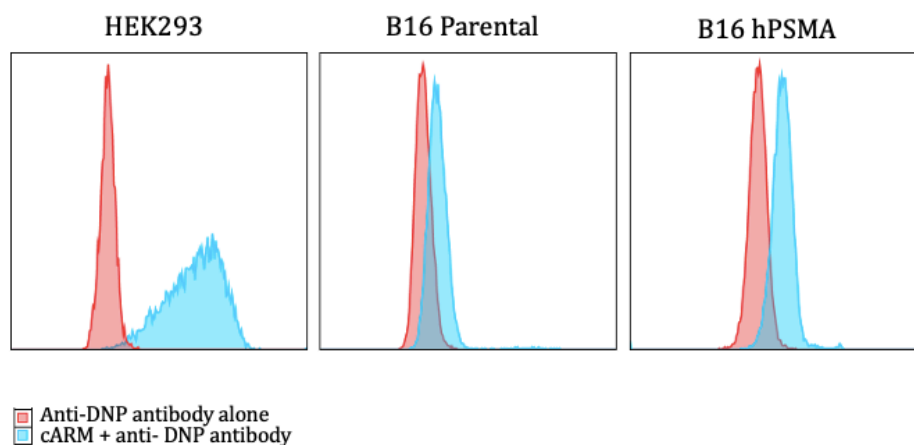


**Figure 3.3. cARM – B16 hPSMA binding.** Flow cytometry results to confirm cARM binding to B16-hPSMA cells. HEK293hPSMA, B16 parental and B16hPSMA (L5A-A) cells were stained with a polyclonal anti-DNP antibody (AlexaFluor 647) alone and cARM labeled anti-DNP antibody. The corresponding shift for each cell line shows the difference in anti-DNP antibody recruitment to cells due to cARM binding. Background staining of anti-DNP antibody is shown in red. HEK293hPSMA cells were used as a positive control and B16 parentals were used as a comparative control.

### 3.1.3 Anti-DNP Antibody Boosting in Mice

*Passive antibody transfer allows for the transfer of anti-DNP antibodies from vaccinated mice into naïve mice.*

Following the development of B16hPSMA cells, the mouse model required sufficient antibody levels. As the ABD domain of ARM and cARM bind specifically to anti-DNP antibodies, mice were vaccinated with DNP to enhance antibody levels. To boost anti-DNP antibody titers in mice, mice were injected with increasing doses of DNP-keyhole limpet hemocyanin (KLH) and monophosphoryl lipid A (MPLA) every other day for a span of two weeks (**Figure 3.4A**).

To confirm anti-DNP antibody presence, mouse serum containing antibodies was run on an enzyme linked-immunosorbent assay (ELISA) wherein DNP-bovine serum albumin (BSA) is immobilized onto plates and acts as a capture antigen. Diluted serum samples from vaccinated and naïve mice were tested on ELISA to view anti-DNP antibody levels. There is an increase in absorbance correlating to increased anti-DNP antibody levels in the vaccinated mice when compared to basally low amounts that were found in naïve mice (**Figure 3.4B**).

To examine if passive antibody transfer would be a viable option to transfer anti-DNP antibodies from vaccinated to naïve mice, naïve mice were injected with DNP boosted serum. ELISA results confirmed that passive antibody transfer works as an alternative to boost anti-DNP antibody levels without the 2-week vaccination period (**Figure 3.4B**). While not reaching anti-DNP antibody levels in vaccinated mice, there was a significant increase in antibody presence in serum from naïve mice with passive antibody transfer.

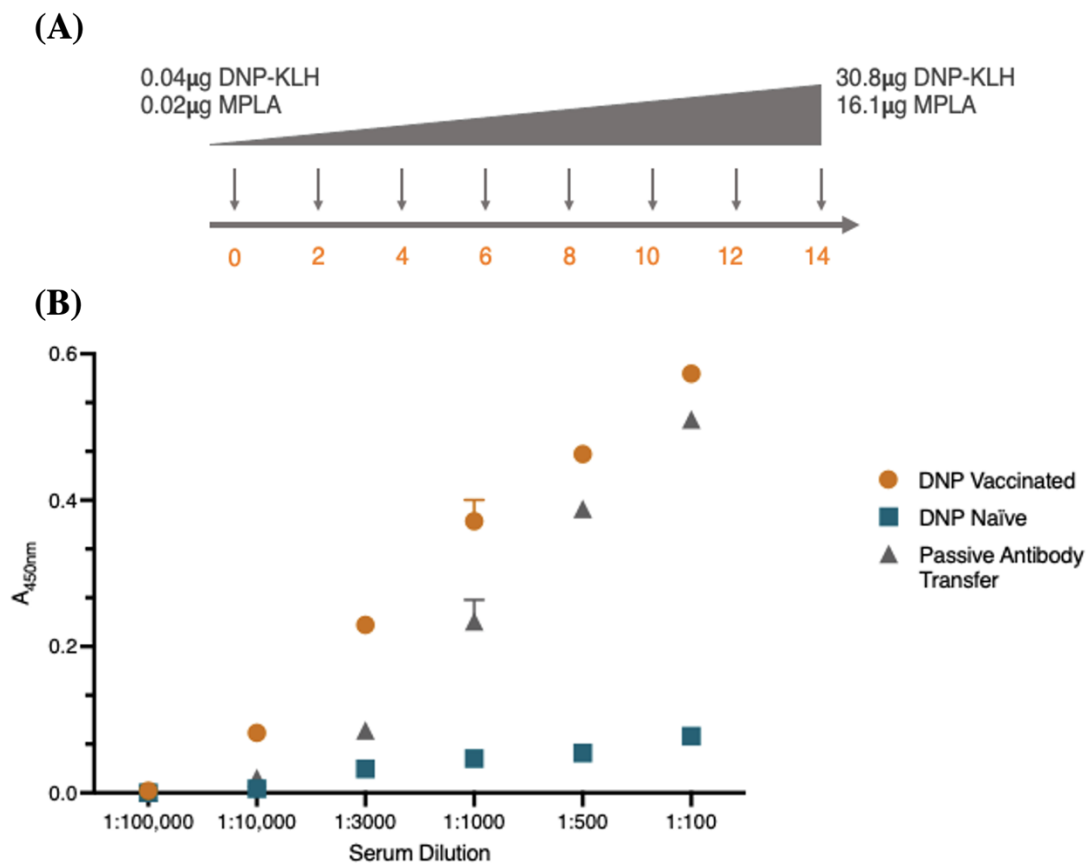


**Figure 3.4. DNP vaccination to boost anti-DNP antibodies.** (A) Mice were injected subcutaneously with increasing doses of DNP-keyhole limpet hemocyanin (KLH) and increasing doses of monophosphoryl lipid A (MPLA – adjuvant) on the indicated days. (B) DNP-immobilized ELISA results showing anti-DNP antibody presence in serum samples of DNP vaccinated and naïve mice. Naïve mice that were injected with serum from vaccinated mice are shown as passive antibody transfer samples. Anti-DNP antibodies presence is depicted as absorbance at 450nm.

To quantify anti-DNP antibody concentrations, an ELISA standard curve was developed (**Figure 3.5**). Quantitation analysis revealed that DNP vaccination yielded  $\sim 35\mu\text{M}$  boosted anti-DNP IgG in vaccinated mice. Similarly, mice that received passive antibody transfer displayed  $\sim 30\mu\text{M}$  boosted anti-DNP IgG in circulation.

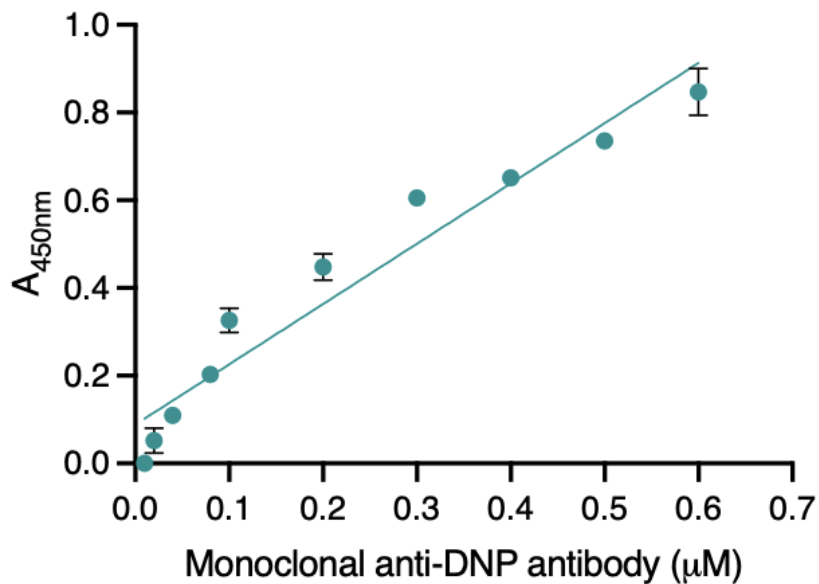


**Figure 3.5. Anti-DNP antibody ELISA standard curve.** A standard curve via DNP-immobilized ELISA was developed using mouse monoclonal anti-DNP antibody.  $R^2 = 0.9364$ , Equation of line of best fit:  $Y = 1.375x + 0.08845$ .



### 3.1.4 B16hPSMA Tumour Growth in Mice

#### ***Depletion of CD8+ T-cells allows for B16hPSMA tumour growth in mice. CD8+ T cell and CD20 depletion allows for NK cell expansion.***

Following the development of B16hPSMA cells as well as anti-DNP antibody vaccination platforms, mice were challenged with B16hPSMA tumours. Two groups of mice (female C57BL/6, n=5) were vaccinated to enhance anti-DNP antibody levels and received 200,000 B16hPSMA cells intradermally. PBS mice (**Figure 3.6A**) acted as the negative control and received 200 $\mu$ L of PBS 3x weekly. The cARM treatment group (**Figure 3.6B**) was dosed 3x weekly with 200 $\mu$ L of 10 $\mu$ M cARM ( $\sim$ 1 $\mu$ M *in vivo* concentration). Both tumour volume and survival were monitored. Tumour volume as well as survival between both groups were similar. Most importantly, at days 7-10, both groups displayed spontaneous tumour regression. By day 20, most mice were completely tumour free.

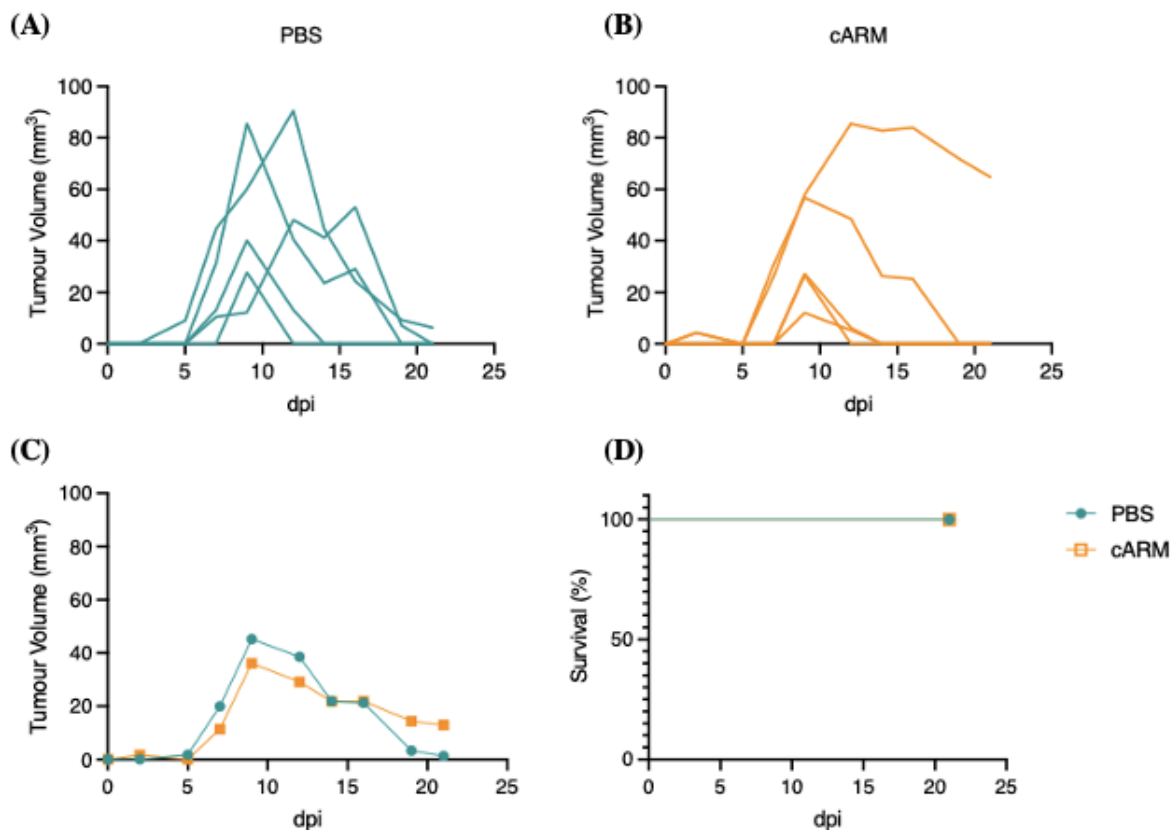


**Figure 3.6. cARM effect on tumour volumes.** B16hPSMA tumour volumes (mm<sup>3</sup>) were assessed at the indicated time points.  $2 \times 10^5$  B16hPSMA cells were intradermally injected into the back of all mice and tumours were measured for 21 days post implantation (dpi). B16hPSMA tumour-bearing mice were treated with 200 $\mu$ L of PBS or 200 $\mu$ L of  $\mu$ M cARM (1 $\mu$ M in mouse blood) intravenously 3x times a week starting from the day of tumour cell implantation. **(A)** Individual mouse (n=5, mice) tumour volumes compared to dpi. **(B)** Individual mouse (n=5) tumour volumes compared to dpi from the cARM treatment group. **(C)** Averages of tumour volumes in cARM and PBS groups. **(D)** Survival curve of PBS and cARM groups.

To examine if the spontaneous tumour regression was mediated by an adaptive immune response against hPSMA, we studied the effects of CD8<sup>+</sup> T cells against hPSMA as well as the effects of increasing the number of tumour cells during implantation. Tumour bearing mice received increased amounts of B16hPSMA cells as well as CD8<sup>+</sup> T cell depleting antibody (n=2). Mice that received only increased amounts of tumour cells displayed previously observed spontaneous tumour regression (**Figure 3.7A**). Mice received 500,000 - 1,000,000 B16hPSMA cells and all mice were able to reject tumour growth. Consequently, none of these mice reached endpoint (1000mm<sup>3</sup>) (**Figure 3.7B**). Conversely, mice that received tumour cells along with 100µg of anti-CD8 depletion antibody on days 0 and 10, displayed high tumour volumes reaching endpoint. Two groups received CD8<sup>+</sup> T cell depleting antibody as well as increasing amounts of tumour cells (200,000 & 500,000 cells). Both groups, regardless of tumour cell amounts, displayed similar results.

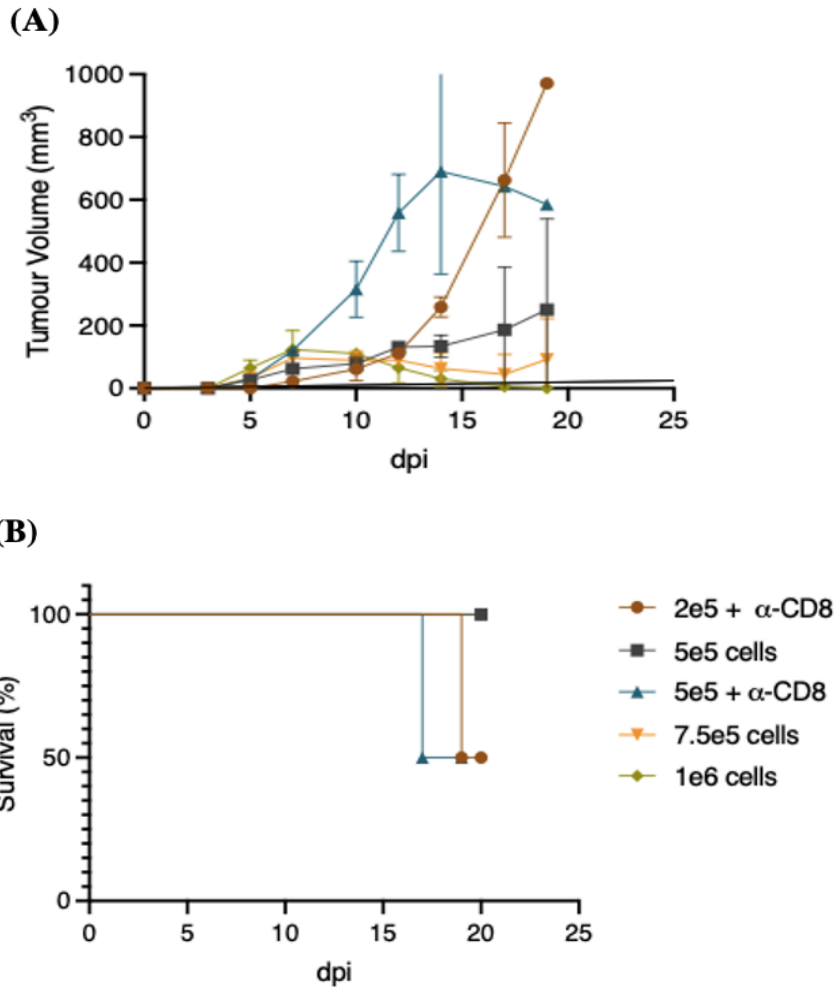


**Figure 3.7. Mitigating effects of B16hPSMA tumour regression. (A)** Averages tumour volumes in mice groups (n=2) of increasing B16hPSMA cells/CD8+ T cell depletion (100µg). Mice received two doses of depletion antibody on days 0 and 10. Volumes are shown as mean with SD **(B)** Survival curve of all indicated mouse groups.

To confirm immune cell levels in depleted mice, mice were given anti-CD8, as well as anti-CD20 depletion antibodies (from later studies). Blood samples were taken 1 week post depletion and analyzed to examine at CD8+, CD19+ and NK1.1+/CD27+ lymphocyte levels (**Figure 3.8A-C**). As a substantial mechanism of action against B16hPSMA in cARM treated mice is hypothesized to be ADCC, NK cell levels were assessed in depleted and non-depleted mice.

CD8+ T cell population was found at 10% in untreated mice (**Figure 3.8A**) whereas it was found at 0% in mice that were given with CD8+ T cell depletion antibody as well as mice that were given with both CD8 and CD20 depletion antibodies. CD20+ B cell population was found at ~50% in untreated mice and increased to 60% in mice treated with CD8+ T cell depletion antibody (**Figure 3.8B**). B cells were found at 0% in mice that were co-depleted with anti-CD8 and anti-CD20 depletion antibodies. Lymphocytes were also stained for NK1.1 and CD27 markers to view NK cell populations compared to total cell populations (**Figure 3.8C**). Untreated mice displayed 2.5% NK cells whereas mice that were depleted with anti-CD8 depletion antibody increased to 5% NK cells. Finally, mice that were co-depleted displayed increased levels of NK cells (~10%) when compared to untreated or CD8+ T cell depletion alone.

Results showed that when mice are depleted of specific lymphocyte populations, other populations increased. In the case of singular depletion (CD8+), B cell levels and NK cells levels increased by 10% and 2.5% respectively when compared to untreated mice. Similarly, when mice are co-depleted of two lymphocyte populations, NK cell levels increased ~8% from untreated mice.

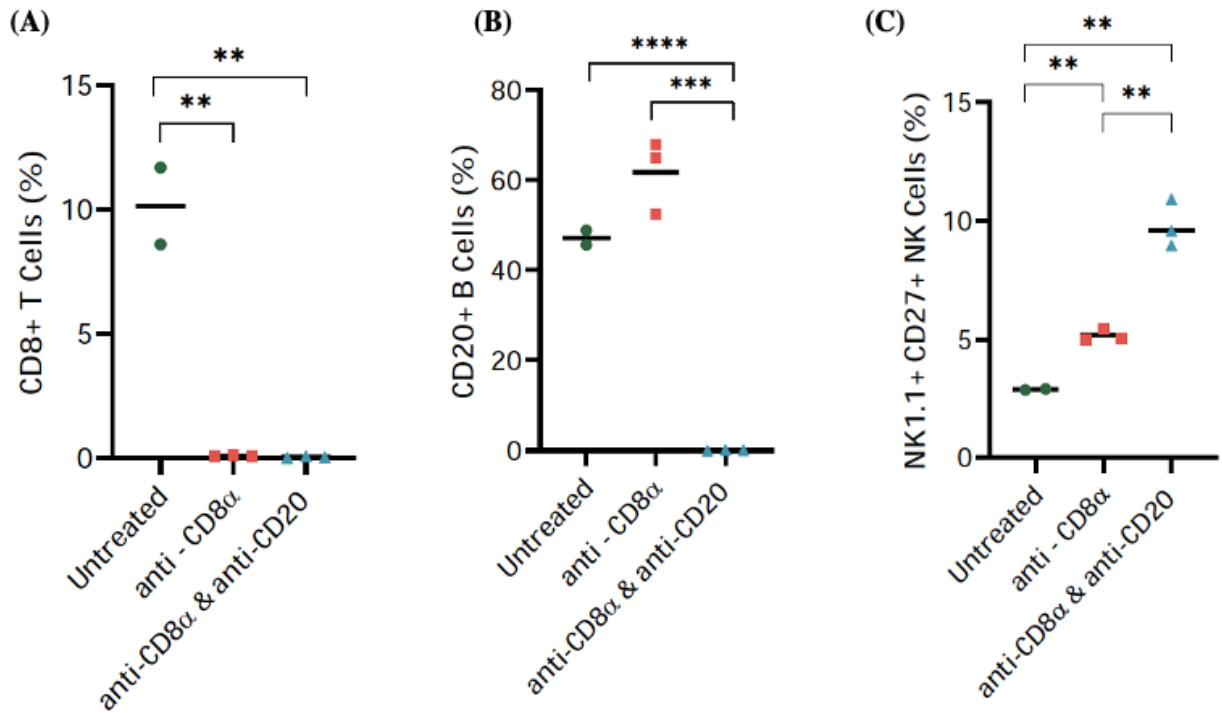


**Figure 3.8. Immune cell presence in depleted vs. untreated mice. (A)** CD8+ T cell (%) in blood samples of mice in the absence of depletion, CD8+ T cell depletion and CD8 & CD20 co-depletion. **(B)** % of CD20 B cells in blood samples of mice in the absence of any depletion, CD8+ depletion and CD8+ depletion with CD20 depletion in conjunction. **(C)** NK 1.1+ CD27+ NK cells (%) in blood of mice with no depletion, CD8+ T cell depletion and co-depletion with CD8 and CD20. Data in A-C represent each mouse as individual values and are shown with the mean. \*\* $P < 0.01$ , \*\*\* $P < 0.001$  and \*\*\*\* $P < 0.0001$  by 2-tailed Student's *t* test.

### 3.1.5 Mouse Model Development - Discussion

To evaluate ARM and cARM function and efficacy *in vivo*, we aimed to develop a mouse model to test these molecules. B16 cells required adequate hPSMA expression for ARM/cARM function. Additionally, we intended to maximize hPSMA expression on cell surfaces by limiting protein internalization. Previous literature demonstrated that the N-terminal amino acids MWNLL within hPSMA mediate internalization<sup>85</sup>. Specifically, the methionine and leucine residues were shown to be essential for internalization and incorporation of an alanine residue at the 5-leucine significantly reduced hPSMA internalization<sup>85</sup>. Importantly, mutations made in the cytoplasmic tail have no effect on ARM/cARM binding via the TBD as these residues are not near the binding site. As such, alongside the transduction of WT hPSMA, clones containing hPSMA L5A mutants were co-cultured.

While there was a range of hPSMA expression on monoclonal B16 populations, one of the L5A clones had the highest hPSMA expression. This clone was chosen for future work and for use *in vivo* as maximal hPSMA expression should yield maximal ARM/cARM efficacy. As increased hPSMA expression will allow for more ARM and cARM mediated antibody recruitment, ternary complex, and subsequent quaternary complex formation. Comparative analysis of hPSMA expression on transduced B16hPSMA cells to HEK293hPSMA cells showed successful hPSMA expression. However, B16hPSMA cells did not express hPSMA as highly as HEK293hPSMA cells which have been successfully used in the lab due to their high hPSMA expression. This could play an important role in the efficacy of ARMs as higher cancer protein expression allows for high avidity binding of ARMs to hPSMA and antibody<sup>81</sup>. This effect enhances binding of molecules to the tumour cell surface and influences quaternary complex stability. Conversely, lower target protein expression prevents avidity interactions<sup>81</sup>. While

cARMs do not require high avidity interactions due to covalent stabilization, lower hPSMA expression results in decreased numbers of immune active complexes for clustering and subsequent immune mediated killing<sup>81</sup>.

Following the development and validation of B16hPSMA cells, cARM binding was analyzed. The data suggest that labeled anti-DNP antibodies are capable of binding to B16hPSMA cells. When compared with B16 parental cells, there was increased binding of cARM labeled antibody to transduced cells. This increase in binding could be correlated with hPSMA expression on cell surfaces. However, when compared to HEK293hPSMA cells, B16hPSMA cells displayed less cARM binding. This is likely due to enhanced hPSMA expression on HEK293 cells.

DNP vaccination successfully boosted anti-DNP antibody titers in mice. Mice underwent prolonged exposure to DNP-KLH and MPLA, which acted as an adjuvant. This vaccination platform combined extended antigen exposure and exponentially increasing doses to augment vaccination responses<sup>86</sup>. It was shown that increasing antigen doses resulted in enhanced and prolonged antigen retention within lymph nodes. This dosing method was also observed to amplify the germinal center response<sup>86</sup>. As such, vaccinated mice displayed significantly increased anti-DNP antibody titers. Quantitation of ELISA absorbance reading using standard curve analysis yielded a boosted anti-DNP IgG concentration estimation of  $\sim 35\mu\text{M}$ . Previous work in DNP immunization in mice yielded  $\sim 23\mu\text{M}$  boosted anti-DNP IgG<sup>80</sup>. As such, this augmented vaccination protocol produced increased levels of anti-DNP IgG compared to previous attempts. Naïve mice displayed basally low anti-DNP antibody titers, suggesting that mice do endogenously express this antibody. Mice that received passive antibody transfer via DNP boosted serum displayed similar anti-DNP antibody titers to DNP vaccinated mice.



Quantitation of standard curve analysis provided a concentration estimation of  $\sim 30.68 \mu\text{M}$  of anti-DNP IgG in circulation. It was found that sera from immunized mice offered a high degree of protection in unimmunized mice<sup>87</sup>. This correlates with observed anti-DNP antibody passive immunity and the data implies that passive antibody transfer is a viable and successful approach to transfer antibodies into naïve mice. This approach provides a treatment advantage wherein mice can be injected with pre-formed antibody-ARM/cARM complex. Furthermore, mice do not need to undergo the 2-week vaccination period.

B16hPSMA tumours did not successfully grow in C57BL/6 mice. Following tumour cell implantation, both treatment and PBS groups displayed spontaneous tumour regression occurring 7-10 dpi. This posed a serious concern wherein tumour growth was not substantial enough to view anti-tumour effects via our treatment. To probe this further, we hypothesized immunogenicity against hPSMA could be implicated in the observed tumour rejection. Previous work utilizing hPSMA in mouse *in vivo* tumour studies were completed using NOD/SCID and hu-PBL-SCID mice and displayed robust tumour growth<sup>64,88</sup>. This could imply that hPSMA tumour growth in mice required a lack of immune response. Studies in mice have shown that early immune responses occur in the first 5 days followed by an adaptive immune response from days 5-14<sup>89</sup>, correlating with the days of tumour regression observed in hPSMA tumour bearing mice. Further analysis revealed that mouse PSMA (mPSMA) and hPSMA share 86% sequence identity, as such, differences in sequence identity or protein folding could result in a mounted immune response against hPSMA that prevents tumour growth<sup>90</sup>. To overcome this, we attempted to stimulate tumour growth by increasing the amount of tumour cells and utilized CD8+ T cell depletion. We observed tumour regression in mice that solely received  $5 \times 10^5$ ,  $7.5 \times 10^5$  and  $1 \times 10^6$  B16hPSMA tumour cells. While increasing the amount of tumour cells

proved to be unsuccessful, treatment with anti-CD8 monoclonal antibodies caused robust B16hPSMA tumour growth in mice. Mice that received  $2 \times 10^5$  or  $5 \times 10^5$  B16hPSMA tumour cells along with anti-CD8 depletion antibody reached endpoint by 17-20 dpi. This data suggests that a CD8<sup>+</sup> T cell response could be present against hPSMA post tumour cell implantation. While CD8<sup>+</sup> T cell depletion solved the issue of tumour growth, this results in a lack of cytotoxic T cell function in tumour bearing mice treated with cARM/ARM. This limitation would result in less efficacious anti-tumour effects as we would expect some T cell involvement mediated by innate immune cells recruited by ARM/cARM. While mPSMA was a consideration for use instead of hPSMA, there were a few limitations with this approach. Firstly, cARM and ARM contain GUL on the TBD as the binding partner of hPSMA. GUL competitively binds to the enzymatic active site and is strengthened by a specific arene-binding cleft within hPSMA and this interaction has been validated in literature using crystal structures and modeling<sup>78</sup>. mPSMA currently has no published crystal structure available, consequently, it was not possible to confirm cARM/ARM binding to mPSMA through modelling. While hPSMA protein expression patterns are varied between human and mouse, enzymatic function remains largely the same<sup>91</sup>. As such, conserved sequences at the active site could allow for cARM/ARM binding. However, hPSMA expressing B16 cells had been developed and validated for use. Additionally, the final goal of ARM/cARMs is the treatment of human disease with human proteins. As such, hPSMA optimization was prioritized. Thus, while we decided to utilize hPSMA expressing cells, it is important to note that data will not reflect fully intact immune responses as CD8<sup>+</sup> T cells were depleted to allow for tumour growth. Nevertheless, future work may focus on utilizing mPSMA to view fully intact immune responses mediated by ARM/cARM as the lab is currently developing B16mPSMA cells for binding validation and use. Conversely, transgenic adenocarcinoma mouse prostate

(TRAMP)-C2 cells have demonstrated endogenous mPSMA expression and is a possible alternative mouse model to test PSMA targeting ARM/cARM<sup>92</sup>.

Following CD8<sup>+</sup> T cell and CD20<sup>+</sup> B cell depletion, NK cell population increased in peripheral blood. NK1.1<sup>+</sup>/CD27<sup>+</sup> NK cell populations were shown to increase in mice that were depleted of CD8<sup>+</sup> T cells by 2%. Furthermore, NK cell populations increased by 8% in mice that were depleted of both CD8<sup>+</sup> T cells and B cells. Previous work highlighted that NK cell populations significantly increased following CD8<sup>+</sup> T cell depletion by utilizing the immune space previously taken by CD8<sup>+</sup> T cells<sup>93</sup>. Specifically, CD27<sup>+</sup> populations were examined as murine CD27<sup>high</sup> NK cells have been shown to exhibit powerful cytokine production, increased migratory abilities and higher cytotoxic function<sup>17</sup>. This data suggests that by depleting mice of CD8<sup>+</sup> T cells, lymphocyte repopulation results in the increase of CD27<sup>high</sup> cytotoxic NK cells. As such, this effect could inadvertently play a role in enhancing the ADCC effects mediated by cARM/ARM.

Alongside hPSMA, there are many tumour-specific antigens that cARMs/ARMs can be designed to bind to. Multiple cancers including breast, ovarian, colon etc. display up-regulated folate receptors (FOLR)<sup>94</sup>. As such, FOLR makes a promising tumour target. The lab has produced molecules that contain folic acid on the TBD to target folate receptor. To test these molecules, a mouse model needs to be developed. Development of this mouse model may involve enhancing FOLR expression on mouse tumour cells however, an important consideration is immunogenicity. As seen with the hPSMA mouse model, immune responses prevented hPSMA tumour growth in mice. As such, confirming that folate binding ARM/cARMs can bind to mFOLR would be an important step. To identify a cell line that endogenously expresses mFOLR, we tested 4T1 murine breast cancer cells. These cells were examined for mFOLR

expression alongside two known FOLR expressing human cell lines (**Supplementary Figure 5.6**). Future work using alternative tumour antigens could provide a robust profile of ARM and cARM efficacy.

### **3.2 Examine cARM/ARM efficacy in reducing/delaying tumour growth in mouse model**

#### **3.2.1 ARM Efficacy against B16hPSMA Tumours**

*ARM treated mice demonstrated significantly improved survival compared to PBS controls.*

Once the mouse model was developed with the use of anti-CD8 depletion antibody, we tested ARM function against B16hPSMA tumours (**Figure 3.9**). ARMs were used in this preliminary study as they have been publishing in previous literature and serves as a method to test our mouse model. Four groups (n=5) were used in this study – 2 groups were vaccinated to boost anti-DNP antibody levels and 2 groups were non-vaccinated/naïve groups. All mice following the same treatment regimen (**Figure 3.9A**). The first vaccinated group acted as the negative control and received 200 $\mu$ L of PBS every other day (**Figure 3.9B**). All mice within the PBS group displayed exponential tumour growth and all mice reached endpoint (1000mm<sup>3</sup>) within 22 days (**Figure 3.9G**). The second vaccinated group was treated with injections of 200 $\mu$ L of 10 $\mu$ M ARM every other day (**Figure 3.9C**). Individual tumour volumes were varied among the mice but when compared to PBS mice, showed a slight delay in growth. This group displayed significantly improved survival when compared to PBS control mice.

The first naïve group received injections of 200 $\mu$ L of 10 $\mu$ M ARM every other day (**Figure 3.9D**). This group displayed similar tumour growth patterns as the PBS control mice and displayed no improved survival. The second naïve group received treatments of 200 $\mu$ L of 10 $\mu$ M pre-formed ARM/antibody complex every other day (**Figure 3.9E**). ARM was pre-incubated overnight with serum from vaccinated mice to allow for saturated anti-DNP antibody binding. This group showed a slight delay in tumour growth when compared to PBS control mice. These mice also displayed significantly improved survival when compared to PBS mice.

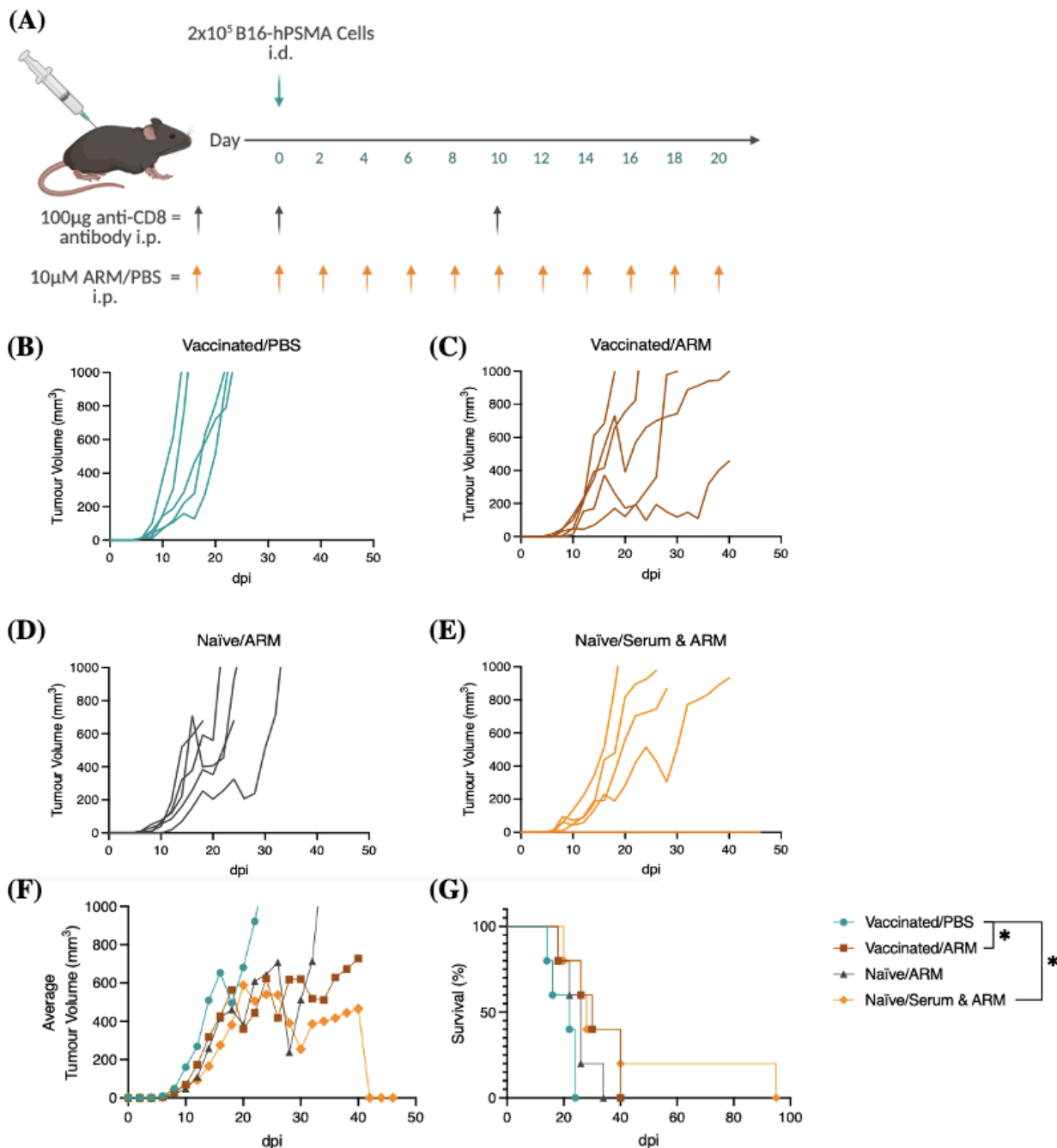


**Figure 3.9. ARM anti-tumour effects on B16hPSMA tumours.** (A) Treatment regimen & dosing. (B-E) Individual B16hPSMA tumour volumes (mm<sup>3</sup>) of mice (n=5) were assessed on the indicated days post implantation (dpi) (B) Tumour growth in DNP vaccinated mice treated with PBS. (C) Tumour growth in DNP vaccinated mice treated with 200µL of 10µM ARM for *in vivo* concentration of ~1µM. (D) Tumour growth in naïve mice treated with 200µL of 10µM ARM for *in vivo* concentration of ~1µM. (E) Tumour growth in naïve mice treated with anti-DNP vaccinated mouse serum incubated with 10µM ARM prior to injection. (F) Average tumour volumes in each treatment group measured on the days indicated. (G) Survival of B-E. Endpoint was measured at tumour ulceration or growth reaching 1000mm<sup>3</sup>. \*P<0.05 by log-rank (Mantel-Cox) test.

***ARMs function in an antibody dependent manner.***

To confirm the antibody dependent functionality of ARMs, naïve mice were depleted of B cells, tumour challenged and then treated with ARM alone (n=5). All mice followed the same treatment regimen (**Figure 3.10A**). The first group was depleted of all B cells and treated with 200µL of PBS every other day (**Figure 3.10B**); this group acted as the negative control. The second group underwent B cell depletion and was treated with 200µL of 10µM ARM every other day (**Figure 3.10C**) The final group was not depleted of B cells and was treated with 200µL of 10µM ARM every other day (**Figure 3.10D**). All groups contained unvaccinated mice and no passive antibody transfer was used to confirm that ARMs do not function independently of anti-DNP antibodies. There was no apparent difference in tumour volume or growth between any of the groups. All mice within the groups reached endpoint by day 21 and none displayed improved survival (**Figure 3.10F**).

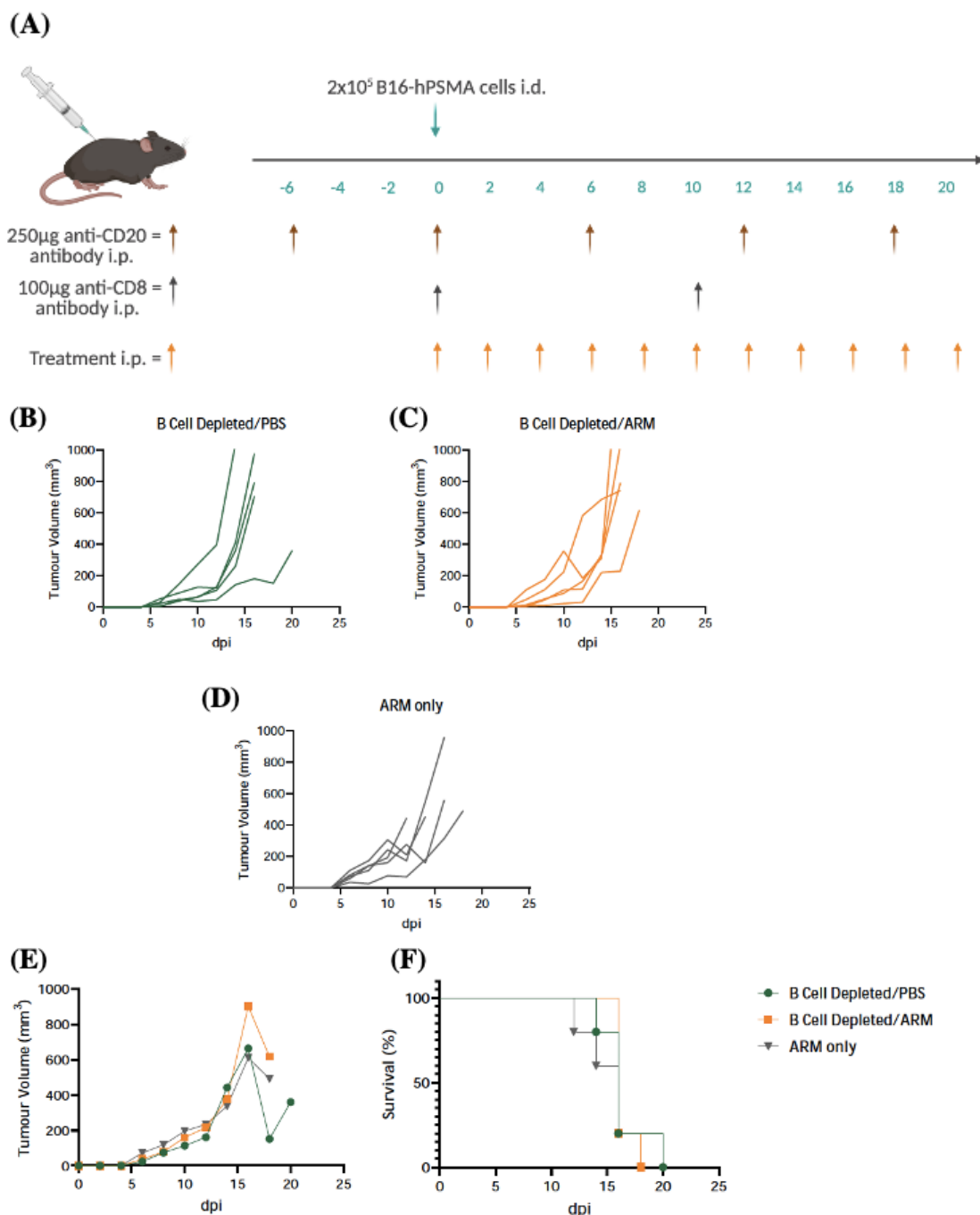


**Figure 3.10. B cell depletion effects on ARM efficacy.** (A) Treatment regimen and dosing. (B-D) Individual B16hPSMA tumour volumes (mm<sup>3</sup>) of mice (n=5) were assessed on the indicated days post implantation (dpi). (B) Individual tumour volumes in mice that were depleted of B cells with anti-CD20 antibodies treated with PBS. (C) Individual tumour volumes in B cell depleted mice treated with 200µL of 10µM ARM. (D) Individual tumour volumes treated with 200µL of 10µM ARM. (E) Average tumour volumes in each treatment group. (F) Survival of B-D.



### 3.2.2 cARM & ARM Efficacy against B16hPSMA Tumours

#### *cARM and ARM treated mice showed significantly improved survival.*

Following the analysis of ARM function and efficacy against B16hPSMA tumours, we next tested the effects of covalency by using cARM alongside ARM. None of the groups underwent prior DNP vaccination and all treatments used passive antibody transfer (n=2-4). All mice followed the same treatment regimen but varied in treatment dosing concentration (**Figure 3.11A**). The first group received 200 $\mu$ L of PBS every other day and acted as the negative control (**Figure 3.11B**). These mice did not survive past 14 dpi – all mice in the group had severe tumour ulceration and had reached endpoint.

There were two ARM treated groups – these were dosed with different concentrations of ARM. The first group received 200 $\mu$ L of 10 $\mu$ M pre-formed ARM/DNP boosted serum (*in vivo* concentration of  $\sim$ 1 $\mu$ M) every other day (**Figure 3.11C**). This group displayed a slight delay in tumour growth when compared to PBS control mice however did not display improved survival. The second group received 200 $\mu$ L of 1 $\mu$ M pre-formed ARM/DNP boosted serum (*in vivo* concentration of  $\sim$ 0.1 $\mu$ M) (**Figure 3.11D**). There was a slight delay in tumour growth within this group compared to PBS mice. Importantly, this group displayed significant improved survival compared to negative control mice.

The two cARM treated groups received two different concentrations of cARM every other day (**Figure 3.11E-F**). The first group received 200 $\mu$ L of 10 $\mu$ M cARM labeled DNP boosted serum (*in vivo* concentration of 1 $\mu$ M cARM) displayed significantly improved survival when compared to PBS mice (**Figure 3.11H**). Conversely, the second cARM treatment group received 200 $\mu$ L of 1 $\mu$ M cARM labeled DNP boosted serum (*in vivo* concentration of 0.1 $\mu$ M cARM) and displayed no improvement in survival.

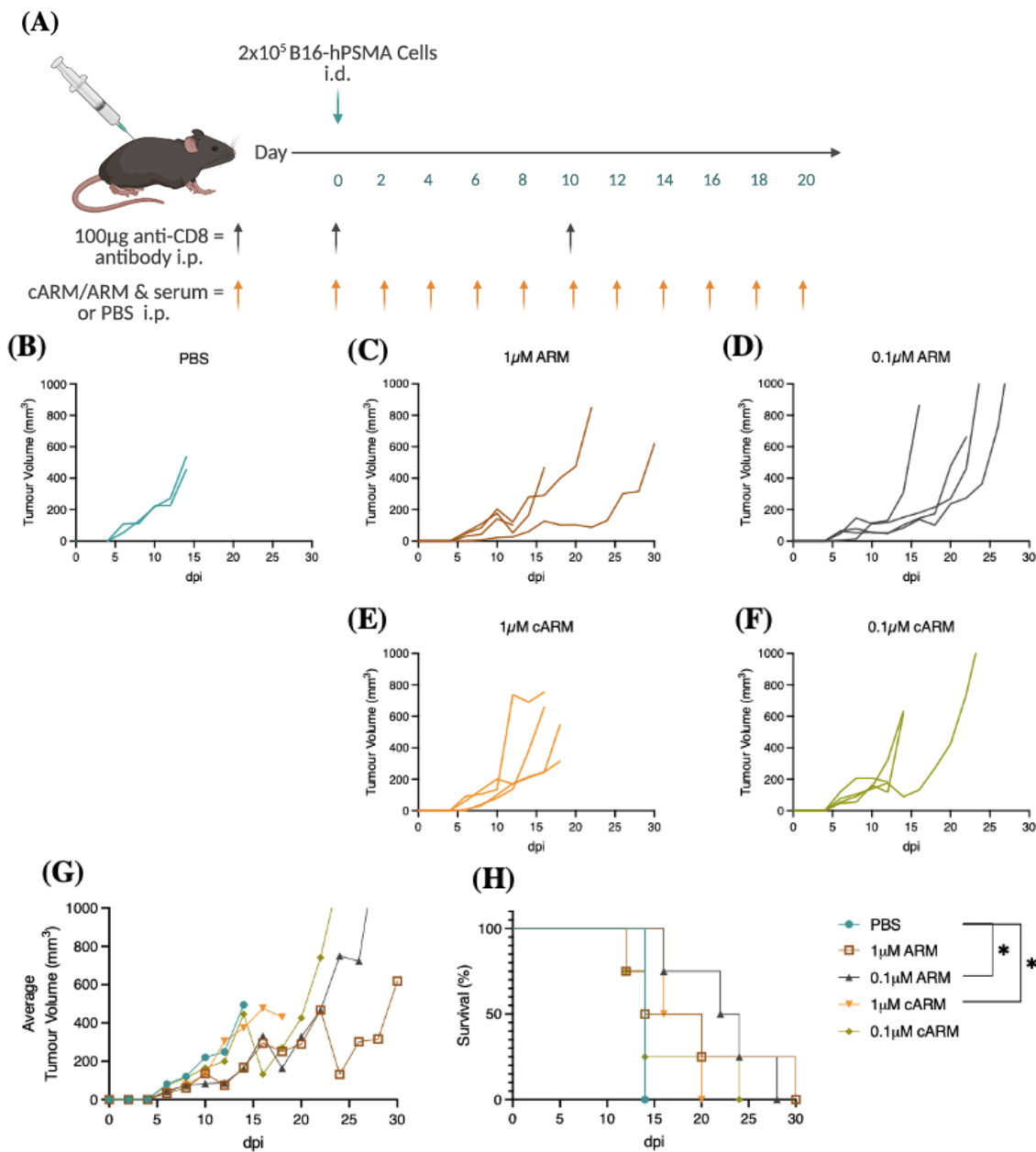


**Figure 3.11. cARM vs. ARM effects on B16hPSMA tumours.** (A) Treatment regimen and dosing. (B-F) Individual B16hPSMA tumour volumes ( $\text{mm}^3$ ) of mice ( $n=2-4$ ) were assessed on the indicated days post implantation (dpi) (B) Tumour growth in mice treated with PBS. (C) Tumour growth in mice treated with pre-incubated complex of  $200 \mu\text{L}$  of  $10 \mu\text{M}$  ARM + vaccinated DNP serum for *in vivo* concentration of  $\sim 1 \mu\text{M}$ . (D) Tumour growth in mice treated with pre-incubated complex of  $200 \mu\text{L}$  of  $1 \mu\text{M}$  ARM + vaccinated DNP serum for *in vivo* concentration of  $\sim 0.1 \mu\text{M}$ . (E) Tumour growth in mice treated with pre-labeled complex of  $10 \mu\text{M}$  cARM + vaccinated DNP serum for *in vivo* concentration of  $\sim 1 \mu\text{M}$ . (F) Tumour growth in mice treated with pre-labeled complex  $1 \mu\text{M}$  cARM + vaccinated DNP serum for *in vivo* concentration of  $\sim 0.1 \mu\text{M}$ . (G) Average tumour volumes in each treatment group measured on the days indicated. (H) Survival of B-F. Endpoint was measured at tumour ulceration or growth reaching  $1000 \text{mm}^3$ . \* $P < 0.05$  by log-rank (Mantel-Cox) test.

### 3.2.3 ARM/cARM Efficacy – Discussion

Following the development of the B16hPSMA mouse model, we examined the efficacy of hPSMA binding ARM. Initial *in vivo* attempts utilized ARM as the treatment platform as it has been extensively studied in literature and provided a basis in which to test treatment conditions, dosing, and concentrations. Two groups of mice were DNP vaccinated to produce anti-DNP IgG antibodies while two groups remained unvaccinated. Following B16hPSMA tumour cell transplantation, mice received treatment starting on the day of transplant and continued every other day until mice reached endpoint. Tumour bearing mice treated with ARM and sufficient anti-DNP antibody levels displayed significantly improved survival. Specifically, DNP vaccinated mice treated with ARM displayed a slight delay in tumour growth and significantly improved survival (median survival = 30 days) when compared to PBS controls (median survival = 22 days). Conversely, naïve mice treated with ARM displayed no improvement in survival (median survival = 26 days). This implies that sufficient anti-DNP antibody titers are required for an ARM mediated response. The data also suggests that ARM function is dependent on specific antibodies wherein ARMs require circulating anti-DNP antibodies. Naïve mice that were treated with ARM and DNP boosted serum displayed a slight delay in tumour growth and significantly improved survival (median survival = 28 days). As this group displayed similar results to the vaccinated/ARM treatment group, this suggests that mice can be treated using passive antibody transfer. This approach offers a therapeutic advantage. As DNP boosted serum was pre-incubated with ARM, this allowed for the formation of ARM-antibody complexes *ex vivo*. Treatments using pre-bound or pre-labeled antibodies permitted mechanistic simplification of immune complexes and controlled dosing. This work represents the preliminary *in vivo* examination of hPSMA targeting ARMs developed in the lab. Importantly, the survival we observed in vaccinated mice treated with ARM and naïve mice treated with ARM + passive antibody

transfer are comparable to previous work in literature that examined uPAR targeting ARMs<sup>65</sup>. Specifically, uPAR-ARM treated mice displayed a median survival of 28-30 days, correlating with the median survival seen in hPSMA targeting ARMs<sup>65</sup>. Furthermore, uPAR-ARMs were used in vaccinated mice and passive antibody transfer was not used to mediate pre-formed complex formation. As such, these results demonstrated the efficacy of ARMs in recruiting anti-DNP antibodies *in vivo* to hPSMA expressing tumour cells and validated the efficiency in utilizing pre-formed complexes.

Further investigation into ARM mediated effects revealed that ARMs function in an antibody dependent manner. When naïve mice were depleted of B cells and treated with ARM, there was no decrease in tumour volume and no improvement in survival. Similarly, naïve mice that were not B cell depleted and treated with ARM displayed no improvement in survival or reduced tumour growth. Previous work demonstrated that B cell depletion decreased humoral immune responses, decreased memory B cell levels and reduced antibody development to recall antigens<sup>95</sup>. It was observed that all naïve mice treated with ARM alone did not display any anti-tumour effects in the absence of sufficient anti-DNP antibody presence. This implies that ARMs may not function independent of anti-DNP antibodies.

Following the testing of our B16hPSMA mouse model with ARM, we examined the effects of covalency in limiting tumour growth and enhancing survival with the use of cARM. Mice were treated with either ARM or cARM every other day and both constructs were incubated with DNP boosted serum prior to injection to allow for ARM binding and cARM labeling of anti-DNP IgG. While ARM and cARM treated mice displayed delays in tumour growth as well as significantly improved survival, it was observed that only certain concentrations of constructs mediate beneficial effects. Interestingly, mice treated with 0.1  $\mu$ M

ARM demonstrated improved survival (median survival = 23 days) compared to PBS controls (median survival = 14 days). On the other hand, mice treated with 1  $\mu$ M ARM displayed no significant change in survival (median survival = 17 days) however, did display some reduced tumour growth. Seemingly, lower concentrations of ARM mediate enhanced anti-cancer effects leading to improved survival. This could imply autoinhibition effects are present with higher concentrations of ARM wherein ARM binds to tumour cell surfaces prior to antibody binding. As such, ternary complex formation is inhibited due to the formation of binary complexes thus, inhibiting quaternary immune active complex formation. Similarly, lower ARM concentrations could allow for stronger antibody binding that is not disrupted by excess ARM leading to improved immune activation and function. Conversely, mice treated with 1  $\mu$ M cARM demonstrated significantly improved survival (median survival = 18 days) whereas 0.1  $\mu$ M cARM treated mice displayed no improvement in survival (median survival = 14 days) compared to control mice. This indicates that the effects of covalency can circumvent possible autoinhibitory limitations seen in the 1  $\mu$ M ARM treated mice. As ARM and anti-DNP antibody binding is reversible, autoinhibitory effects could be resolved with cARM mediated covalent labeling of antibodies wherein ternary and immune complexes are stabilized. Furthermore, this data suggests that perhaps a higher cARM concentration is required to sufficiently label anti-DNP antibodies within DNP boosted serum as the 0.1  $\mu$ M cARM treatment group demonstrated no improvement in survival. Increased recruitment of labeled antibodies in the 1  $\mu$ M cARM treatment group could then allow for more pronounced ADCC/ADCP *in vivo*, thus improving survival. Interestingly, the 0.1  $\mu$ M ARM treatment group demonstrated improved survival whereas the 0.1  $\mu$ M cARM treatment group did not. This could mean that ARM, at lower concentrations, can function uninhibited whereas cARM requires a higher concentration to

induce immune function. As this is preliminary work, *in vivo* tumour studies need to be repeated to confirm these findings. This data represents the first examination of cARMs *in vivo* and treatment dosing and regimen were designed from previous *in vivo* studies utilizing uPAR binding ARMs<sup>65</sup>. However, as cARMs differ from ARM, treatment dosing would likely vary. Unfortunately, we only successfully quantified specific anti-DNP antibody concentrations with DNP boosted serum and DNP vaccinated mice following *in vivo* studies. As such, we could not determine optimal cARM concentrations for maximal anti-DNP antibody labeling in serum at the time. More experiments to analyze optimal cARM concentration and conditions likely need to be completed. As such, future *in vivo* work can contain more informed cARM concentration dosing to improve the treatment platform.

### 3.3 Study ARM/cARM - Anti-DNP Antibody Binding Kinetics & Selectivity

#### 3.3.1 *Ex vivo* Binding/Labeling

*cARM binds more monoclonal anti-DNP antibodies ex vivo.*

To examine ARM vs. cARM *ex vivo* antibody binding, 500nM monoclonal anti-DNP IgG was incubated with 1 $\mu$ M of each molecule and analyzed on ELISA (**Figure 3.12**). ARM was able to bind to anti-DNP IgG antibodies and displayed a low absorbance reading. Conversely, cARM/anti-DNP antibody binding displayed significantly higher absorbance levels.

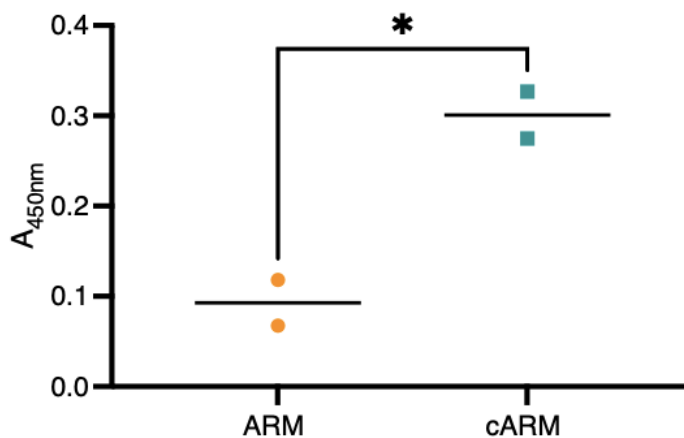


**Figure 3.12. ARM vs. cARM binding of anti-DNP monoclonal antibodies.** ELISA results of labeled monoclonal anti-DNP antibody. Binding/labeling mediated by ARM and cARM.

\* $P < 0.05$  by 2-tailed Student's *t* test.

### 3.3.2 *In vivo* Binding/Labeling

***Multiple doses of cARM show similar in vivo labeling and bind more anti-DNP antibodies than analogous ARM. However, there could be possible auto-inhibitory effects reducing cARM function and efficacy.***

To study ARM binding and cARM labeling of anti-DNP antibodies *in vivo*, DNP vaccinated mice (n=1) were injected with reporter ARM and cARM (biotin on the TBD) which can bind to streptavidin coupled readouts. A modified sandwich ELISA was developed to study levels/presence of bound/labeled antibodies within serum samples. A capture antibody is immobilized onto the ELISA plate to capture all mouse antibodies. This capture step is followed by the addition of streptavidin-horseradish peroxidase (HRP) that only binds to biotin molecules on bound/labeled antibodies. As such, an increase in absorbance correlates to increased bound/labeled antibodies within that sample.

Firstly, to view cARM labeling of antibodies at different timepoints, mice were injected with 200µL of 10µM biotin cARM (*in vivo* concentration of ~1µM) and sampled at different timepoints. When mice were injected with 1 dose of cARM and sampled at 24hrs, 48hrs and 72hrs, similar labeling of anti-DNP antibodies is observed within all three times (**Figure 3.13A**). When mice were injected with 2 doses of cARM at 0hrs and 48hrs and sampled at 72hrs, labeling remained the same as in the mice that received just 1 dose. Naïve mice were also injected with 200µL of 10µM biotin cARM and sampled at 24hrs. This sample acted as a control to establish the specificity of cARM labeling to anti-DNP antibodies. This naïve sample displayed very low labeling levels. Similarly, to examine ARM and anti-DNP antibody binding, mice were injected with 200µL of 10µM biotin ARM (*in vivo* concentration of ~1µM) and sampled at different timepoints (**Figure 3.13A**). When mice were injected with 1 dose of ARM and sampled at 24hrs, 48hrs and 72hrs, similar binding of anti-DNP antibodies is observed within all three times. However, when mice were injected with 2 doses of ARM at 0hrs and



48hrs and sampled at 72hrs, anti-DNP antibody binding decreased. All mice injected with ARM displayed lower absorbance readings at every timepoint when compared to mice injected with cARM. DNP boosted serum was incubated with ARM and cARM *ex vivo* for 24hrs to allow for saturated binding/labeling. These samples were used as a positive control for binding/labeling.

To study the effect of different cARM concentrations on anti-DNP antibody labeling, mice were injected 200 $\mu$ L of biotin cARM and sampled at 24hrs (**Figure 3.13B**). Three *in vivo* concentrations of cARM were examined. Results show that the highest level of labeling occurred with 0.1 $\mu$ M cARM however, this difference is not significant. Similar levels of labeling were observed with 1 $\mu$ M and 5 $\mu$ M cARM.

While at 24hrs there may be similar labeling among differing cARM concentrations, this does not hold true at 72hrs. When mice were dosed at 0hrs and 48hrs and sampled at 72hrs, labeling results differ between 1 $\mu$ M and 5 $\mu$ M cARM. At 5 $\mu$ M cARM, there is a decrease in labeling of anti-DNP antibodies when compared to labeling results with 1 $\mu$ M cARM (**Figure 3.13C**).

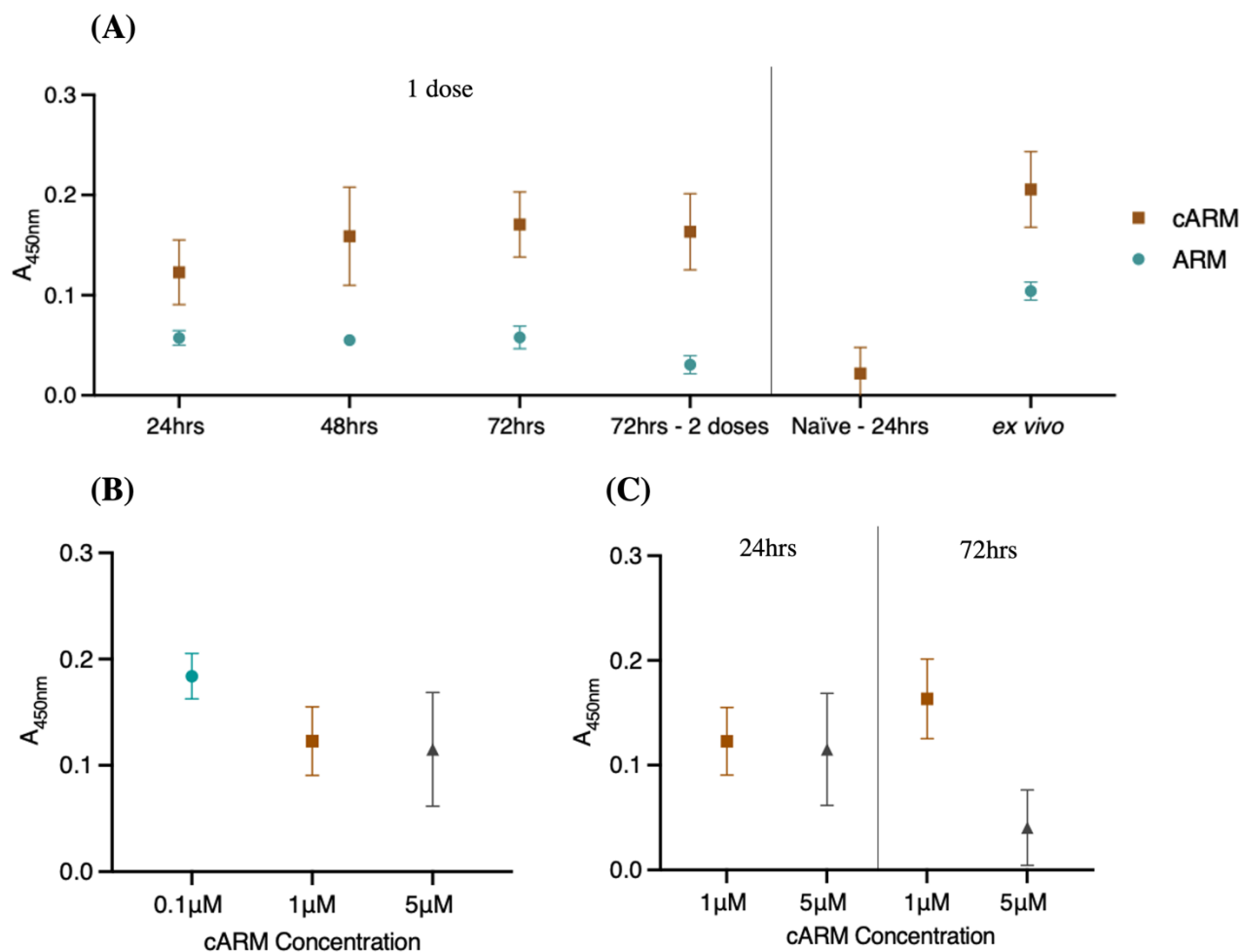


**Figure 3.13. ARM/cARM *in vivo* binding/labeling of anti-DNP antibodies.** (A) Modified sandwich ELISA results of bound/labeled anti-DNP antibodies in DNP vaccinated and naïve mice at the timepoints indicated. Mice were injected with 1 dose of 200  $\mu$ L of 10  $\mu$ M biotin ARM and cARM for an *in vivo* concentration of 1  $\mu$ M and endpoint bled at the indicated timepoints. All mice were injected at 0hrs. Timepoint 72hrs – 2 doses show results from mice that were injected at 0hrs and 48hrs and bled at 72hrs. Naïve - 24hrs point shows results from non-vaccinated mice that were injected at 0hrs and bled at 24hrs. *Ex vivo* serum samples were incubated with ARM and cARM and used as a positive control (B) Anti-DNP antibody labeling results following cARM injections. Mice were injected with varying cARM concentrations and endpoint bled at 24hrs. (C) Anti-DNP antibody labeling of DNP vaccinated mice at both 24hrs and 72hrs at different concentrations. 72hrs timepoint were mice that were injected with two doses (0hrs and 48hrs). (A-C) Each point represents one mouse.

### 3.3.3 ARM & cARM Binding/Labeling – Discussion

ELISA results displayed increased absorbance in monoclonal anti-DNP antibodies incubated with cARM when compared to ARM. This means that cARM displayed increased binding of anti-DNP antibodies. As the same concentrations of construct and antibody were used, the difference in antibody binding is a result of covalent effects. cARMs employ labeling via acyl imidazole chemistry to instigate an irreversible covalent bond between antibody and cARM. Comparatively, ARMs reversibly bind antibodies and this interaction can be disturbed by excess ARM and ARM degradation<sup>80</sup>. This data confirms that cARM induced covalent effects mitigate some of the limitations posed by ARMs. The enhancement in antibody binding allows for augmented antibody recruitment to tumour cell surfaces and increased quaternary immune active complex formation.

To examine construct and anti-DNP IgG binding and labeling *in vivo*, DNP vaccinated mice were injected with 1 dose of the same concentration of construct and sampled at different time points. cARM mediated *in vivo* labeling of anti-DNP antibodies was observed at 24hrs post cARM injection and labeled antibodies remain in circulation for at least 72hrs. The level of labeling remained consistent between 24hrs, 48hrs and 72hrs with 1 dose of cARM. This data implies maximal labeling could be reached by 24hrs and labeled antibodies remain in circulation at a stabilized level. However, the latest timepoint that was analyzed was 72hrs, as such, labeled antibodies could remain in circulation for longer. Further analysis needs to be completed in the future to confirm this. As labeled antibodies remain in circulation for at least 72hrs, cARMs are able to stay in circulation much longer than ARMs, which are rapidly cleared *in vivo* ( $t_{1/2} = 1-2$ hrs) when not bound to antibodies<sup>80</sup>. This is supported by the results of ARM mediated anti-DNP antibody binding *in vivo*. At all sampled timepoints, cARM outperformed ARM in anti-

DNP antibody binding. This is most likely due to labeling chemistry that allows for irreversible covalent bond formation between cARM and anti-DNP IgG in serum. As such, this stabilizes the cARM-anti-DNP IgG complex and allows for increased amounts of labeled antibodies to remain in circulation longer. Furthermore, as all mice were given the same concentration of construct, the reduction in signaling observed in ARM injected mice could be a result of rapid ARM clearance. While ARM-antibody binding is reversible, unbound ARM can be cleared promptly thus resulting in lower levels of ARM that can induce anti-DNP IgG binding. Unvaccinated mice were injected with the same concentration of cARM and sampled at 24hrs. This sample was used as a control for anti-DNP IgG labeling and displayed low absorbance readings which confirmed selective labeling by cARM. Furthermore, DNP boosted serum was incubated with cARM and ARM *ex vivo* to allow for saturated binding/labeling and was used as a positive control. The positive control samples yielded the highest absorbance readings for cARM and ARM respectively – confirming experimental set-up and validity. This analysis represents the first attempt in viewing ARM and cARM mediated antibody binding and labeling *in vivo* as well as the first examination into the longevity of labeled antibodies *in vivo*. This is vital as it provides validation of cARM function *in vivo* as well as provides key details on the pharmacokinetic profile of these novel molecules.

cARM mediated labeling of anti-DNP antibodies *in vivo* remains consistent between dosing whereas ARM binding decreases. Mice that received 1 or 2 doses of 1 $\mu$ M cARM yielded similar antibody labeling. This implies that 1 dose of cARM could be sufficient to label circulating anti-DNP antibodies and an extra dose of cARM does not reduce labeling levels. Conversely, while 1 dose of ARM displayed similar low circulating ARM-anti-DNP IgG levels at all timepoints, this is not observed when excess ARM is in circulation. When mice were given

2 doses of ARM and sampled at 72hrs, the level of bound anti-DNP IgG decreases when compared to mice given 1 dose. This implies excess ARM disrupts ARM-antibody binding and can compete for antibody binding. As such, covalent effects can stabilize cARM-antibody binding and dosing does not interrupt this interaction. This could then correlate to stabilized ternary and immune complexes wherein excess cARM, at this concentration, do not disrupt immune activation and function against target cells.

To study the effects of cARM concentration on anti-DNP IgG labeling *in vivo*, mice were given varying amounts of cARM and sampled at 24hrs. Similar anti-DNP IgG labeling was observed with all cARM concentrations. While 0.1 $\mu$ M cARM displayed slightly higher antibody labeling compared to 1 $\mu$ M or 5 $\mu$ M cARM, this was not a significant difference.

While 1 dose of different cARM concentrations mediated similar labeling at 24hrs, this does not hold true when mice were given multiple doses of higher concentrations. Reduced antibody labeling was observed at 72hrs with 5 $\mu$ M cARM. Comparatively, higher levels of labeling were observed with 1 $\mu$ M cARM. This data implies that there could be autoinhibition of cARM preventing labeling of antibodies and these effects are more pronounced at higher cARM concentrations. A possible reason for autoinhibition could be acyl imidazole hydrolysis. Acyl imidazoles are more reactive than typical esters and are susceptible to nucleophilic attack such as hydrolysis<sup>96</sup>. The ALD contains acyl imidazole chemistry which results in ejection of the ABD group from the cARM as a result of anti-DNP antibody labeling. However, if chemical hydrolysis were to occur, inhibitory fragments containing the TBD and ABD can form. This could result in autoinhibition wherein ABD fragments prevents fully intact cARM from binding and then subsequently labeling antibodies. Similarly, fragments containing the TBD can compete with labeled antibody for target binding sites. Inadvertently, the ALD, which is meant to enhance

cARM function, poses an autoinhibitory issue itself. To circumvent this issue, new non-ejection cARMs were developed (**Supplementary Figure 5.3**). This cARM functions similar to the previous ejection cARM however, acyl imidazole chemistry does not result in the ejection of the ABD from the cARM following antibody labeling. As this acyl imidazole group is not found directly in the linker of the cARM, hydrolysis would not result in inhibitory fragment formation. We hypothesized that hydrolysis of this new non-ejection molecule will not result in autoinhibition. In fact, as there are no ejected ABD fragments, this molecule should not have any impaired function. The non-ejection cARM would then allow for further enhanced antibody labeling and subsequent ternary and quaternary complex formation. Furthermore, new cARMs developed in the lab utilize alternate labeling chemistries that are less susceptible to hydrolysis. It would be vital to test new chemistries to view if labeling increases thereby resulting in enhanced anti-tumour effects.

### **3.4 Enhance & optimize cARM treatment platform utilizing results from previous aims**

#### **3.4.1 Monoclonal Antibody Development**

*Varying heavy: light antibody chain ratios result in differing amounts of antibodies produced.*

To optimize cARM labeling of anti-DNP antibodies, we developed mouse monoclonal anti-DNP antibodies as an alternative to DNP boosted serum. The use of monoclonal antibodies will mitigate serum albumin sequestering of small hydrophobic molecules such as DNP. Two expression vectors incorporating the antibody heavy and light chains were developed and transfected into HEK293T cells for antibody production. To examine which heavy: light chain vector ratio is optimal for producing antibodies in cell culture, HEK293T cells were transfected with varying ratios. Following transfection, cell culture supernatant was collected, purified, and concentrated. A variety of heavy: light chain plasmid ratios were analyzed via ELISA to view optimal anti-DNP antibody production (**Figure 3.14**). Based on ELISA results, there was successful production of anti-DNP antibodies in all transfected cells. While all the plasmid ratios yielded anti-DNP antibody production, the highest antibody levels were seen in samples using the 2:1 heavy: light chain plasmid ratio.

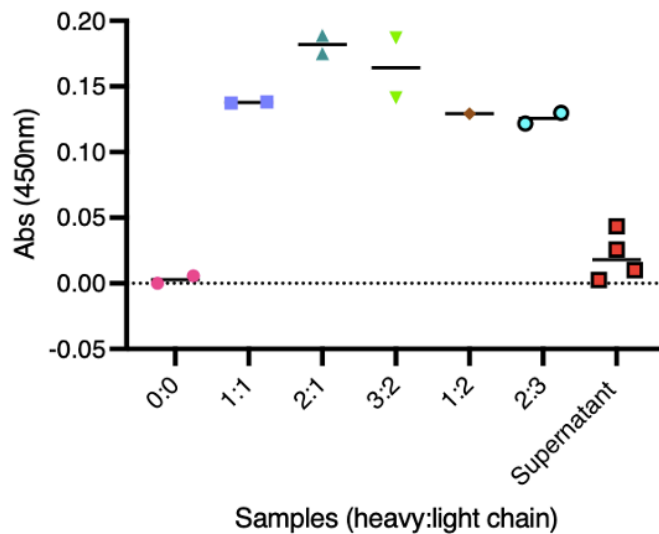


**Figure 3.14. Mouse monoclonal anti-DNP antibody expression.** (A) DNP-immobilized ELISA results with purified and concentrated cell supernatant samples at varying plasmid ratios. Sample mean is shown along with duplicate readings. Supernatant sample is cell culture supernatant prior to ProteinG purification and concentration.



### 3.4.2 ARM vs. Ejection cARM vs. Non-Ejection cARM

#### *Non-ejection cARM recruits more hPSMA compared to ejection cARM.*

To optimize cARM efficacy and labeling, a non-ejection cARM was developed to mitigate hydrolyzation issues posed by the ejection cARM. To evaluate the function of the non-ejection cARM vs. the ejection cARM, we examined both versions using biolayer interferometry. Both constructs were incubated with monoclonal anti-DNP antibodies overnight to allow for labeling. ProteinG probes were used to allow for antibody binding – including labeled antibodies. This was followed by hPSMA association. As such, increased nm shifts correlate to increased amounts of hPSMA associating onto labeled antibodies. Samples using both cARM versions showed increased shift (nm) when compared to the negative control of mAb only (**Figure 3.15**). This confirms that any hPSMA association is due to the presence of labeled antibody and the GUL group within the cARM. It was observed that both concentrations of ejection cARM recruited hPSMA to the probe. However, compared to the ejection cARM, both concentrations of the non-ejection cARM showed a higher increase in nm shift.

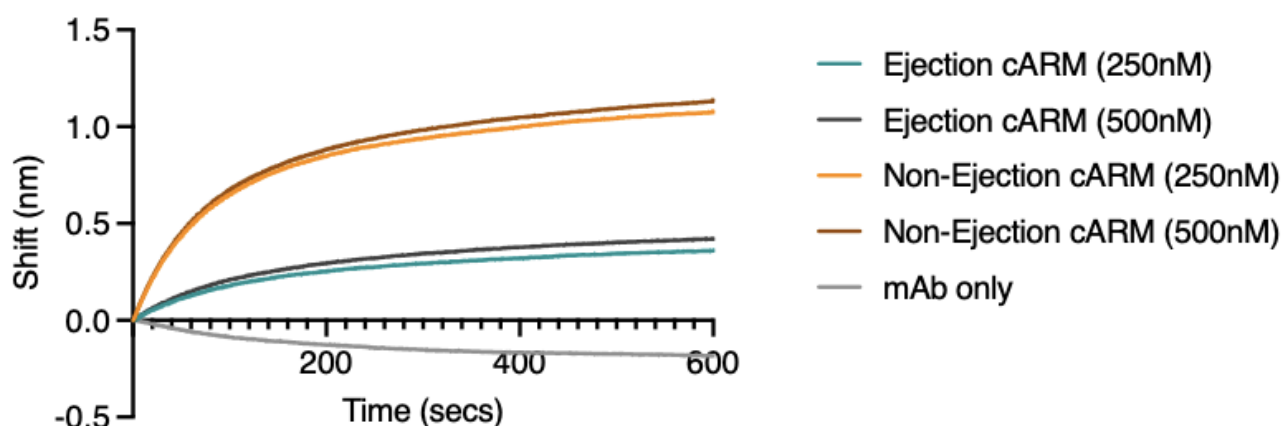


**Figure 3.15. hPSMA recruitment to cARM labeled anti-DNP antibody.** Biolayer interferometry results of cARM labeled monoclonal anti-DNP antibody. Antibody was labeled with ejection cARM and the non-ejection cARM to confirm the function of non-ejection cARM. Shift (nm) correlates to the amount of hPSMA associating onto the labeled antibody which is bound to ProteinG probes.

***Non-ejection cARM labels more anti-DNP antibodies within DNP boosted serum compared to ARM and ejection cARM.***

To examine labeling efficiency of ARM, ejection cARM and non-ejection cARM, a comparative *ex vivo* analysis was completed. DNP boosted serum was incubated with 1 $\mu$ M of each molecule and analyzed on ELISA (**Figure 3.16**). ARM was able to bind to anti-DNP antibodies within boosted serum and displayed a low absorbance reading. Similarly, ejection cARM successfully labeled anti-DNP antibodies found in boosted serum, however also displayed a lower absorbance reading. Conversely, it was observed that DNP boosted serum that was labeled with non-ejection cARM displayed the highest absorbance reading. Non-ejection was able to mediate the highest level of anti-DNP antibody labeling within boosted serum compared to ARM and ejection cARM. A non-boostered serum control was used to confirm the selectivity of these molecules - this sample displayed no absorbance.

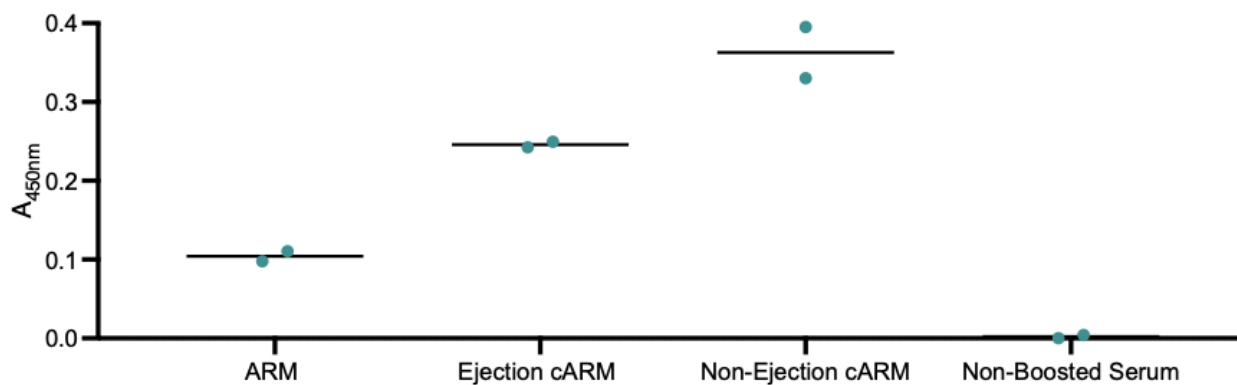


**Figure 3.16. *Ex vivo* labeling of anti-DNP antibodies by ARM, ejection & non-ejection cARMs.** Modified sandwich ELISA results of labeled anti-DNP antibodies in DNP boosted serum. Binding/labeling mediated by ARM, ejection cARM and non-ejection cARM. Non-boostered serum was labeled with ejection cARM to show labeling selectivity towards anti-DNP antibodies.

***Non-ejection cARM mitigates autoinhibitory effects that are seen in higher concentrations of ejection cARM.***

To study the *in vivo* labeling profile of the non-ejection cARM, *in vivo* labeling studies were repeated. DNP vaccinated mice (n=1) were injected with 200 $\mu$ L of either 10 $\mu$ M or 50 $\mu$ M non-ejection cARM (*in vivo* concentrations of  $\sim$ 1 $\mu$ M and  $\sim$ 5 $\mu$ M respectively) and sampled at various times. These samples were run on a modified sandwich ELISA wherein absorbance correlates to labeling. While ejection cARM labeled less antibodies at higher concentrations, it was observed that higher concentrations of non-ejection cARM was able to successfully label increased amounts of anti-DNP antibodies *in vivo* (Figure 3.17A). Compared to an *in vivo* concentration of 1 $\mu$ M, 5 $\mu$ M non-ejection cARM displayed increased labeling of antibodies.

When mice are sampled at 24hrs and 72hrs, non-ejection cARM displayed the same labeling profile. 5 $\mu$ M of circulating non-ejection cARM, at both 24hrs and 72hrs, displayed higher labeling than 1 $\mu$ M at those same times (Figure 3.17B).

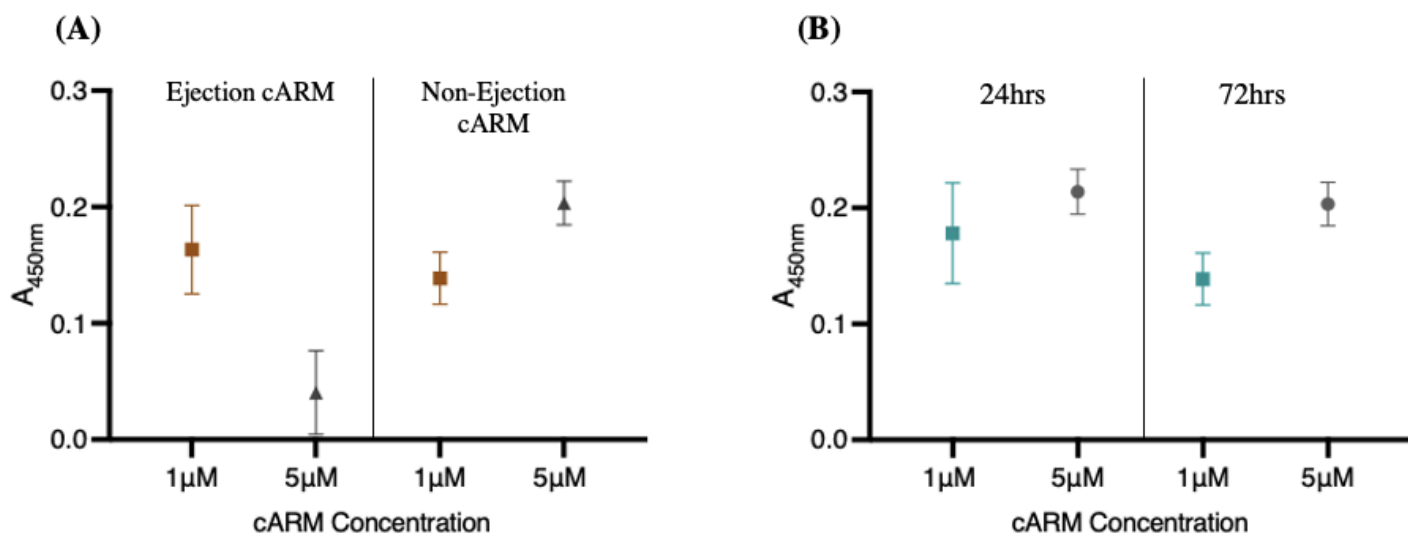


**Figure 3.17. Mouse *in vivo* labeling with ejection and non-ejection cARMs in vaccinated mice.** Modified sandwich ELISA results of labeled anti-DNP antibodies in DNP vaccinated mice. (A) Anti-DNP antibody labeling of DNP vaccinated mice at 72hrs at different concentrations of both cARMs. (B) Anti-DNP antibody labeling with non-ejection cARM of DNP vaccinated mice at indicated timepoints and concentrations. (A-B) Each point represents one mouse.

### 3.4.3 ARM vs. cARMs *in vivo*

***Tumour bearing mice treated with non-ejection cARM every 4 days display significantly improved survival compared to ejection cARM and traditional ARM.***

Following the confirmation of non-ejection cARM's enhanced labeling capacity, we sought to evaluate the construct *in vivo* against B16hPSMA tumours. We aimed to optimize the treatment platform by increasing labeling through a new ALD as well as using isolated monoclonal anti-DNP antibodies. In conjunction, we wanted to evaluate different treatment regimens by altering treatment days. Thus, we studied the effects of pre-formed monoclonal anti-DNP antibody and ARM/ejection cARM/non-ejection cARM complex when given to tumour bearing mice every other day as well as every 4 days. All mice were given 200 $\mu$ L of 1 $\mu$ M construct and 500nM monoclonal anti-DNP antibody (n=4). Mice groups varied in treatment regimen but dosing concentrations remained constant (**Figure 3.18A**).

We observed that ARM treated groups, regardless of treatment day, had no significant delay in tumour growth or survival when compared to PBS control mice (**Figure 3.18C-D**). Similarly, ejection cARM treated groups, regardless of treatment day, also had no significant delay in tumour growth or survival compared to PBS control mice (**Figure 3.18E-F**). Likewise, the non-ejection cARM group (every other day) had no significant delay in tumour growth or survival when compared to PBS control mice. Interestingly, the non-ejection cARM treatment group (every 4 days) had a delay in tumour growth as well as significantly improved survival when compared to PBS control mice and multiple other treatment groups (**Figure 3.18H**). We observed significantly improved survival between the non-ejection cARM treatment group (every 4 days) and PBS, ARM (every other day), ejection cARM (every other day) and ejection cARM (every 4 days) groups (**Figure 3.18J**).

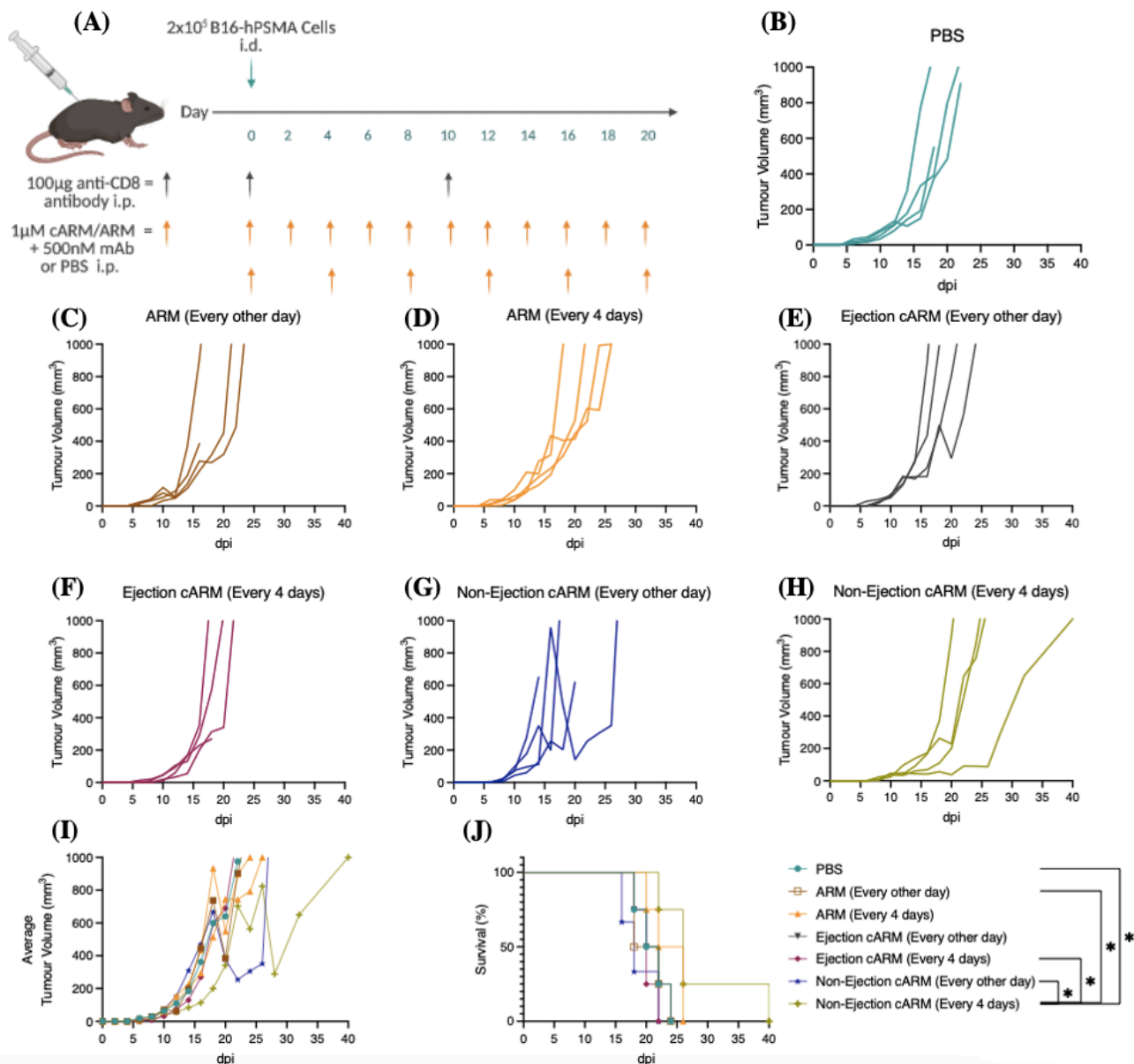


**Figure 3.18. ARM vs. Ejection vs. Non-ejection cARM effects on B16hPSMA tumours.** (A) Treatment regimen and dosing. (B-H) Individual B16hPSMA tumour volumes ( $\text{mm}^3$ ) of mice ( $n=4$ ) were assessed on the indicated days post implantation (dpi) (B) Tumour growth in mice treated with PBS. (C-D) Tumour growth in mice treated every other day (C) and every 4 days (D) with pre-incubated complex of  $200\mu\text{L}$  of  $1\mu\text{M}$  ARM +  $500\text{nM}$  monoclonal anti-DNP antibody. (E-F) Tumour growth in mice treated every other day (E) and every 4 days (F) with pre-labeled complex of  $200\mu\text{L}$  of  $1\mu\text{M}$  ejection cARM +  $500\text{nM}$  monoclonal anti-DNP antibody. (G-H) Tumour growth in mice treated every other day with (G) and every 4 days (H) with pre-labeled complex of  $200\mu\text{L}$  of  $1\mu\text{M}$  non-ejection cARM +  $500\text{nM}$  monoclonal anti-DNP antibody. (I) Average tumour volumes in each treatment group measured on the days indicated. (J) Survival of B-H. Endpoint was measured at tumour ulceration or growth reaching  $1000\text{mm}^3$ . \* $P < 0.05$  by log-rank (Mantel-Cox) test.

### 3.4.4 Immune Cell Presence in Tumour Bearing Mice

#### ***Tumour bearing mice treated with ARM and ejection cARM results in increased circulating macrophages and NK cells within peripheral blood.***

Following examination of tumour growth and survival of ARM, ejection cARM and non-ejection cARM treatment groups, we sought to analyze innate immune cell presence in peripheral blood of tumour bearing mice during treatment. All mice (n=3) were injected with the appropriate molecule every 4 days. We observed no significant increase in circulating CD11c+/F4/80+ macrophages in mice that were treated with ARM in comparison to PBS control mice (**Figure 3.19A**). Similarly, there was no apparent increase in macrophages within peripheral blood of mice that were treated with non-ejection cARM. However, there was an increase in peripheral blood macrophages in mice that were treated with ejection cARM.

Concurrently, we sought to identify NK1.1+/CD27+ NK cell populations within peripheral blood samples of tumour bearing mice during treatment. We observed a significant increase in NK cell populations within mice treated with ARM every 4 days (**Figure 3.19B**). Similarly, mice treated with ejection cARM also displayed increased NK cell levels within peripheral blood. Conversely, there was no change in NK cell levels in the blood of mice treated with non-ejection cARM.

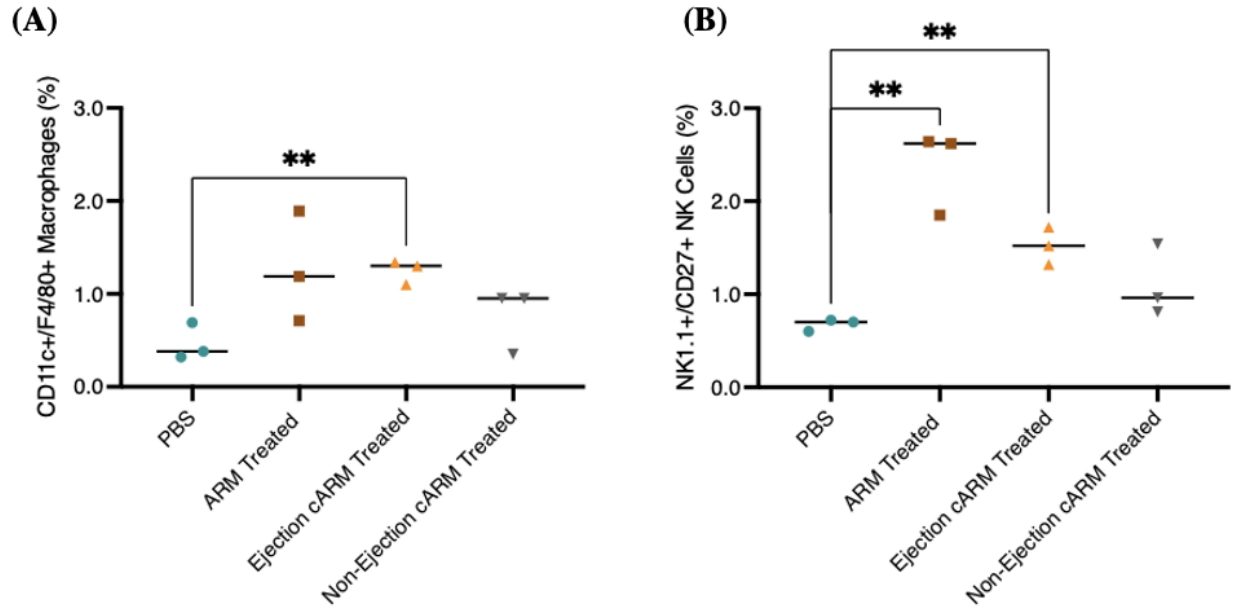


**Figure 3.19. Immune cell presence in peripheral blood of tumour bearing mice treated with constructs.** All mice were sampled at 17 dpi **(A)** CD11c+/F4/80+ Macrophage (%) in blood samples of tumour bearing mice treated with PBS, ARM, ejection cARM and non-ejection cARM every 4 days. **(B)** NK 1.1+ CD27+ NK cells (%) (%) in blood samples of tumour bearing mice treated with PBS, ARM, ejection cARM and non-ejection cARM every 4 days. Data in **A-B** represent each mouse as individual values and are shown with the mean. \*\* $P < 0.01$  by 2-tailed Student's  $t$  test.

### 3.4.5 Treatment Platform Optimization - Discussion

In an effort to optimize anti-DNP antibody labeling, DNP boosted serum was no longer used in ARM/cARM treatments. While DNP boosted serum provided a supply of anti-DNP IgG antibodies, it posed antibody labeling limitations. DNP is a small hydrophobic molecule and can interact with various other molecules, specifically serum albumin. This poses an issue in terms of selectivity with ARMs and cARMs bearing a DNP group in the ABD. Previous work established serum albumin labeling via cARMs<sup>80</sup>. Problematically, treatments using DNP boosted serum contained high natural levels of serum albumin. To mitigate albumin sequestering of cARMs, plasmids were designed to express and produce mouse monoclonal IgG2a anti-DNP antibodies. This antibody subtype was selected as murine IgG2a was observed to be most successful in directing ADCC by effector cells through activation of mFcγRIV<sup>97,98</sup>. As such, the use of IgG2a monoclonal antibodies was hypothesized to result in isolated labeling of antibodies by cARM as well as facilitate potent ADCC function. Furthermore, this would ensure that all available cARM/ARM interacted with antibodies instead of other serum proteins. Thus, mouse monoclonal anti-DNP antibodies were successfully produced, purified, and concentrated. To confirm increased IgG labeling, cARM was incubated with both monoclonal anti-DNP IgG and DNP boosted serum. ELISA results demonstrated that cARM was able to label significantly more monoclonal anti-DNP IgG antibodies when compared to antibodies found in DNP boosted serum (**Supplementary Figure 5.2**).

To resolve possible cARM autoinhibition, a new non-ejection cARM was developed. The development of this molecule aimed to reduce the detrimental effects of cARM hydrolysis. Non-ejection cARMs displayed increased hPSMA recruitment in biolayer interferometry studies when compared to ejection cARM. As both cARMs were incubated with the same concentration of



mAb, this suggests that there is increased labeling of antibody with the non-ejection cARM. Additionally, we observed enhanced labeling of anti-DNP antibodies within DNP boosted serum by non-ejection cARM compared to ARM and ejection cARM. Similarly, *in vivo* labeling was enhanced with the non-ejection cARM. Where previous *in vivo* labeling studies demonstrated decreasing labeling with 5 $\mu$ M ejection cARM, *in vivo* labeling utilizing 5 $\mu$ M non-ejection cARM displayed more antibody labeling than 1 $\mu$ M non-ejection cARM. Furthermore, non-ejection cARM displayed similar antibody labeling *in vivo* at 24hrs and 72hrs wherein increased antibody labeling was observed with increased cARM concentration *in vivo*. This data confirms that autoinhibition reduced the labeling capacity of ejection cARM due to ALD hydrolysis. Furthermore, this demonstrates the superior labeling capacity of non-ejection cARMs while circumnavigating autoinhibitory effects posed by the ejection cARM. Future work should focus on the quantification of cARM labeling *in vivo* and *in vitro*. The quantification of labeling could then be correlated to anti-DNP antibody IgG titers to view % labeling by both cARMs. This would offer vital information on cARM functionality and hydrolysis effects. Furthermore, this approach would provide a method to study and optimize cARM treatment dosing and concentration.

Following examination of *in vivo* efficacy of ARM and ejection cARM on tumour growth and survival, we next sought to optimize the treatment platform further. Firstly, we analyzed the *in vivo* efficacy of non-ejection cARM when compared to ejection cARM and ARM. Next, we examined the treatment regimen by analyzing the effects of treatments given every other day compared to every 4 days. For this, all construct concentrations remained the same at 1 $\mu$ M. Simultaneously, we attempted to optimize cARM labeling by utilizing purified monoclonal anti-DNP IgG2a antibodies to allow for more potent immune effector function *in vivo* and reduce

albumin labeling. 1  $\mu$ M construct and 500nM monoclonal anti-DNP IgG was incubated overnight to allow for ARM binding and cARM labeling. A 1:2 antibody to construct ratio was used as anti-DNP IgG have two locations of possible ARM binding and cARM labeling. Upon analysis, non-ejection cARM treatment reduced tumour volume and significantly improved survival (median survival = 26 days) in tumour bearing mice when injected every 4 days as compared to PBS controls (median survival = 21 days). In fact, when compared to multiple treatment groups, non-ejection cARM treated mice displayed significantly improved survival. Interestingly, we observed that only mice treated with non-ejection cARM labeled anti-DNP IgG antibodies every 4 days displayed any anti-cancer effects. In comparison, mice treated with non-ejection cARM every other day displayed no improved survival (median survival = 18 days). While non-ejection cARM proved to be successful in improving the survival of tumour bearing mice, less frequent dosing of non-ejection cARM could mediate enhanced anti-tumour effects. Conversely, literature review of ARM treatment regimen revealed that more frequent dosing of molecules resulted in improved *in vivo* efficacy<sup>60,64,65</sup>. The difference in optimal treatment regimen could be a result of covalency wherein less cARM is required to stimulate a response. These *in vivo* results are varied from previous attempts wherein ARM and ejection cARM displayed anti-cancer effects and modulated improved survival in tumour bearing mice. This could be due to the use of DNP boosted serum in previous studies or because of the high variance *in vivo*. Thus, *in vivo* tumour studies need to be repeated to confirm these findings.

To examine construct effects on immune cell presence, we analyzed peripheral blood of tumour bearing mice treated with ARM, ejection cARM and non-ejection cARM. An increase in CD11c+/F4/80+ macrophages was observed in mice treated with ejection cARM. Interestingly, there was no increase in macrophage populations in mice treated with ARM or non-ejection

cARM. Conversely, we observed an increase in CD27<sup>+</sup>/NK1.1<sup>+</sup> NK cells in mice treated with ARM and ejection cARM. This data conflicts with tumour studies as only non-ejection cARM treated mice displayed significantly improved survival and no apparent increase in macrophages and NK cells were found in peripheral blood of these mice. However, as we were unsuccessful in analyzing immune cell recruitment and activation in the TME of tumour bearing mice, we could not compare immune cell levels between the tumour, blood, and spleen. As such, more analysis needs to be completed on immune cell recruitment to the TME as well as immune cell activation in treatment mice compared to PBS control mice. This approach offers a mechanistic view into cARM/ARM mediated anti-tumour effects as well as a readout alongside survival. This would allow for more detailed analysis into anticancer effects, examination of dosing regimen, molecule concentrations, and overall optimization of the treatment platform.

To continue the optimization of cARM/ARM efficacy, it may be beneficial to recruit alternative antibodies. ARMs and cARMs can differ in their ABD and can be synthesized to selectively recruit other populations of antibodies. While anti-DNP antibodies are found in human serum, other studies have indicated that there is a large subset of antibodies found in humans directed against L-rhamnose<sup>99</sup>. These antibodies could pose for an advantageous target as they mitigate the hydrophobic effects of DNP. The lab has synthesized ARMs and analogous cARMs that successfully recruit anti-rhamnose antibodies. For future *in vivo* studies, we have developed both mouse rhamnose monoclonal IgG antibodies as well as a rhamnose antibody vaccination platform (**Supplementary Figures 5.4 & 5.5**). The rhamnose mouse model offers a platform to test cARM/ARMs that recruit anti-rhamnose antibodies in comparison to anti-DNP antibody recruiting molecules.

### 3.5 Fc Dependent Target Cell Killing via cARM in *in vitro* Assays

#### 3.5.1 Mouse Effector Cells for use in ADCC Assays

##### *HEK293T expresses mCD16 following successful transduction.*

To assess mouse Fc dependent target cell killing via ARM and cARMS, we aimed to develop mouse effector cells to use in ADCC assays. To this end, we attempted to develop a NK-92 cell line that expresses mCD16. To develop this cell line, we developed a lentivirus to transduce NK-92 cells. While NK-92 transduction was repeatedly unsuccessful, we transduced HEK293T cells as an alternative cell line for use in Fc binding assays. Transduced and parental HEK293T cells were analyzed via flow cytometry to view mCD16 expression levels (**Figure 3.20**). We observed an increase in fluorescence in transduced HEK293T cells.

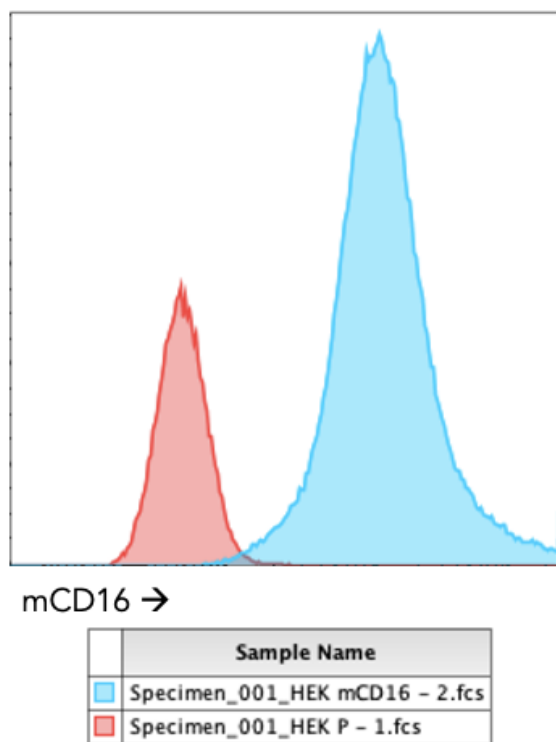


**Figure 3.20. mCD16 expression in HEK293T cells.** HEK293T-mCD16 transduced cell fluorescence compared to HEK293T parental cells. mCD16 expression is shown as PE fluorescence.

### 3.5.2 Antibody Dependent Cellular Phagocytosis

#### *Sufficient hPSMA expression is required for ADCP mediated by RAW macrophages.*

Following attempts to develop NK cells for ADCC assays, we sought to identify alternative Fc dependent *in vitro* assays to study ARM and cARM mediated function. We identified a mouse macrophage line (RAW 264.7) to utilize in ADCP *in vitro* assays. To conduct ADCP assays, constructs were pre-incubated with DNP boosted serum and mouse monoclonal anti-DNP antibody to allow for binding and labeling. ARM bound antibodies and cARM labeled antibodies were added to target B16hPSMA cells and effector RAW264.7 cells and incubated together to allow for phagocytosis. Anti-PSMA antibody was used as a positive control whereas effector + target only, monoclonal antibody alone and serum alone samples were used as negative controls.

Basal phagocytosis was observed at around ~12% and positive control samples yielded ~16% phagocytosis (**Figure 3.21**). ARM, ejection cARM and non-ejection cARM incubated with monoclonal antibody displayed similar phagocytosis levels at ~12% for all constructs. Constructs incubated with DNP boosted serum resulted in slightly higher phagocytosis at ~16%. There was no significant increase in phagocytosis among the positive control or experimental samples when compared to basal level phagocytosis.

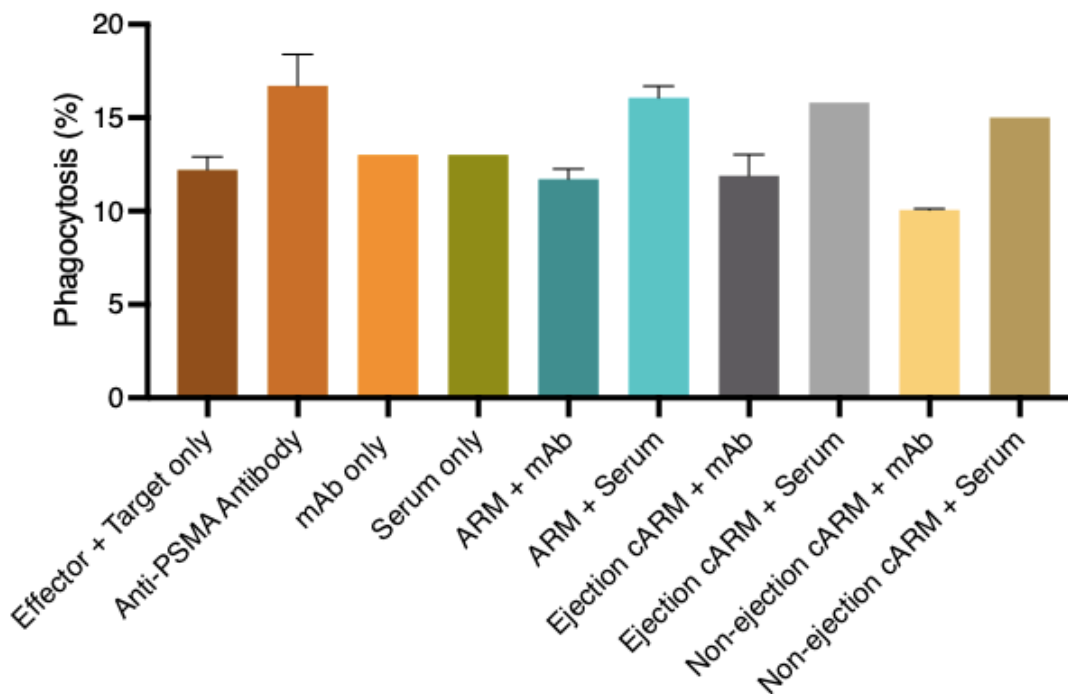


**Figure 3.21. RAW264.7 induced antibody dependent cellular phagocytosis against B16hPSMA cells.** Phagocytosis (%) is shown in different conditions using both DNP boosted serum as well as mouse monoclonal mAb. Negative controls are shown as effector + target only, mAb only and serum only. Positive control shown as anti-PSMA antibody. ARM, ejection cARM and non-ejection cARM were incubated with DNP boosted serum and mAb overnight to allow for saturated labeling.

### 3.5.3 *In vitro* Approaches - Discussion

Previous *in vitro* work in analyzing ARM and cARM function utilized human effector and target cells. To develop an ADCC assay to complement *in vivo* studies, we aimed to develop a mouse NK cell line to use as effector cells. We initially attempted to use *in vivo* derived mouse NK cells. However, these cells were not sustainable in cell culture or available in large amounts. To circumnavigate the issues posed by *in vivo* derived NK cells, we attempted to produce our own NK cell line. We identified that the human NK-92 cell line could be a viable option for use *in vitro* assays<sup>100</sup>. These cells, once armed with mCD16 displayed specific and potent ADCC function against target cells<sup>100</sup>. Thus, we intended to develop our own mCD16 expressing NK-92 line. However, this proved to be difficult as NK-92 cells would rapidly die following lentiviral transduction and antibiotic selection. This is likely due to NK cell resistance to transduction as well as inefficient transduction of NK cells by lentiviral vectors<sup>101,102</sup>. Studies have identified robust NK cell transduction by specific pseudotyped viral vectors and future work in developing this line should focus on the use of alternate transduction pathways<sup>103</sup>. Alternatively, we developed mCD16 expressing HEK293 cells. These cells, while not being able to mediate effector function, can still be used in future binding assays to test mCD16 recruitment to cARM labeled antibodies, target cells and quaternary complex formation.

As a complementary approach to ADCC assays, mouse ADCP assays were developed to examine ARM, ejection cARM and non-ejection cARM mediated effects. RAW264.7 mouse macrophages displayed no significant increase in phagocytosis in conditions using ARM, ejection cARM and non-ejection cARM. Interestingly, all construct conditions resulted in basal level phagocytosis (%) that was observed in negative control samples. In fact, there was no discernable difference between ARM, ejection cARM and non-ejection cARM incubated

samples. Likewise, there was no difference in ADCP with the use of anti-DNP IgG boosted serum or mouse monoclonal anti-DNP IgG. To examine this further, we attempted to alter construct/antibody concentrations, effector:target ratios and experimental procedure steps. However, all attempts proved to be unsuccessful. Interestingly, when anti-hPSMA IgG antibody was utilized as the positive control, there was no increase in phagocytosis (%) from basal levels. Previous work demonstrated robust ADCP functionality by RAW 264.7 macrophages against high antigen expressing target cells<sup>104</sup>. The lack of effector function in our attempts indicates that hPSMA expression on B16hPSMA cell surfaces was not sufficient to mediate ADCP. As such, results from this ADCP experiment are not indicative of ARM or cARM functionality. Future work should utilize higher antigen expressing cells to view ADCP directed by ARM and cARM constructs.

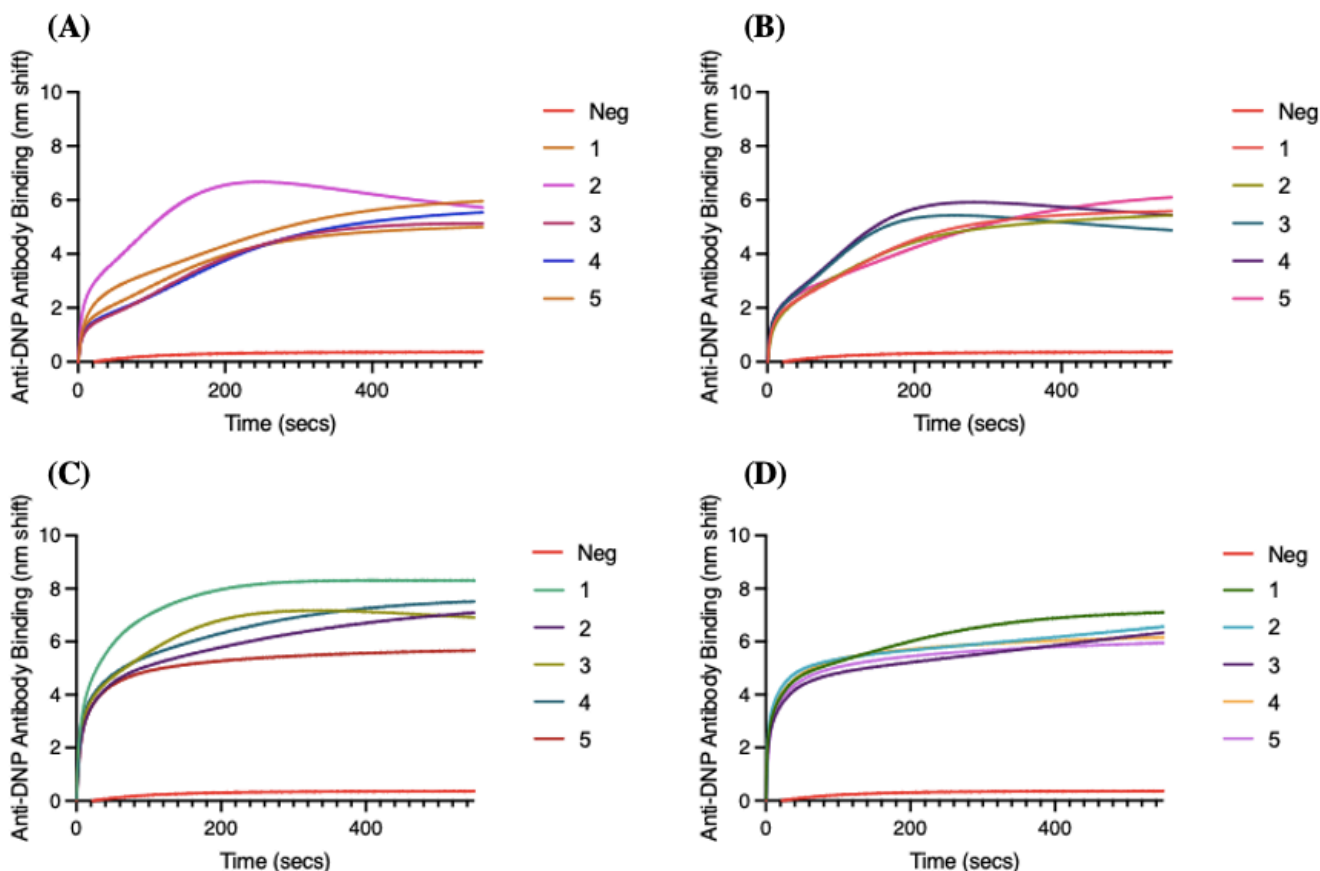


## Chapter 4: Conclusion

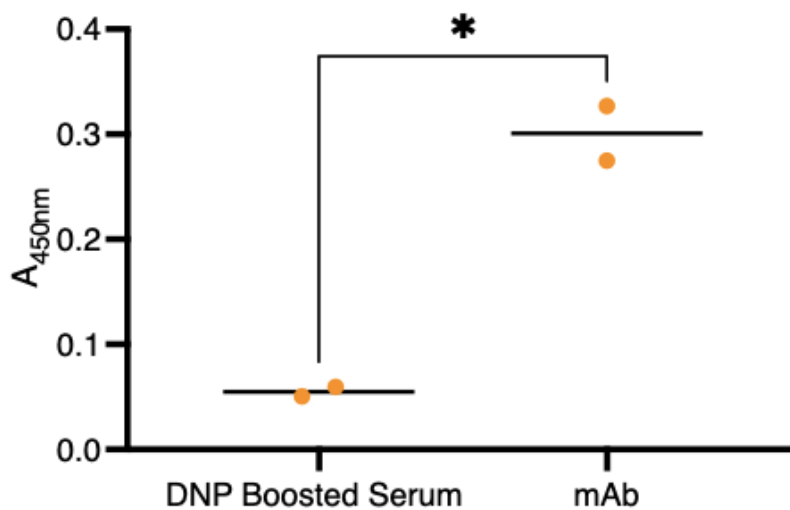
Synthetic immunology allows for the manipulation and modulation of the immune system by synthetic compounds. ARMs have shown efficacy in the past however, is limited by ternary complex instability. This led to the development of cARMs to stabilize ternary and quaternary complexes. While cARM function has been demonstrated *in vitro*, these molecules had yet to be tested *in vivo*. Thus, this thesis has revealed the *in vivo* and *in vitro* efficacy of first-generation cARMs in comparison to reversible binding ARMs. In this work, a mouse model to evaluate and examine ARM/cARM function was developed. ARMs were shown to successfully mediate anti-tumour effects in an antibody dependent manner in DNP vaccinated and in naïve mice with the use of passive antibody transfer. In a novel study, cARMs were shown to be efficacious in reducing tumour growth and improving survival. *In vitro* binding studies demonstrated the advantage of covalent labeling in binding significantly more anti-DNP IgG than analogous ARM. This enhanced antibody binding can then be correlated to improved recruitment to tumour cell surfaces, increased ternary complex and subsequent quaternary complex formation. Studies into antibody binding/labeling *in vivo* revealed the presence of circulating cARM labeled antibodies for at least 72hrs at stable and considerably higher levels compared to ARM bound anti-DNP IgG. However, autoinhibition effects of cARM caused by ALD hydrolysis were shown to hinder labeling capacity. To resolve this, a new non-ejection cARM was developed. The non-ejection cARM exhibited increased labeling at higher cARM concentrations *in vivo*, increased selective antibody labeling in serum, and improved survival in tumour bearing mice. Analysis of peripheral blood of tumour bearing mice revealed increased macrophages in cARM treated mice and increased NK cell populations in ARM and cARM treated mice. This proof-of-concept work can lay the groundwork for the future *in vivo* testing of cARMs that utilize alternative novel labeling chemistries and recruit various immune machinery to different tumour antigens. Ultimately, cARMs have potential as a novel immunotherapeutic that labels specific antibody populations, mediates immune effector function and circumnavigates limitations posed by traditional ARMs.

## Chapter 5: Supplementary Figures

## 5.1 Anti-DNP Antibodies

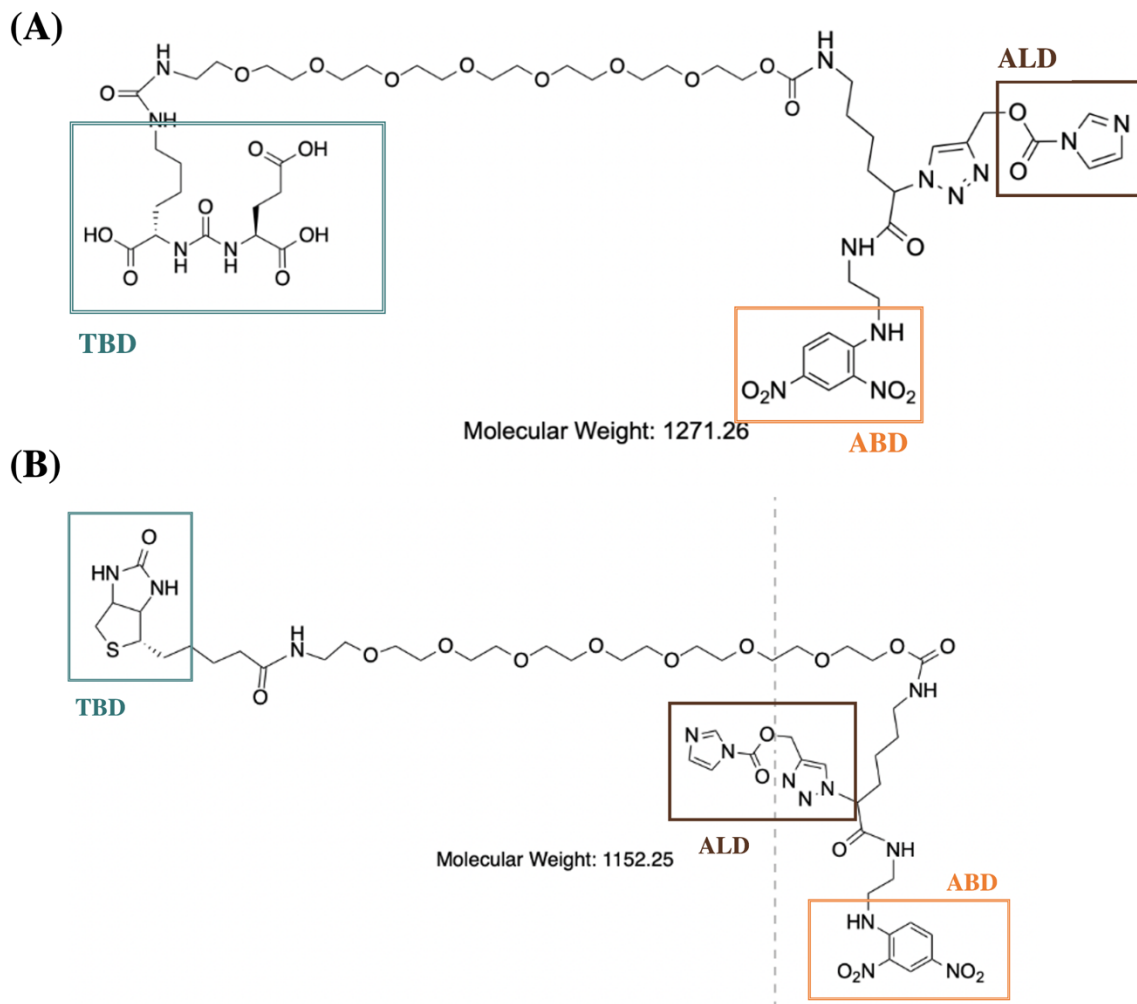


**Figure 5.1. Anti-DNP antibody presence in boosted mouse sera.** Biolayer interferometry results of anti-DNP antibody presence in DNP-KLH vaccinated mice. Streptavidin probes were loaded with biotin ARM and associated with mouse sera samples. Shift (nm) correlates to the amount of anti-DNP antibodies associating onto loaded probes. All boosted sera samples were compared with serum from non-vaccinated mice (negative). **(A)** Mice from **Figure 3.9A**. **(B)** Mice from **Figure 3.9B**. **(C)** DNP boosted serum donor mice. **(D)** DNP boosted serum donor mice.



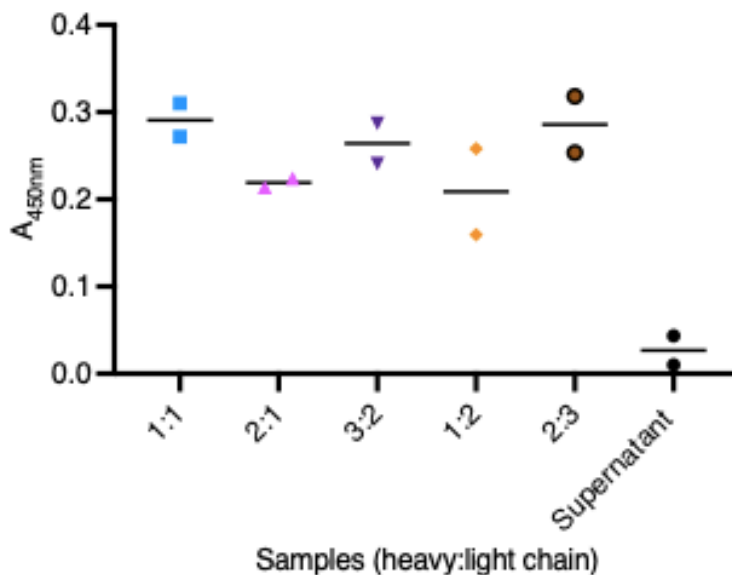
**Figure 5.2. Anti-DNP antibody labeling by ejection cARM.** Anti-DNP antibody labeling mediated by ejection cARM of DNP boosted serum and monoclonal anti-DNP IgG.  $1\mu\text{M}$  cARM was incubated with  $500\text{nM}$  anti-DNP antibodies.  $*P < 0.05$  by 2-tailed Student's  $t$  test.

## 5.2 Non-Ejection cARM Structures

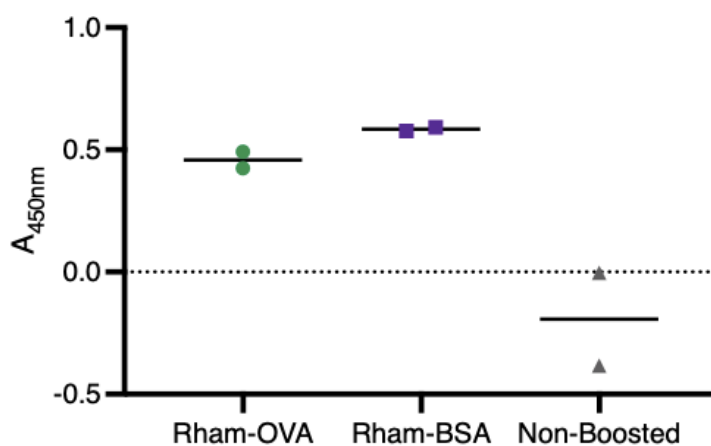


**Figure 5.3. Chemical structures of non-ejection cARMs.** Non-ejection cARMs developed to mitigate autoinhibition caused by ALD hydrolysis. **(A)** Chemical structure of hPSMA binding non-ejection cARM. TBD contains GUL to bind to hPSMA expressing cells. ABD contains a DNP group to bind to anti-DNP antibodies. ALD acyl imidazole group is found on the side of linker. **(B)** Chemical structure of streptavidin binding non-ejection cARM. TBD contains biotin moiety to bind to streptavidin. ABD contains DNP group to bind to anti-DNP antibodies. ALD acyl imidazole group is found on the side of linker.

### 5.3 Rhamnose Mouse Model

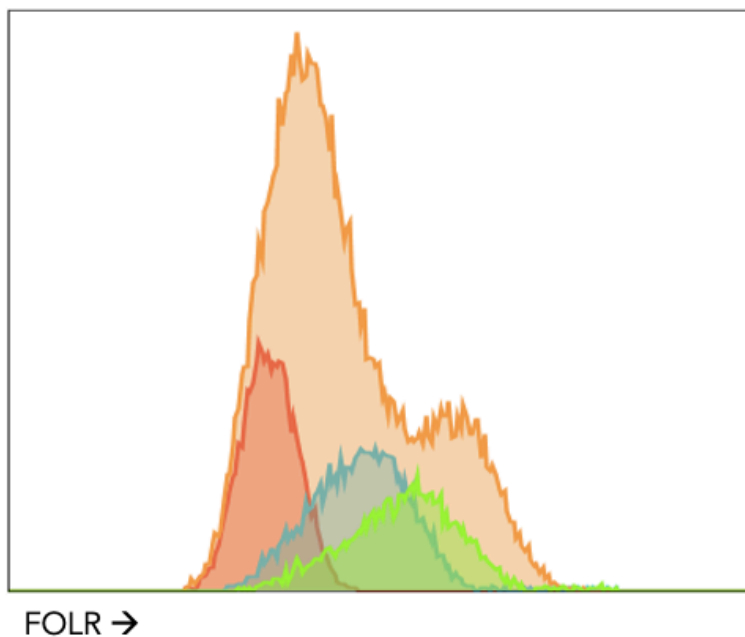


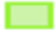



**Figure 5.4. Mouse monoclonal anti-rhamnose antibody expression.** Rhamnose-immobilized ELISA results with purified and concentrated cell supernatant samples at varying plasmid ratios (heavy:light chain). Sample mean is shown along with duplicate readings. Supernatant sample is HEK293T cell culture supernatant from transfected cells prior to ProteinG purification and concentration.



**Figure 5.5. *In vivo* boosting of anti-rhamnose antibodies.** Rhamnose-immobilized ELISA results with serum from boosted mice. Mice were boosted with a lab synthesized rhamnose-ovalbumin (OVA) conjugate as well as with rhamnose-BSA. Non-boosted mouse serum was used as a negative control.

### 5.4 Folate Mouse Model



	Sample Name
	MDA-MB-231
	4T1
	KB
	Secondary antibody only

**Figure 5.6. Endogenous folate receptor expression on human and mouse cancer cell lines.**

Flow cytometry results of surface FOLR $\alpha$  expression on MDA-231 human breast cancer cells, 4T1 mouse breast cancer cells and KB human epithelial cells. Both MDA-MD-231 and KB cells were used as a positive control for FOLR expression. A primary antibody against human/mouse FOLR $\alpha$  was used in conjugation with a secondary antibody conjugated with AlexaFluor647.

## Chapter 6: Materials & Methods

### Cell Culture

All cells were maintained at 37°C and 5% CO<sub>2</sub>. B16 cell lines were maintained with Minimum Essential Medium (MEM) with Earle's salts supplemented with 1% sodium pyruvate, 1% HEPES, 1% L-glutamine, 1% MEM vitamin solution and 10% fetal bovine serum (FBS). B16 hPSMA transduced cell lines were selected with 5µg/mL blasticidin. HEK293T cells were maintained in Dulbecco's Modified Eagle Medium (DMEM) supplemented with 10% FBS and 1% L- glutamine. RAW264.7 mouse macrophages were cultured in DMEM supplemented with 10% FBS and 5% L-glutamine and activated prior to ADCP with 30µL (0.1mg/mL) of interferon-gamma (IFN-γ).

### Transfection of HEK293T Cells

HEK293T cells were transfected to produce virus to create stable cell lines or to produce monoclonal antibodies. 24hrs prior to transfection, HEK293T cells were plated in a 10cm dish. Appropriate plasmids (**Table 1**) were added to a tube with 2mL basal DMEM and added into another tube containing 2mL basal DMEM and Lipofectamine 2000 (ThermoFisher). Following incubation of plasmids and Lipofectamine for 20min at RT, mixture is added on top of HEK293T cells. 12hrs post transfection, the media was changed. Supernatant containing antibodies are harvested once a day for 4 days. Supernatant containing virus is harvested 24 to 48hrs post media change.

Plasmid	Amount
pMD2.G	3µg
pRSV-REV	1µg
pMDLg-pRRE	10µg
Plasmid of interest	10µg

**Table 6.1. Transfection plasmids & amounts.** Plasmids used for transfection of HEK293T cells to develop lentiviral vectors.

### Transduction of Cell Lines

Following virus harvest from HEK293T cells, supernatant containing virus was centrifuged at 3000rpm for 5min to sediment any collected cells. Supernatant was filtered through a 0.45µm syringe filter. Virus was added directly to cells to be transduced in increasing doses. 24hrs post transduction, cells were split into a new 10cm dish with new media containing a selection marker to generate a polyclonal cell line with varied expression levels. Monoclones were generated by limited dilution cloning. Cells were trypsinized and suspended in selection containing media at 5 cells/mL. Cells were placed into a flat bottom 96-well plate at 200µL per well. Monoclones were grown to be screened for expression levels.

### *In vitro* Antibody Production

Following antibody harvest from transfected HEK293T cells, supernatant was collected every 24hrs for 3-4 days post transfection. Supernatant containing antibodies were spun down at 1500rpm for 5mins to sediment any collected cells. Supernatant was added to Protein G beads or antigen linked cyanogen bromide (CNBr) for incubation in a roller overnight at 4°C.

### Antibody Purification & Concentration

Supernatant containing antibodies and beads were placed into a Polypropylene column following incubation. Supernatant was collected as flow through for analysis. Columns containing beads were washed 2x column amounts with PBS. Antibodies were eluted with 10mL of 0.1M glycine-HCl (pH 2.3) into 15mL falcon tubes containing 1mL of 2M Tris-HCl (pH 10). Eluate was concentrated using 30kDa Amicon Ultra Centrifugal Filters.



## Cell Staining & Flow Cytometry

### cARM Binding

Antibodies used for flow cytometry were purchased from ThermoFisher and R&D systems. For labeled antibodies, 1 $\mu$ M cARM and 500nM anti-DNP antibody (Alexa fluor 488) were incubated at 4°C approximately 24hrs prior to flow analysis to allow for binding to create a prebound cARM-Ab mixture. Isotype controls were used. Cells were trypsinized, pelleted and resuspended in flow cytometry staining buffer (FACS) buffer in a 96- well plate at 1.5x10<sup>5</sup> cells/200 $\mu$ L. After the plate was spun down, cells were resuspended in 50 $\mu$ L of FVS780 (1:1000 dilution), covered from light and incubated for 20min at RT. The plate was washed and resuspended in 75 $\mu$ L of FACS buffer along with 25 $\mu$ L of antibody (1:100) or prebound cARM-DNP Ab mixture. The cells were incubated with antibody for 30mins. Wells were washed and resuspended in 200 $\mu$ L of FACS buffer. Samples were filtered into FACS tubes. cARM-Ab mixtures were not washed from the plate and filtered into FACS tubes and analyzed by LSRII flow cytometry machine. Plots were further analyzed using FlowJo11 software.

### Extracellular Staining

The cells were pelleted in a 96-well plate and incubated with Fc block for 20min at 4°C. Surface antibodies and isotype controls were added (25 $\mu$ L in FACS buffer) and incubated at 4°C for 30mins. The cells were washed in FACS buffer and resuspended in 100 $\mu$ L. All cells were filtered into FACS tubes and analyzed by LSRII flow cytometry. Data was further analyzed using FlowJo11 software.

Antibody	Catalog #	Fluorophore	Company	Dilution/Conc.
Polyclonal anti-DNP	A-11097	Alexa fluor 488	ThermoFisher	500nM
Anti-PSMA	FAB4234R	Alexa fluor 647	R&D Systems	1:100
Anti-CD8 (depletion)	BE0061	N/A	BioxCel	100µg
Anti-CD8	11-0081-82	FITC	ThermoFisher	1:100
Anti-CD20 (depletion)	MB20-11	N/A	BioxCel	200µg
Anti-NK1.1	108708	PE	BioLegend	1:100
Anti-CD27	124212	APC	BioLegend	1:100
Anti-CD19	115555	BV711	BioLegend	1:100
Anti- F4/80	743282	BV650	BD Biosciences	1:100
Anti- CD11c	117318	PECy7	BioLegend	1:100
Anti-mouse IgG	115-005-003	N/A	Jackson Immunoresearch Labs	5µg/well
Anti-mouse IgG - HRP conjugated	62-6520	HRP	ThermoFisher	1:3000
Anti-CD16	156606	PE	BioLegend	1:100
Anti-FOLR	PA5-116453	N/A	ThermoFisher	1:100
Anti-rabbit IgG	A-21245	Alexa fluor 647	ThermoFisher	1:100

**Table 6.2. Flow cytometry antibodies.** All antibodies & dilutions/concentrations used in flow cytometry and ELISA experiments.

#### Antibody-Dependent Cellular Phagocytosis

Concentrated saturated antibodies and small molecules were prepared to ensure antibody binding/labeling. RAW264.7 mouse macrophage cells were activated with IFN- $\gamma$  (0.1mg/mL) 24hrs prior to assay. RAW264.7 cells were suspended with TRYPLE Express, counted, washed, and suspended to a concentration of 1million cells/mL and stained with 1.9µM Vybrant DiD Cell-Labeling solution for 30mins at 4°C. Target cell cells were suspended with TRYPLE Express, washed, and resuspended to a concentration of 1million cells/mL. Target cells were stained with 5.79µM Vybrant DiO Cell-Labeling solution for 30mins at 4°C. Cells were washed and plated into a 96-well U-bottom plate prior to phagocytosis. Effector cells were allowed to

bind to the plate for 2hrs prior to adding target cells and appropriate treatments. Plate was softly pelleted for 2mins at 800rpm and incubated for 2hrs at 37°C. Plate was then put onto ice for 15mins before all wells were washed, resuspended in 100uL FACS buffer prior to filtering. All samples were analyzed using the LSRII machine and plots were analyzed with FlowJo11 software.

### Mice

Female C57BL/6 mice (aged 6-8 weeks) were purchased from Charles River Laboratories and housed in a level-2 clean room in the Central Animal Facility at McMaster University. All the animal studies were approved by the Animal Research Ethics Board and regulations set by the Canadian Council on Animal Care were followed. All animal work was completed under AUP #20-01-05.

### Blood Collection & Processing

For serum collection, blood was collected from anesthetized mice from the retro-orbital vein with non-heparinized capillary tubes. The blood was collected into Eppendorf tubes and left to clot for 45 minutes at RT. Following clotting, the tubes were centrifuged at 1500rpm, and serum was carefully transferred into new tubes for analysis. For flow analysis, blood was collected from the retro-orbital vein with heparinized capillary tubes. The blood was collected into Eppendorf tubes containing 50µL of heparin. Once the blood was transferred into FACS tubes, 2mL Ammonium-Chloride-Potassium (ACK) lysis buffer was added to the tubes. Tubes were vortexed gently following incubation for 5mins at RT, Hank's buffered salt solution was added. The tubes were centrifuged for 5mins at 1500rpm. The supernatant was poured off and cells were resuspended in 1mL of ACK lysing buffer, vortexed and incubated for 5mins. Hank's buffer was added and centrifuged for 5mins at 1500rpm. Supernatant was poured off once again and cells

were resuspended in complete media. Resuspended cells were plated into 96-well plates for staining and further analysis. Mice that were not endpoint bleeds received replenishing amounts of saline subcutaneously. Gauze was used to stop bleeding and drops of eye lubricant were added.

### Mouse Vaccination

All mice were subcutaneously injected at the base of the tail with the designated doses of DNP-keyhole limpet hemocyanin (KLH) and monophosphoryl lipid A (MPLA) in 100 $\mu$ L PBS on the specified days. Mice were also injected with Rham-OVA and Rham-BSA constructs.

	Day 0	Day 2	Day 4	Day 6	Day 8	Day 10	Day 12	Day 14
<b>Antigen (<math>\mu</math>g) Total 50<math>\mu</math>g</b>	0.04	0.1	0.26	0.676	1.76	4.56	11.88	30.8
<b>MPLA (<math>\mu</math>g) Total 25 <math>\mu</math>g</b>	0.02	0.052	0.135	0.352	0.91	2.37	6.17	16.1

**Table 6.3. Vaccination dosing profile.** Antigen/MPLA dosing amounts and days. A total of 50 $\mu$ g antigen and 25 $\mu$ g MPLA was injected into mice over the course of two weeks. This vaccination protocol was adapted from Tam et al<sup>86</sup>.

### Bi-layer Interferometry – Serum

Streptavidin probes were soaked in PBS for 20mins prior to the experiment. Following a baseline of PBS for 240secs, 500nM of biotin ARM analog (consisting of a biotin moiety and a DNP group) was loaded onto the probes for 180secs. 5% w/v milk powder in PBS was added as a quencher to block non-specific binding for 150secs. After 300secs in PBS, mouse sera (1:2 dilution in PBS) was associated onto the probes for 600secs.

### Bi-layer Interferometry – cARM Labeling

125nM anti-DNP monoclonal antibody was incubated with 250nM cARM and 250nM non-ejection cARM for 24hrs at 4°C to allow for labeling. ProteinG probes were soaked in PBS for

20mins prior to experiment. Following a baseline of PBS for 240secs, 200 $\mu$ L of labeled antibody was loaded onto the probes for 180secs. 5% w/v milk powder in PBS was added as a quencher to block non-specific binding for 150secs. Following a wash in PBS, 500nM PSMA was associated onto the probes for 600secs.

#### Biolayer Interferometry – Anti-DNP Antibody Presence

Streptavidin probes were soaked in PBS for 20mins prior to the experiment. Following a baseline of PBS for 240secs, 500nM of non-reactive cARM analog (consisting of a biotin moiety and a DNP group) was loaded onto the probes for 180secs. 5% w/v milk powder in PBS was added as a quencher to block non-specific binding for 150secs. After 300secs in PBS, mouse sera (1:2 dilution in PBS) was associated onto the probes for 600secs.

#### *In vivo* Tumour Study

2x10<sup>5</sup> B16hPSMA cells in 30 $\mu$ L PBS was intradermally injected in the back of all mice.

Treatments began on the day of tumour cell transplant and were injected every other day till the mice reached endpoint. For CD8<sup>+</sup> T cell depletion, mice were injected interperitoneally with one dose of 100 $\mu$ g of anti-CD8 depletion antibody on the day of tumour cell transplant and were given another dose on day 10. For B cell depletion, mice received one dose of 200 $\mu$ g of anti-CD20 depletion antibody 6 days prior to start of treatment and were dosed once a week intraperitoneally. Initial *in vivo* study utilized intravenous injections. For PBS/negative control mice, 200 $\mu$ L of PBS was intraperitoneally injected into the mice. For the treatment groups, 200 $\mu$ L of cARM/ARM (molecule alone or pre-labeled antibody) was intraperitoneally injected into the mice on the indicated days. cARMs/ARM were incubated with DNP boosted serum or mouse monoclonal anti-DNP antibody overnight at 4°C to allow for labeling. Tumours were measured every other day with a caliper following injections.

### Indirect & Modified Sandwich ELISAs

200ng of antigen/well in PBS was immobilized onto a 96-well ELISA plate overnight at 4°C. Following washing (3x) with 0.05% Tween in PBS, plates were blocked with normal goat serum (5% v/v solution) for 2hrs at 37°C. 50µL of samples were added to corresponding wells along with appropriate controls and incubated for 2hrs at 37°C. Plates were washed, and a secondary antibody conjugated with HRP (ThermoFisher, 1:3000 dilution) was added and left to incubate for 1hr at 37°C. For sandwich ELISAs, 5µg/mL of capture antibody (ThermoFisher) in PBS was immobilized onto an ELISA plate overnight at 4°C. Following washing (3x) with 0.05% Tween in PBS, plates were blocked with normal goat serum (5% v/v solution) for 2hrs at 37°C. 50 µL of samples were added to corresponding wells along with appropriate controls and incubated for 2hrs at 37°C. Plates were then washed, and 50µL of 1:5000 streptavidin-HRP (ThermoFisher) was added to plates and left to incubate for 1hr at 37°C. For all ELISAs, 50µL of 1:1 HRP substrate and H<sub>2</sub>O<sub>2</sub> was added to wells and left until a colour gradient is formed. 50µL of H<sub>2</sub>SO<sub>4</sub> was then used to quench the reaction. Absorbance was read at 450nm on the plate reader.

### *In vivo* Labeling

DNP boosted mice were injected with 200µL of cARM constructs of varying concentrations. Mice were retro-orbitally bled at various timepoints using non-heparinized capillary tubes into 1.5mL Eppendorf tubes. Blood samples were left at RT for 50mins to clot. Samples were spun down at 4°C at 10,000rpm for 15mins. Serum supernatant was carefully pipetted out and used for further analysis.

**Chapter 7: Works Cited**

1. Sung, H. *et al.* Global Cancer Statistics 2020: GLOBOCAN Estimates of Incidence and Mortality Worldwide for 36 Cancers in 185 Countries. *CA. Cancer J. Clin.* **71**, 209–249 (2021).
2. Varmus, H. The new era in cancer research. *Science (80-. )*. **312**, 1162–1165 (2006).
3. Schreiber, R. D., Old, L. J. & Smyth, M. J. Cancer immunoediting: Integrating immunity's roles in cancer suppression and promotion. *Science* vol. 331 1565–1570 (2011).
4. Grivennikov, S. I., Greten, F. R. & Karin, M. Immunity, inflammation, and cancer. *Cell* **140**, 883–899 (2010).
5. Demaria, O. *et al.* Harnessing innate immunity in cancer therapy. *Nature* **574**, 45–56 (2019).
6. Vesely, M. D., Kershaw, M. H., Schreiber, R. D. & Smyth, M. J. Natural innate and adaptive immunity to cancer. *Annu. Rev. Immunol.* **29**, 235–271 (2011).
7. Radoja, S., Rao, T. D., Hillman, D. & Frey, A. B. Mice bearing late-stage tumors have normal functional systemic T cell responses in vitro and in vivo. *J. Immunol.* **164**, 2619–2628 (2000).
8. Malmberg, K. J. Effective immunotherapy against cancer. *Cancer Immunol. Immunother.* *2004 5310* **53**, 879–892 (2004).
9. Van Pel, A. & Boon, T. Protection against a nonimmunogenic mouse leukemia by an immunogenic variant obtained by mutagenesis. *Proc. Natl. Acad. Sci. U. S. A.* **79**, 4718–4722 (1982).
10. Morvan, M. G. & Lanier, L. L. NK cells and cancer: you can teach innate cells new tricks. *Nat. Rev. Cancer* *2016 161* **16**, 7–19 (2015).
11. Ferlazzo, G. *et al.* The Abundant NK Cells in Human Secondary Lymphoid Tissues Require Activation to Express Killer Cell Ig-Like Receptors and Become Cytolytic. *J. Immunol.* **172**, 1455–1462 (2004).
12. Zamai, L. *et al.* NK Cells and Cancer. *J. Immunol.* **178**, 4011–4016 (2007).
13. Lanier, L. L. Up on the tightrope: natural killer cell activation and inhibition. *Nat. Immunol.* **9**, 495–502 (2008).
14. Shimasaki, N., Jain, A. & Campana, D. NK cells for cancer immunotherapy. *Nat. Rev. Drug Discov.* *2020 193* **19**, 200–218 (2020).
15. Narni-Mancinelli, E. *et al.* Complement factor P is a ligand for the natural killer cell-activating receptor NKp46. *Sci. Immunol.* **2**, (2017).
16. Waldhauer, I. & Steinle, A. NK cells and cancer immunosurveillance. *Oncogene* *2008 2745* **27**, 5932–5943 (2008).
17. Hayakawa, Y., Huntington, N. D., Nutt, S. L. & Smyth, M. J. Functional subsets of mouse natural killer cells. *Immunological Reviews* vol. 214 (2006).
18. Geissmann, F. *et al.* Development of monocytes, macrophages, and dendritic cells. *Science (80-. )*. **327**, 656–661 (2010).
19. Clynes, R. A., Towers, T. L., Presta, L. G. & Ravetch, J. V. Inhibitory Fc receptors modulate in vivo cytotoxicity against tumor targets. *Nat. Med.* **6**, 443–446 (2000).
20. Tay, M. Z., Wiehe, K. & Pollara, J. Antibody dependent cellular phagocytosis in antiviral immune responses. *Front. Immunol.* **10**, 332 (2019).
21. Gonzalez, H., Hagerling, C. & Werb, Z. Roles of the immune system in cancer: from

- tumor initiation to metastatic progression. *Genes Dev.* **32**, 1267 (2018).
22. Hanna, R. N. *et al.* Patrolling monocytes control tumor metastasis to the lung. *Science* **350**, 985–990 (2015).
  23. Guerriero, J. L. *et al.* Class IIa HDAC inhibition reduces breast tumours and metastases through anti-tumour macrophages. *Nature* **543**, 428–432 (2017).
  24. Vidarsson, G., Dekkers, G. & Rispens, T. IgG Subclasses and Allotypes: From Structure to Effector Functions. *Front. Immunol.* **5**, (2014).
  25. Clynes, R. Antitumor Antibodies in the Treatment of Cancer: Fc Receptors Link Opsonic Antibody with Cellular Immunity. *Hematol. Oncol. Clin. North Am.* **20**, 585–612 (2006).
  26. Scott, A. M., Wolchok, J. D. & Old, L. J. Antibody therapy of cancer. *Nat. Rev. Cancer* **2012 124** **12**, 278–287 (2012).
  27. Vidarsson, G., Dekkers, G. & Rispens, T. IgG subclasses and allotypes: From structure to effector functions. *Front. Immunol.* **5**, 520 (2014).
  28. Yu, J., Song, Y. & Tian, W. How to select IgG subclasses in developing anti-tumor therapeutic antibodies. *J. Hematol. Oncol.* **13**, 1–10 (2020).
  29. Lo, M. *et al.* Effector-attenuating Substitutions That Maintain Antibody Stability and Reduce Toxicity in Mice. *J. Biol. Chem.* **292**, 3900–3908 (2017).
  30. Buss, N. A. P. S., Henderson, S. J., McFarlane, M., Shenton, J. M. & De Haan, L. Monoclonal antibody therapeutics: History and future. *Current Opinion in Pharmacology* vol. 12 615–622 (2012).
  31. Mellor, J. D., Brown, M. P., Irving, H. R., Zalcborg, J. R. & Dobrovic, A. A critical review of the role of Fc gamma receptor polymorphisms in the response to monoclonal antibodies in cancer. *Journal of Hematology and Oncology* vol. 6 1 (2013).
  32. Smyth, M. J. *et al.* Activation of NK cell cytotoxicity. *Molecular Immunology* vol. 42 501–510 (2005).
  33. Wang, W., Erbe, A. K., Hank, J. A., Morris, Z. S. & Sondel, P. M. NK Cell-Mediated Antibody-Dependent Cellular Cytotoxicity in Cancer Immunotherapy. *Front. Immunol.* **6**, 1 (2015).
  34. Wang, W., Erbe, A. K., Hank, J. A., Morris, Z. S. & Sondel, P. M. NK cell-mediated antibody-dependent cellular cytotoxicity in cancer immunotherapy. *Front. Immunol.* **6**, 368 (2015).
  35. Gwalani, L. A. & Orange, J. S. Single Degranulations in NK Cells Can Mediate Target Cell Killing. *J. Immunol.* **200**, 3231–3243 (2018).
  36. Lieberman, J. The ABCs of granule-mediated cytotoxicity: new weapons in the arsenal. *Nat. Rev. Immunol.* **3**, 361–370 (2003).
  37. Yeap, W. H. *et al.* CD16 is indispensable for antibody-dependent cellular cytotoxicity by human monocytes. *Sci. Reports 2016 61* **6**, 1–22 (2016).
  38. Zent, C. S. & Elliott, M. R. Maxed out macs: physiologic cell clearance as a function of macrophage phagocytic capacity. *FEBS J.* **284**, 1021–1039 (2017).
  39. Cao, X. *et al.* Promoting antibody-dependent cellular phagocytosis for effective macrophage-based cancer immunotherapy. *Sci. Adv.* **8**, 9171 (2022).
  40. Sarma, J. V. & Ward, P. A. The complement system. *Cell Tissue Res.* **343**, 227 (2011).
  41. Müller-Eberhard, H. J. Molecular Organization and Function of the Complement System. *Annu. Rev. Biochem.* **57**, 321–347 (1988).
  42. Debela, D. T. *et al.* New approaches and procedures for cancer treatment: Current perspectives. *SAGE Open Med.* **9**, 205031212110343 (2021).



43. Yang, Y. Cancer immunotherapy: harnessing the immune system to battle cancer. *J. Clin. Invest.* **125**, 3335–3337 (2015).
44. Sunada, H., Magun, B. E., Mendelsohn, J. & MacLeod, C. L. Monoclonal antibody against epidermal growth factor receptor is internalized without stimulating receptor phosphorylation. *Proc. Natl. Acad. Sci. U. S. A.* **83**, 3825–3829 (1986).
45. Alley, S. C., Okeley, N. M. & Senter, P. D. Antibody-drug conjugates: Targeted drug delivery for cancer. *Current Opinion in Chemical Biology* vol. 14 529–537 (2010).
46. Capala, J. & Bouchelouche, K. Molecular imaging of HER2-positive breast cancer: A step toward an individualized ‘image and treat’ strategy. *Current Opinion in Oncology* vol. 22 559–566 (2010).
47. Clynes, R., Takechi, Y., Moroi, Y., Houghton, A. & Ravetch, J. V. Fc receptors are required in passive and active immunity to melanoma. *Proc. Natl. Acad. Sci. U. S. A.* **95**, 652–656 (1998).
48. Thomas, A., Maltzman, J. & Hassan, R. Farletuzumab in lung cancer. *Lung Cancer* **80**, 15–18 (2013).
49. Henry, M. D. *et al.* A Prostate-Specific Membrane Antigen-Targeted Monoclonal Antibody–Chemotherapeutic Conjugate Designed for the Treatment of Prostate Cancer. *Cancer Res.* **64**, 7995–8001 (2004).
50. Kinoshita, T., Nagai, H., Murate, T. & Saito, H. CD20-negative relapse in B-cell lymphoma after treatment with Rituximab. *J. Clin. Oncol.* **16**, 3916–3916 (1998).
51. Loibl, S. & Gianni, L. HER2-positive breast cancer. *Lancet* **389**, 2415–2429 (2017).
52. Harding, F. A., Stickler, M. M., Razo, J. & DuBridge, R. B. The immunogenicity of humanized and fully human antibodies: Residual immunogenicity resides in the CDR regions. *MAbs* **2**, 256–265 (2010).
53. Hansel, T. T., Kropshofer, H., Singer, T., Mitchell, J. A. & George, A. J. T. The safety and side effects of monoclonal antibodies. *Nature Reviews Drug Discovery* vol. 9 325–338 (2010).
54. Jackisch, C. *et al.* Subcutaneous versus intravenous formulation of trastuzumab for HER2-positive early breast cancer: Updated results from the phase III HannaH study. *Ann. Oncol.* **26**, 320–325 (2015).
55. Coulson, A., Levy, A. & Gossell-Williams, M. Monoclonal Antibodies in Cancer Therapy: Mechanisms, Successes and Limitations. *West Indian Med. J.* **63**, 650 (2014).
56. Tabrizi, M. A., Tseng, C. M. L. & Roskos, L. K. Elimination mechanisms of therapeutic monoclonal antibodies. *Drug Discov. Today* **11**, 81–88 (2006).
57. Presta, L. G. Engineering of therapeutic antibodies to minimize immunogenicity and optimize function. *Advanced Drug Delivery Reviews* vol. 58 640–656 (2006).
58. Veber, D. F. *et al.* Molecular properties that influence the oral bioavailability of drug candidates. *J. Med. Chem.* **45**, 2615–2623 (2002).
59. Chames, P., Van Regenmortel, M., Weiss, E. & Baty, D. Therapeutic antibodies: Successes, limitations and hopes for the future. *British Journal of Pharmacology* vol. 157 220–233 (2009).
60. Sasaki, K. *et al.* Fc-binding antibody-recruiting molecules exploit endogenous antibodies for anti-tumor immune responses. *Chem. Sci.* **11**, 3208–3214 (2020).
61. Spiegel, D. A. A call to ARMs: The promise of immunomodulatory small molecules. *Expert Review of Clinical Pharmacology* vol. 6 223–225 (2013).
62. Imai, K. & Takaoka, A. Comparing antibody and small-molecule therapies for cancer.

- Nature Reviews Cancer* vol. 6 714–727 (2006).
63. Wu, A. M. & Senter, P. D. Arming antibodies: prospects and challenges for immunoconjugates. *Nat. Biotechnol.* **23**, 1137–1146 (2005).
  64. McEnaney, P. J., Parker, C. G., Zhang, A. X. & Spiegel, D. A. Antibody-Recruiting Molecules: An Emerging Paradigm for Engaging Immune Function in Treating Human Disease. *ACS Chem. Biol.* **7**, 1139 (2012).
  65. Rullo, A. F. *et al.* Antitumor Agents Re-engineering the Immune Response to Metastatic Cancer: Antibody-Recruiting Small Molecules Targeting the Urokinase Receptor. doi:10.1002/anie.201510866.
  66. McEnaney, P. J., Parker, C. G., Zhang, A. X. & Spiegel, D. A. Antibody-recruiting molecules: An emerging paradigm for engaging immune function in treating human disease. *ACS Chemical Biology* vol. 7 1139–1151 (2012).
  67. Murelli, R. P., Zhang, A. X., Michel, J., Jorgensen, W. L. & Spiegel, D. A. Chemical control over immune recognition: A class of antibody-recruiting small molecules that target prostate cancer. *J. Am. Chem. Soc.* **131**, 17090–17092 (2009).
  68. Murelli, R. P., Zhang, A. X., Michel, J., Jorgensen, W. L. & Spiegel, D. A. Chemical control over immune recognition: A class of antibody-recruiting small molecules that target prostate cancer. *J. Am. Chem. Soc.* **131**, 17090–17092 (2009).
  69. Hong, H. *et al.* Site-specific C-terminal dinitrophenylation to reconstitute the antibody Fc functions for nanobodies. *Chem. Sci.* **10**, 9331–9338 (2019).
  70. Jakobsche, C. E. *et al.* Exploring binding and effector functions of natural human antibodies using synthetic immunomodulators. *ACS Chem. Biol.* **8**, 2404–2411 (2013).
  71. Ghosh, A. & Heston, W. D. W. Tumor target prostate specific membrane antigen (PSMA) and its regulation in prostate cancer. *Journal of Cellular Biochemistry* vol. 91 (2004).
  72. Donin, N. M. & Reiter, R. E. Why Targeting PSMA Is a Game Changer in the Management of Prostate Cancer. *J. Nucl. Med.* **59**, 177 (2018).
  73. Murphy, G. P. *et al.* Measurement of prostate-specific membrane antigen in the serum with a new antibody. *Prostate* **28**, 266–271 (1996).
  74. Palamiuc, L. & Emerling, B. M. PSMA brings new flavors to PI3K signaling: A role for glutamate in prostate cancer. *J. Exp. Med.* **215**, 17 (2018).
  75. Wolf, P. *et al.* Preclinical evaluation of a recombinant anti-prostate specific membrane antigen single-chain immunotoxin against prostate cancer. *J. Immunother.* **33**, 262–271 (2010).
  76. Bander, N. H. *et al.* Phase I trial of 177Lutetium-labeled J591, a monoclonal antibody to prostate-specific membrane antigen, in patients with androgen-independent prostate cancer. *J. Clin. Oncol.* **23**, 4591–4601 (2005).
  77. Hummel, H.-D. *et al.* Phase 1 study of pasotuxizumab (BAY 2010112), a PSMA-targeting Bispecific T cell Engager (BiTE) immunotherapy for metastatic castration-resistant prostate cancer (mCRPC). [https://doi.org/10.1200/JCO.2019.37.15\\_suppl.5034](https://doi.org/10.1200/JCO.2019.37.15_suppl.5034) **37**, 5034–5034 (2019).
  78. Zhang, A. X. *et al.* A Remote Arene-Binding Site on Prostate Specific Membrane Antigen Revealed by Antibody-Recruiting Small Molecules. *ACS Chem. Biol.* **132**, 12711– 12716 (2010).
  79. Chivers, C. E., Koner, A. L., Lowe, E. D. & Howarth, M. How the biotin–streptavidin interaction was made even stronger: investigation via crystallography and a chimaeric tetramer. *Biochem. J.* **435**, 55 (2011).

80. Lake, B., Serniuck, N., Kapcan, E., Wang, A. & Rullo, A. F. Covalent Immune Recruiters: Tools to Gain Chemical Control over Immune Recognition. *ACS Chem. Biol.* **15**, 1089–1095 (2020).
81. Kapcan, E. *et al.* Covalent Stabilization of Antibody Recruitment Enhances Immune Recognition of Cancer Targets. (2021) doi:10.1021/acs.biochem.1c00127.
82. Lu, Y. & Low, P. S. Folate targeting of haptens to cancer cell surfaces mediates immunotherapy of syngeneic murine tumors. *Cancer Immunol. Immunother.* **51**, 153–162 (2002).
83. Akiyama, K. *et al.* Targeting Apoptotic Tumor Cells to FcγR Provides Efficient and Versatile Vaccination Against Tumors by Dendritic Cells. *J. Immunol.* **170**, 1641–1648 (2003).
84. Huynh, V. *et al.* Improved Efficacy of Antibody Cancer Immunotherapeutics through Local and Sustained Delivery. *ChemBioChem* vol. 20 747–753 (2019).
85. Rajasekaran, S. A. *et al.* A Novel Cytoplasmic Tail MXXXL Motif Mediates the Internalization of Prostate-specific Membrane Antigen. *Mol. Biol. Cell* **14**, 4835–4845 (2003).
86. Tam, H. H. *et al.* Sustained antigen availability during germinal center initiation enhances antibody responses to vaccination. *Proc. Natl. Acad. Sci. U. S. A.* **113**, E6639–E6648 (2016).
87. Gorer, P. A. & Amos, D. B. Passive Immunity in Mice against C57BL Leukosis E.L.4 by Means of Iso-immune Serum. *Cancer Res.* **16**, (1956).
88. Friedrich, M. *et al.* Regression of human prostate cancer xenografts in mice by AMG 212/BAY2010112, a novel PSMA/CD3-bispecific BiTE antibody cross-reactive with non-human primate antigens. *Mol. Cancer Ther.* **11**, 2664–2673 (2012).
89. Miao, H. *et al.* Quantifying the Early Immune Response and Adaptive Immune Response Kinetics in Mice Infected with Influenza A Virus. *J. Virol.* **84**, 6687 (2010).
90. Simons, B. W., Turtle, N. F., Ulmert, D. H., Abou, D. S. & Thorek, D. L. J. PSMA expression in the Hi-Myc model; extended utility of a representative model of prostate adenocarcinoma for biological insight and as a drug discovery tool. *Prostate* **79**, 678–685 (2019).
91. Schmittgen, T. D. *et al.* Expression pattern of mouse homolog of prostate-specific membrane antigen (FOLH1) in the transgenic adenocarcinoma of the mouse prostate model. *Prostate* **55**, 308–316 (2003).
92. Muthumani, K. *et al.* Novel prostate cancer immunotherapy with a DNA-encoded anti-prostate-specific membrane antigen monoclonal antibody. *Cancer Immunol. Immunother.* **66**, 1577 (2017).
93. Rodriguez-Barbosa, J. I. *et al.* Therapeutic implications of NK cell regulation of allogeneic CD8 T cell-mediated immune responses stimulated through the direct pathway of antigen presentation in transplantation. *MAbs* **10**, (2018).
94. Sega, E. I. & Low, P. S. Tumor detection using folate receptor-targeted imaging agents. *Cancer Metastasis Rev.* **27**, 655–664 (2008).
95. Van Der Kolk, L. E., Baars, J. W., Prins, M. H. & Van Oers, M. H. J. Rituximab treatment results in impaired secondary humoral immune responsiveness. *Blood* **100**, (2002).
96. Stone, E. A., Mercado, B. Q., Miller, S. J. & Lett Author manuscript, O. Structure and Reactivity of Highly Twisted N-Acyl Imidazoles HHS Public Access Author manuscript. *Org Lett* **21**, 2346–2351 (2019).

97. Kipps, T. J., Parham, P., Punt, J. & Herzenberg, L. A. IMPORTANCE OF IMMUNOGLOBULIN ISOTYPE IN HUMAN ANTIBODY-DEPENDENT, CELL-MEDIATED CYTOTOXICITY DIRECTED BY MURINE MONOCLONAL ANTIBODIES. doi:10.1084/jem.161.1.1.
98. Nimmerjahn, F. *et al.* FcY $\gamma$ RIV deletion reveals its central role for IgG2a and IgG2b activity in vivo. *Proc. Natl. Acad. Sci. U. S. A.* **107**, 19396–19401 (2010).
99. Hossain, M. K., Vartak, A., Karmakar, P., Sucheck, S. J. & Wall, K. A. Augmenting Vaccine Immunogenicity through the Use of Natural Human Anti-rhamnose Antibodies. *ACS Chem. Biol.* **13**, 2130–2142 (2018).
100. Clémenceau, B. *et al.* The human natural killer cytotoxic cell line NK-92, once armed with a murine CD16 receptor, represents a convenient cellular tool for the screening of mouse mAbs according to their ADCC potential. *MAbs* **5**, 587 (2013).
101. Colamartino, A. B. L. *et al.* Efficient and Robust NK-Cell Transduction With Baboon Envelope Pseudotyped Lentivector. *Front. Immunol.* **10**, 2873 (2019).
102. Bari, R. *et al.* A distinct subset of highly proliferative and lentiviral vector (LV)-transducible NK cells define a readily engineered subset for adoptive cellular therapy. *Front. Immunol.* **10**, 2001 (2019).
103. Micucci, F. *et al.* High-efficient lentiviral vector-mediated gene transfer into primary human NK cells. *Exp. Hematol.* **34**, (2006).
104. Zou, N. *et al.* Macrophages Receptors on  $\gamma$  Vivo by Interaction with Fc High HER2 Cancer Cells In Vitro and In Trastuzumab Triggers Phagocytic Killing of. (2015) doi:10.4049/jimmunol.1402891.